

EXPERIMENTAL INVESTIGATION OF THERMAL STRATIFICATION IN
BOILING WATER REACTOR SUPPRESSION POOLS DURING REACTOR CORE
ISOLATION COOLING SYSTEM OPERATION AND REACTOR SAFETY
IMPLICATIONS

A Thesis

by

DALLIN JACOB KEESLING

Submitted to the Graduate and Professional School of
Texas A&M University
in partial fulfillment of the requirements for the degree of

MASTER OF SCIENCE

Chair of Committee,	Karen Vierow Kirkland
Committee Members,	Mark Kimber
	Lesley Wright
Head of Department,	Michael Nastasi

August 2021

Major Subject: Nuclear Engineering

Copyright 2021 Dallin Jacob Keesling

ABSTRACT

The primary safety concern at a nuclear reactor is to maintain water inventory inside the reactor core so that the nuclear fuel is adequately cooled. The Reactor Core Isolation Cooling system is designed to automatically provide make-up water to the reactor pressure vessel during isolation events by passing steam from the reactor pressure vessel through a turbine which drives a pump to inject water into the reactor pressure vessel. Exemplary performance of the RCIC system during the Fukushima Daiichi nuclear accident of 2011 showed the RCIC system's potential utility as a safety device during Beyond Design Basis Accidents as well. This has led to increased interest in maximizing the performance of RCIC systems installed in about 25 US BWR nuclear power plants.

RCIC system performance is dependent on conditions in the suppression pool which serves as the RCIC pump water source. To investigate the development of thermal stratification within the pool, a model facility was constructed at the Laboratory for Nuclear Heat Transfer Systems at Texas A&M University. The facility was modified for this work to produce the first high-resolution 3-D temperature measurements in a large water pool. Addition of a scaled-down Terry Turbine of the same design as those used in the RCIC system increases data fidelity to real-world RCIC system behavior.

Development of thermal stratification in the suppression pool was investigated by changing two parameters: the steam flowrate and suppression pool pressure conditions.

Thermal stratification was most strongly influenced by suppression chamber pressure, with a maximum thermal separation between the top and bottom of the pool of

40.9 °C observed under high pressure while the thermal separation under low pressure with the same steam flowrate was only 18.2 °C. Increased steam flowrate tended to improve mixing, which decreased the duration of thermal stratification.

RCIC system performance was found to be strongly influenced by thermal stratification within the pool, showing an improvement in heat removal of up to 6% for thermally stratified pools, compared to well-mixed pools. Inducing thermal stratification in BWR suppression pools could maximize the RCIC system's ability to safely cool the reactor core.

DEDICATION

To God, for without his guidance and strength I would not be the person I am today, capable of producing this work. To the love of my life, Kendra Keesling, for her patience, love, and never-ending support. To Jonathan and Robyn Keesling for teaching me the importance of hard work and dedication that have helped me along this path.

ACKNOWLEDGEMENTS

This research would not have been possible without the support of several individuals. The guidance and support of my advisor, Dr. Karen Kirkland, was crucial. I would also like to give a special thanks to Matthew Solom, whose experience and advice were critical throughout the facility construction process. The efforts of (in no particular order) Ashraf Alfandi, Thomas Freyman, Gage Green, Benjamin Lear and Joshua Vandervort are greatly appreciated.

Finally, thanks to my mother and father for their encouragement and to my wife for her patience and love.

CONTRIBUTORS AND FUNDING SOURCES

Contributors

This work was supervised by a thesis committee consisting of Dr. Karen Kirkland and Dr. Mark Kimber of the Department of Nuclear Engineering and Dr. Lesley Wright of the Department of Mechanical Engineering.

Dr. Matthew Solom aided substantially in the design and construction of the experimental facility. The facility Piping and Instrumentation Diagrams included in Appendix A were prepared by a fellow graduate student, Ashraf Alfandi. All other work conducted for the thesis was completed by the student independently.

Funding Sources

This work was also made possible by the Office of Nuclear Energy, U.S. Department of Energy through the Nuclear Energy University Program under Award Number DE-NE0008763 as part of the project “Coupled Application of Accident Tolerant Fuels and the RCIC System to Enhance LWR Safety”. Its contents are solely the responsibility of the authors and do not necessarily represent the official views of the Department of Energy

NOMENCLATURE

API	American Petroleum Institute
ASME	American Society of Mechanical Engineers
BWR	Boiling Water Reactor
CAD	Computer-Aided Design
CV	Coefficient of flow
DAQ	Data Acquisition
DI	Deionized/deionization (water)
GPM	Gallons per Minute
HDPE	High-density Polyurethane
HRS	Heat Rejection System
HP	Horsepower
IAPWS	International Association for the Properties of Water and Steam
LOCA	Loss of Cooling Accident
NHTS	Nuclear Heat Transfer Systems
MHz	Megahertz
NPS	Nominal Pipe Size
NPT	National Pipe Thread
PID	Proportional Integral Derivative
PRV	Pressure Relief Valves
psi	pounds per square inch

psia	pounds per square inch (absolute)
psig	pounds per square inch (gauge)
PWR	Pressurized Water Reactor
RCIC	Reactor Core Isolation Cooling
URL	Upper Range Limit
URV	Upper Range Value
US	United States
VAC	Volts Alternating Current

TABLE OF CONTENTS

	Page
ABSTRACT	ii
DEDICATION.....	iv
ACKNOWLEDGEMENTS	v
CONTRIBUTORS AND FUNDING SOURCES.....	vi
NOMENCLATURE	vii
TABLE OF CONTENTS.....	ix
LIST OF FIGURES	xii
LIST OF TABLES.....	xvii
1. INTRODUCTION	1
1.1. Problem Statement	3
1.2. Technical Approach	3
2. BACKGROUND	5
2.1. Reactor Core Isolation Cooling System Design	5
2.2. Boiling Water Reactor Containment Design	6
2.3. Justification for Designing Facility to Reflect Mark I Containment Design.....	9
2.4. RCIC System Operational Limits	9
2.5. Previous Experimental Studies on Suppression Pool Behaviors during RCIC System Operation.....	11
3. EXPERIMENTAL FACILITY	13
3.1. Water Deionization System	13
3.2. Suppression Chamber Analog	17
3.3. Steam Generator.....	22
3.4. ZS-1 Terry Turbine	28
3.5. Flowmeters	30
3.5.1. Foxboro Vortex Flowmeter.....	30
3.5.2. Azbil Magnetic Flowmeter	31

3.6. Control Valves	32
3.6.1. Main Steam Control Valve	32
3.6.2. Feedwater Control Valve	34
3.7. Thermocouples.....	36
3.8. Pressure Transmitters.....	39
3.8.1. Emerson 3051CA	41
3.8.2. Honeywell STA 940	41
3.8.3. Honeywell STD 924	41
3.8.4. Omega PX309-V150-GI	42
3.9. Feedwater Pump.....	43
3.10. Heat Rejection System	45
3.10.1. Heat Rejection System Heat Exchanger	45
3.10.2. Cooling Tower.....	47
3.10.3. Heat Rejection System Water Supply Tank.....	48
3.10.4. Heat Rejection System Water Treatment System	51
3.10.5. Heat Rejection System Primary-Side Pump	53
3.10.6. Heat Rejection System Secondary-Side Pump.....	55
3.10.7. Heat Rejection System Piping.....	57
3.11. Data Acquisition System	69
3.11.1. Hardware.....	69
3.11.2. Software	71
3.12. Air Compressor.....	80
4. TESTING	82
4.1. Testing plan	82
4.2. Test Matrix.....	82
4.3. Operating Procedures	84
4.3.1. Pre-startup procedures	87
4.3.2. Water Level Verification	88
4.3.3. Warmup Mode.....	89
4.3.4. Data Collection Mode.....	92
4.3.5. Shut-down Procedure.....	96
4.4. Results	99
4.4.1. Test #1.....	99
4.4.2. Test #2.....	106
4.4.3. Test #3.....	109
4.4.4. Test #4.....	113
4.4.5. Test #5.....	116
4.4.6. Test #6.....	118
4.4.7. Test #7.....	122
5. ANALYSIS	127

5.1. Goal of Analysis.....	127
5.2. Effect of Thermal Stratification on RCIC System Performance	128
5.2.1. Error Analysis	131
5.2.2. Optimal Conditions to Maximize the Benefit of Thermal Stratification.....	132
5.2.3. Optimal conditions to promote thermal stratification.....	138
5.3. Discussion of Reactor Safety Implications.....	142
5.4. Scaling Discussion	144
6. CONCLUSIONS	146
6.1. Key Findings.....	148
6.2. Future Work.....	148
REFERENCES	150
APPENDIX A FACILITY P&ID.....	158
APPENDIX B DATA PROCESSING SCRIPTS	161
B.1 Guidelines	161
B.2 Python Scripts	163
B.2.1 Master Script.py.....	163
B.2.2 Read_Data.py	172
B.2.3 SteamProperties.py	187
B.2.4 search.py.....	195
B.2.5 SteadyStateDetection.py	196

LIST OF FIGURES

	Page
Figure 3.1. Culligan® water filtration system indicator light. Turns red when the tank needs to be replaced.	15
Figure 3.2. Culligan® DI water filtration system on mobile cart.....	16
Figure 3.3. Suppression chamber analog with associated piping.....	18
Figure 3.4. CAD model of the suppression chamber analog. Transparent to show internal spargers.....	19
Figure 3.5. Suppression chamber analog water level meter.....	21
Figure 3.6. Steam generator vessel.	23
Figure 3.7. 50 kW heater prior to installation into the steam generator.	24
Figure 3.8. One of the 50kW heaters (Left) and one of the 2kW heaters (Right) on the steam generator.....	25
Figure 3.9. Steam Generator Control Board.....	26
Figure 3.10. Steam generator water level indicator.....	27
Figure 3.11. ZS-1 Terry Turbine with insulation coupled to dynamometer.	29
Figure 3.12. Masoneilan 21124 Top-Guided Globe Valve, used to control steam flow rate.....	33
Figure 3.13. CV curve for equal-percentage Masoneilan 88-21124 globe valve. Data from [25].	34
Figure 3.14. Fisher D041TV1 DN25 GX air-to-open globe valve. Used to control the flowrate of water returning to the steam generator.....	35
Figure 3.15. CV curve for Fisher D041TV1 DN 25 GX air-to-open globe valve. Data from [26]	35
Figure 3.16. CAD model of the suppression chamber analog with thermocouple locations marked in red.....	37
Figure 3.17. Top view of suppression chamber analog CAD model with thermocouple locations indicated in red.....	38

Figure 3.18. Side view of suppression chamber analog CAD model with thermocouples locations indicated in red.....	38
Figure 3.19. Feedwater Pump. Dayton 5UXF5 5-stage centrifugal pump coupled to an electric motor.....	44
Figure 3.20. Pump Curve for Dayton UXF5 5-stage centrifugal pump. Data from [30].	44
Figure 3.21. HRS Heat Exchanger.....	46
Figure 3.22. HRS Cooling Tower.....	47
Figure 3.23. Photo of HRS Storage Tank as installed in facility.....	48
Figure 3.24. Water suction manifold.	49
Figure 3.25. Water return line from HRS cooling tower supported by stainless steel channel strut.....	51
Figure 3.26. HRS Water Treatment System.....	52
Figure 3.27. HRS Primary-side Pump.	53
Figure 3.28. Performance Curves for Liquiflo® 621 Centrifugal Pump. Used as primary-side coolant pump. [33]	54
Figure 3.29. HRS secondary-side coolant pump. Dayton 12N813 Self-Priming Centrifugal Pump.....	56
Figure 3.30 Pump curve for the Dayton 12N813 self-priming centrifugal pump. Data from [32].	56
Figure 3.31. HRS piping connections to HRS heat exchanger.	57
Figure 3.32. HRS Primary Side pump with piping. Red globe valve controls flow rate of primary coolant to the heat exchanger. Pump inlet comes from suppression tank.....	59
Figure 3.33. HRS Tank outlet. 3-inch pipe with red ball valve leads to HRS secondary pump. 1.5-inch pipe with blue ball valve leads to floor drain.....	61
Figure 3.34. HRS secondary-side piping. Water passes through the Y-strainer before entering the pump.	61
Figure 3.35. 3-inch pipes penetrating the wall route to the inlet and outlet of the HRS cooling tower. 3-inch pipe extending upward from the HRS secondary-side	

pump goes to the HRS heat exchanger and water treatment systems. Red globe valve controls the flow rate through the HRS piping system.	62
Figure 3.36. CAD model close-up of HRS pipe support structure.....	63
Figure 3.37. Triangular supports bear the weight of the main support structure and fix it to the wall.....	64
Figure 3.38. HRS elevated piping section #1.....	65
Figure 3.39. HRS elevated piping section #2.....	65
Figure 3.40. HRS elevated piping section #3. Black flexible hose helps to account for thermal expansion.....	67
Figure 3.41. HRS elevated piping section #4. Blue and White instrumentation wires run along the top of the pipe support structure.....	67
Figure 3.42. HRS vertical piping section.....	68
Figure 3.43. HRS piping. Red ball valves allow for heat exchanger bypass.....	69
Figure 3.44. NI PXIe-1075 with modules installed.....	71
Figure 3.45. Main Control Panel on LabVIEW VI.....	73
Figure 3.46. Suppression pool monitoring panel for LabVIEW VI.....	74
Figure 3.47. Heat Rejection System monitoring panel for LabVIEW VI.....	75
Figure 3.48. PID constants panel for LabVIEW VI.....	76
Figure 3.49. Quincy Air Compressor.....	80
Figure 3.50. Quincy Compressed Air Dryer.....	81
Figure 4.1. Average temperature at each monitored elevation within the suppression pool for test #1.....	100
Figure 4.2. Plot of the temperature inside the turbine exhaust line, 4 inches from the outlet, and the water temperature at the outlet for test #1.....	101
Figure 4.3 Plots of temperatures over time at each axial location measured within the suppression pool for Test #1.....	102

Figure 4.4. Plot of temperature measured at each lateral position at the turbine-side weld for test #1.	103
Figure 4.5. Plot of temperature measured at each lateral position at the center of the tank for test #1.	104
Figure 4.6. Plot of temperature measured at each lateral position at the plate-side weld for test #1.	104
Figure 4.7. Average temperature at each monitored elevation within the suppression pool for test #2.	107
Figure 4.8. Plot of the temperature inside the turbine exhaust line, 4 inches from the outlet, and the water temperature at the outlet for test #2.	108
Figure 4.9. Average temperature at each monitored elevation within the suppression pool for test #3.	110
Figure 4.10. Plot of the pressure in the suppression tank during test #3.	111
Figure 4.11. Plot of the temperature inside the turbine exhaust line, 4 inches from the outlet, and the water temperature at the outlet for test #3.	112
Figure 4.12. Average temperature at each monitored elevation within the suppression pool for test #4.	113
Figure 4.13. Plot of the pressure in the suppression tank during test #4.	114
Figure 4.14. Plot of the temperature inside the turbine exhaust line, 4 inches from the outlet, and the water temperature at the outlet for test #4.	115
Figure 4.15. Average temperature at each monitored elevation within the suppression pool for test #5.	117
Figure 4.16. Average temperature at each monitored elevation within the suppression pool for test #6.	119
Figure 4.17. Plot of the pressure in the suppression tank during test #6.	120
Figure 4.18. Plot of the temperature inside the turbine exhaust line, 4 inches from the outlet, and the water temperature at the outlet for test #6.	121
Figure 4.19. Average temperature at each monitored elevation within the suppression pool for test #7.	122

Figure 4.20. Degrees of thermal stratification from the highest elevation thermocouples to the lowest elevation thermocouples during test #7.	124
Figure 4.21. Plot of the pressure in the suppression tank during test #7.	125
Figure 4.22. Plot of the temperature inside the turbine exhaust line, 4 inches from the outlet, and the water temperature at the outlet for test #7.	126
Figure 5.1. Plot of heat rate improvement as a function of suppression chamber pressure.	134
Figure 5.2. Plot of Heat Rate Improvement as a function of the average degrees of thermal stratification.	135
Figure 5.3. Plot of heat rate improvement as a function of water mass flowrate.	136
Figure 5.4. Heat Removal Rate Improvement as a function of a combined variable, mass flowrate \times degrees of thermal stratification.	137
Figure 5.5. Plot of maximum thermal stratification as a function of steam mass flowrate.	140
Figure 5.6. Plot of maximum thermal stratification as a function of steam mass flowrate for tests performed at atmospheric pressure.	141
Figure 5.7. Plot of the maximum degrees of thermal stratification observed in the suppression pool as a function of suppression pool pressure.	142

LIST OF TABLES

	Page
Table 3.1. Accuracy of Azbil MagneW 3000 PLUS converter in combination with a detector <Size 2.5 to 15 mm (0.1 to ½ inch)> [24] Vs = Velocity of setting range.....	32
Table 3.2 Summary of pressure transmitters in the facility	40
Table 4.1. Test matrix	83
Table 4.2 Default valve positions	85
Table 5.1. Effect of Thermal Stratification on RCIC System Heat Removal	130
Table 5.2. Effect of Thermal Stratification on RCIC System Heat Removal Rate	133
Table 5.3 Test conditions and maximum thermal stratification observed for each test	139

1. INTRODUCTION

On March 11th, 2011, the Great East Japan Earthquake struck off the northeastern coast of the Japanese island of Honshu. The magnitude 9.0 quake spawned a series of very destructive tsunami waves, measuring as high as 33 ft. 730,299 structures were damaged by the earthquake, including 121,991 which suffered total collapse [1]. In total, the disaster resulted in 15,899 dead, 2,529 missing, and 6,157 injured [1]. Additionally, the earthquake and subsequent tsunamis led to loss of onsite and offsite power at the Fukushima Daiichi nuclear power plant, which ultimately resulted in core damage to Units 1, 2, and 3 [2]. During the accident, the Reactor Core Isolation Cooling (RCIC) system, which was installed in both Units 2 and 3, performed far beyond its design basis.

The RCIC system works by routing steam from the reactor pressure vessel through a turbine which drives a pump to supply cooling water to the core. The amount of steam allowed to pass through the turbine is controlled by a battery-powered governor valve to avoid a turbine overspeed trip. With no access to onsite power, the RCIC steam governor valve was left to operate on battery power alone, which is designed to last 4-8 hours. Once the battery is drained, the governor valve is expected to fail open, allowing an uncontrolled flow of steam into the RCIC turbine. This uncontrolled flow is expected to result in a turbine overspeed trip, disabling the RCIC system. In general, “one should not expect the RCIC system to run much beyond 8 hours in a station blackout (SBO)” [3]. Contrary to expectation, the RCIC system continued to operate long after the 8-hour threshold, providing essential core cooling and decay heat removal for 21 hours in Unit

3, and approximately 70 hours in Unit 2. The specific cause of failure for the RCIC system is unknown in both cases [2].

This unexpectedly successful performance by the RCIC system has been the cause of increased interest in the nuclear industry about the performance limits of the RCIC system and methods to maximize RCIC system performance. Extended RCIC system operation can lead to high temperature and pressure conditions in the BWR containment suppression pool, which serves as the heat sink for steam routed through the RCIC turbine. In addition, the suppression pool serves as an alternate source of cooling water for the RCIC system if the condensate storage tank is depleted or otherwise unavailable for use. The suppression pool's dual-purpose introduces an optimization problem when it comes to pool mixing. A well-mixed suppression pool maintains a uniform temperature distribution which minimizes the suppression pool surface temperature avoiding water saturation. If the upper levels of the pool are thermally saturated, steam may not be fully condensed which would lead to excess pressure in the containment airspace. On the other hand, if the suppression pool is well-mixed, the water being suctioned from the bottom of the pool by the RCIC pump will be warmer than if the pool could thermally stratify based on temperature-dependent density differences in the water. Allowing thermal stratification to develop by delaying pool mixing will minimize the temperature of the water being supplied to the reactor pressure vessel which is beneficial both for survivability of the RCIC pump and the RCIC system's ability to maintain water inventory in the reactor pressure vessel. To maximize the

overall performance of the RCIC system, the development of thermal stratification in the suppression pool must be well understood.

1.1. Problem Statement

The goal of this research is to investigate factors contributing to the development of thermal stratification in BWR suppression pools during extended RCIC system operation. The analytical focus will be to identify conditions that maximize RCIC system performance.

1.2. Technical Approach

Thermal stratification will be experimentally investigated in a facility representing the RCIC system as found in US BWR containments. Particularly, this research will show the effects that suppression pool conditions have on the development of thermal stratification within the pool and the RCIC system's ability to remove heat from the reactor core. An extensive three-dimensional array of thermocouples installed throughout the suppression pool will provide the most detailed data to date on the spatial and temporal temperature distributions within a large water pool subjected to prolonged steam injection. The development of thermal stratification will be explored using different steam injection rates and suppression pool pressures. The RCIC system facility at the Laboratory for Nuclear Heat Transfer Systems is the only known integral experimental test facility for the RCIC system, incorporating a scaled-down Terry turbine of the same design as the RCIC turbine found in US BWR power plants. This distinction will increase data fidelity by enabling test execution with boundary and initial conditions which reflect those in an actual RCIC system.

Once data is recorded for each experimental test, further analysis will be performed focusing on the theoretical heat removal potential of the water being pumped from the suppression pool to the steam generator, which represents the reactor pressure vessel. This heat removal will be compared to the theoretical heat removal potential if the suppression pool were well-mixed instead of stratified, and optimal conditions will be identified that maximize the improvement in RCIC system performance due to thermal stratification. Based on these results, implications for reactor safety and potential strategies to improve RCIC system operations will be discussed.

2. BACKGROUND

2.1. Reactor Core Isolation Cooling System Design

The Reactor Core Isolation Cooling system is designed to maintain reactor water inventory during design basis isolation events in boiling water reactors. An isolation event refers to any situation where the isolation valves are closed, cutting the reactor pressure vessel off from the main steam turbines, its primary heat sink. Without the normal heat sink, the significant amount of decay heat produced by the scrambled reactor would boil off the reactor water inventory and lead to core damage within a few hours at most. The RCIC system is triggered either manually by operator action, or automatically when the reactor pressure vessel water level reaches a low limit. The RCIC system supplies cooling water by passing the steam produced in the reactor pressure vessel through a Terry turbine and exhausting it into the suppression pool. The turbine is directly coupled to a multistage centrifugal pump which injects water into the reactor pressure vessel at a rate that can match the boiloff rate due to decay heat 15 minutes after reactor shutdown [4]. The default water source for the RCIC system is the condensate storage tank; however, in cases where the condensate storage tank is unavailable or has been depleted, the RCIC pump is aligned to draw water from the suppression pool instead [4]. For this work's investigation of extended RCIC system operation, the suppression pool will be considered the water source since the condensate storage tank will have been depleted.

The turbine exhaust outlet into the suppression pool is a sparger whose design varies from unit to unit. For example, the Fukushima Daiichi Unit 2 RCIC turbine exhaust sparger consists of a simple open-ended vertical pipe submerged near to the bottom of the suppression pool [5], while Unit 3 uses a different design: a vertical pipe capped at the end with a series of holes along the length of the pipe [6]. The design of steam exhaust spargers in suppression pools has been shown to have a significant effect on suppression pool integrity due to changes in steam condensation modes [7].

2.2. Boiling Water Reactor Containment Design

While the exact details of each plant design differ slightly, BWR containments in the United States are broadly based on one of three main containment designs, designated Mark I, Mark II, and Mark III, respectively. The three designs are similar in several respects. Each design consists of a drywell and a suppression chamber. The drywell refers to the portion of containment without water, whose main purpose is to contain steam and fission products during a loss of cooling accident (LOCA) and direct it to the suppression pool for condensation. In addition to condensation of steam during a LOCA, the suppression pool fulfills various other functions. It serves as the heat sink for steam released by safety/relief valves, the High-Pressure Coolant Injection system, and the RCIC turbine exhaust. The suppression pool also serves as water source for the HPCI and RCIC systems, the residual heat removal system, and core spray system [8]. Each of the three BWR containment designs depends on pressure suppression via steam condensation in a suppression pool as the primary means of minimizing the pressure

inside containment. Two significant differences between the three designs are the shape and positioning of the suppression pool.

The BWR Mark I containment suppression chamber is a toroidal vessel, encircling the space below the reactor pressure vessel. The light-bulb shaped drywell is connected to the suppression pool via a system of vents that extend outward and downward in all directions around the reactor pressure vessel. These vents provide an avenue for pressurized steam to pass from the drywell to the suppression pool, as well as a route for non-condensable gases in the suppression chamber to return to the drywell [8]. This system of vents consists of eight large pipes (81" in diameter), spaced equidistantly around the drywell, extending out and down to the suppression chamber. Upon entry to the suppression chamber, steam from all eight pipes enter a communal toroidal vent header from which steam is routed through 96 equivalent downcomer pipes which outlet 3 feet below the surface of the minimum suppression pool level. Injecting steam into the suppression pool through these downcomer pipes with a circumferentially uniform spacing promotes good mixing in the suppression pool and minimizes hot spots. Vacuum breakers are installed between the suppression chamber and the drywell to ensure external pressure on the drywell never exceeds 2 psi. Similar vacuum breakers exist between the suppression chamber and the reactor building to minimize vacuum formation in the primary containment [8].

The BWR Mark II suppression chamber is cylindrical and positioned directly underneath the drywell. This is commonly referred to as the "over-and-under" configuration [8]. The drywell and suppression chamber are connected by downcomer

pipes that penetrate the drywell floor, allowing steam and inert gas to be pushed to the suppression pool where the steam is condensed. The Mark II containment employs a similar vacuum breaker system as described above for the Mark I containment, allowing the inert gas to return to the drywell to avoid vacuum formation as the drywell cools.

Unlike the Mark I and Mark II designs, the BWR Mark III containment does not include a dedicate suppression chamber. Instead, the Mark III design utilizes a large containment building, like the dry containment found in PWR designs, which houses the suppression pool. The drywell in this design is cylindrical and performs the same function as described for the Mark I and Mark II containments. Namely, the drywell confines any steam that is released during a LOCA, and routes it to the suppression pool. The interface between the drywell and suppression pool is quite different in the Mark III design. Instead of downcomer vents, the drywell and suppression pool are connected by horizontal vents submerged at different depths below the suppression pool level. Pressurization of the drywell forces the water level inside the drywell lower until the first horizontal vent is exposed, at which point steam can be vented to the suppression pool. As the pressure in the drywell increases further, the water level decreases in the drywell until more of the horizontal vents are uncovered, increasing the steam injection rate into the suppression pool as needed. This removes the need for vacuum breakers between the drywell and the rest of containment since the system will naturally equalize the pressure throughout.

2.3. Justification for Designing Facility to Reflect Mark I Containment Design

While the BWR Mark I containment is the oldest BWR containment design still in service in the United States and does not represent the state-of-the-art engineering design, it is the most prevalent with 23 of the 32 BWR power units in operation in the United States having Mark I containments [9] [10]. Furthermore, Fukushima Daiichi units 2 and 3 were both BWR units with Mark I containment [11]. Since the detailed accident progression for these two units, including the RCIC system's performance, are well documented, the Mark I containment is an advantageous configuration to investigate.

2.4. RCIC System Operational Limits

The operational limits of the RCIC system depend on three primary pieces of equipment. The RCIC turbine, the suppression pool, and the RCIC pump. If any of these three pieces of equipment are compromised, it will be impossible for the RCIC system to continue supplying cooling water to the reactor pressure vessel.

The RCIC turbine is a GS-series Terry steam turbine, which is an impulse-type turbine that resembles a simple water wheel. Each RCIC system will use either a GS-1 or GS-2 Terry turbine, depending on their flowrate needs. The GS-1 model has 5 steam inlet nozzles along the bottom half of the casing, while GS-2 models have 10 steam inlet nozzles spaced around the entire casing [12]. These non-condensing turbines are not exceptionally efficient since they do not harness the steam's latent heat, but when the goal is to consistently and reliably provide cooling water to the reactor pressure vessel under non-ideal circumstances, turbine efficiency is not a high priority. Terry turbines

excel in their reliability and ruggedness; Terry turbines have even been shown to perform admirably when subjected to two-phase flow and air/water mixtures [13]. While they are quite versatile, the RCIC turbine does have some limitations. The GS-series turbines are designed to operate at a nominal rotational speed of 4030 rpm, with a minimum speed of 1000 rpm. The turbine trip mechanism is set to disengage the turbine if the rotational speed exceeds 4600 rpm [14]. An additional concern with Terry turbines during prolonged operation is the lubricating oil. A combination of prolonged increased oil temperature and exposure to moisture has the potential to degrade the oil's lubricating ability [15], which could result in turbine shaft seizure and remove the turbine from operation. Although the turbine oil is typically actively cooled during operation, in a loss of power situations the temperature could rise considerably over time which promotes oil degradation [16] [17]. Finally, although it is unlikely to damage the turbine, increased back-pressure or decreased supply pressure can affect the amount of power the turbine can apply to the RCIC pump, thus reducing the amount of cooling water supplied to the reactor pressure vessel.

The suppression chamber operating limits differ depending on the containment design. For the Mark I and Mark II containments, the suppression chamber serves as a pressure boundary, while in the Mark III containment the suppression pool is open to the containment building atmosphere. The Mark I design pressure is 60 psig, while the Mark II design pressure is 45 psig [18]. In theory, with all incoming steam being condensed in the suppression pool, the increase in suppression chamber pressure should be due primarily to the temperature increase of non-condensable gases in the airspace.

Application of the ideal gas law suggests that for the airspace pressure to increase from atmospheric pressure to 45 psig would require the air temperature to far exceed the boiling point of the water in the suppression pool, meaning the suppression chamber should remain stable if all the steam is being condensed. Suppression pool damage has been seen in cases where the suppression pool nears its saturation temperature leading to incomplete steam condensation that results in rapid pressure increases [7]. Effective condensation of steam from safety relief valves discharging into the suppression pool at high temperatures is strongly dependent on the sparger design and pool mixing [7].

The RCIC pump itself is built to withstand high temperatures and pressures in excess of anything it would experience during RCIC system operation. However, the water inlet temperature can lead to other problems for the pump. For proper operation of the RCIC pump, the inlet water must have sufficient Net Positive Suction Head. As the inlet water temperature increases throughout RCIC system operation, and approaches the saturation temperature, the likelihood of cavitation inside the RCIC pump increases. Cavitation inside the pump leads to poor pump performance, as well as lasting damage if cavitation is severe or continues for an extended period.

2.5. Previous Experimental Studies on Suppression Pool Behaviors during RCIC System Operation

A PhD dissertation by Matthew Alan Solom, “Experimental Study on Suppression Chamber Thermal-Hydraulic Behavior for Long-term Reactor Core Isolation Cooling System Operation” [19] details a previous experimental investigation performed in this lab of the development of thermal stratification in a BWR Mark I

suppression pool. Results from that investigation have shown that thermal stratification is most significant in the vertical direction, and that suppression tank pressure has a strong effect on the extent of stratification [20]. However, there were some limitations with the experimental facility used. Coarse thermal resolution within the pool limited the ability to monitor the development of the thermal layer, and the previous facility did not have a Terry Turbine as used in the RCIC system. Instead of a turbine, an orifice plate and a loop in the piping were used to simulate the turbine's effects on the steam.

The current work builds upon the limitations recognized during the previous experimental investigation by improving the number and placement of thermocouples used to measure thermal stratification in the pool. Based on the results of the previous work, care was taken to maximize the vertical resolution of temperature readings. Additionally, a ZS-1 Terry turbine has been acquired and is included in the experimental facility to maximize the work's fidelity to conditions found in a power plant RCIC system.

3. EXPERIMENTAL FACILITY

The experimental facility for this work builds upon a previously existing setup in the NHTS lab at Texas A&M University. That facility consisted of a steam generator, water deionization system, a 5-stage centrifugal pump, air compressor, piping and instrumentation, and a large cylindrical tank referred to here as the suppression chamber Analog. Additional pieces of equipment that were incorporated to the facility for the purposes of this work include:

- A ZS-1 Terry Turbine
- Automated Control Valves
- Additional instrumentation
- Heat Rejection System including a heat exchanger, cooling tower, water treatment station, and a water storage tank.
- A new data acquisition system

Detailed P&IDs for the experimental facility are found in Appendix A. What follows are descriptions of the main pieces of equipment used in the facility.

3.1. Water Deionization System

To prevent corrosion and reflect conditions in a suppression pool as found in a nuclear power plant, the water used for these experiments must be purified prior to introducing it to the suppression chamber analog. This is accomplished by running water through Culligan® mixed-bed filtration tanks, which are capable of filtering approximately 350 gallons of water before they need to be replaced. These tanks direct

water through an activated charcoal filter, a cartridge filter, two mixed bed resin tanks, and a final cartridge filter. The filtration tanks have an indicator light (Figure 3.1) that turns red when it is time to exchange the tank. In this facility, deionization tanks are installed on a mobile cart (Figure 3.2) that allows deionized (DI) water to be introduced at various points throughout the facility. The two main injection locations are the steam generator and the pump outlet manifold connected to the suppression chamber analog. The DI water is also used to fill pressure instrument lines to avoid subjecting those instruments directly to steam.



Figure 3.1. Culligan® water filtration system indicator light. Turns red when the tank needs to be replaced.



Figure 3.2. Culligan® DI water filtration system on mobile cart.

3.2. Suppression Chamber Analog

The suppression chamber analog represents the suppression pool as found in BWR Mark I containment. In contrast to the toroidal shape of an actual Mark I suppression pool used in a nuclear power plant; the suppression chamber analog is a horizontally oriented cylindrical vessel. Originally constructed in 1952 by Wyatt Metal & Boiler Works, it is made of 304 stainless steel, and rated to 88 psi at 400°F. The main cylindrical body of the vessel measures 96” from weld to weld with an inner diameter of 59”. Each head-cap adds 3” to the straight length of the body before beginning to curve, totaling 102” of straight cylindrical shape. The internal distance between head-caps is approximately 122”. Overall, the vessel has the capacity to hold approximately 1400 gallons of water, making it well-suited to serve in a steam suppression capacity for this experiment. For the purposes of this description, the front of the vessel will be considered the head which has the ASME-API stamped plate on it. The vessel has a total of ten penetrations. Four identical ¾” NPS flanges are located on the front, arranged in a rectangle measuring 18” horizontally and 52” vertically. Each of these flanges extends out approximately 6” from the face of the vessel. Two of these flanges serve as connection points for a water level meter, while the other two are used for water recirculation. The vessel drain is a 6” NPS flange located on the bottom of the tank, near to the front of the vessel, which supplies water to the pump inlet manifold. This flange is modified to admit 12 thermocouples and has three penetrations for future use. There are four penetrations on the top of the tank, which are in a line down the center of the tank. Starting from the front of the tank: A 1.5” NPS flange; a 20” ASME blind flange which

is removed to access the tank internals during construction; a 2” NPS flange which serves as a secondary route for steam to enter the pool, with tubing that leads to a tee placed approximately 3 inches off the floor of the tank; and a 4” NPS flange which is used to introduce 60 thermocouples to the pool, as well as cooled water from the heat rejection system. Finally, the rear face of the tank has a 6” NPS flange centered near the top, which serves as the primary steam injection port. Figure 3.3 shows the suppression chamber analog in its current condition with associated piping. The suppression chamber analog is insulated with 2” of fiberglass insulation around the main body, while the lid is insulated with a 2” slab of mineral wool.



Figure 3.3. Suppression chamber analog with associated piping.

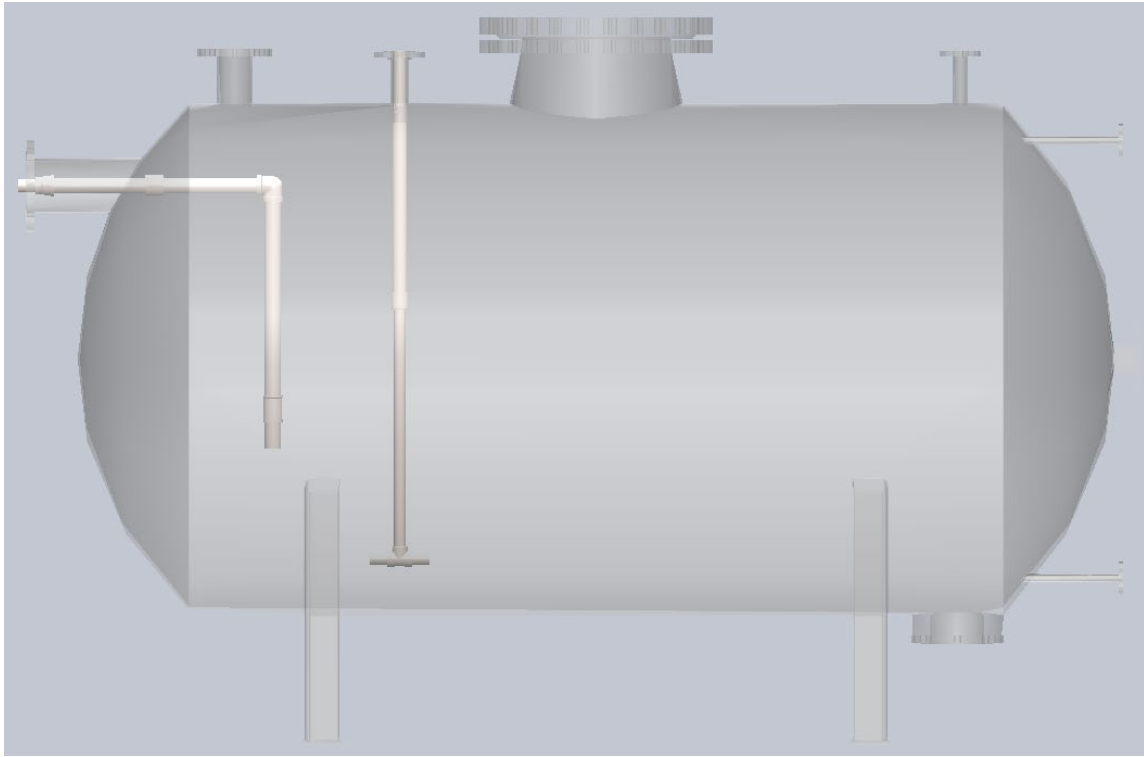


Figure 3.4. CAD model of the suppression chamber analog. Transparent to show internal spargers.

As shown in Figure 3.4, there are two spargers installed in the suppression chamber analog that can be used to inject steam into the suppression pool. The turbine exhaust sparger, which is used in this work, is the one on the left which terminates in an open-ended pipe, like the sparger used in Fukushima Daiichi Unit 2. The other sparger, meant to represent safety relief valve spargers as found in BWR containment, are unused during this work. The suppression chamber analog is filled with water to an elevation of approximately 31 inches, which corresponds to a turbine exhaust sparger outlet depth of 12 inches from the water surface. While the suppression pool water level is measured

electronically, in case of instrument failure the suppression chamber Analog has been equipped with a visual water level indicator as shown in Figure 3.5. This water level meter is essentially a stainless-steel pipe with a magnetic float inside which follows the water level. A small orange indicator shuttle outside the pipe follows the magnetic float, providing a reliable method for operators to check the water level without introducing a sight-glass into the suppression chamber analog which would be a potential safety risk during pressurized tests. The water level is maintained at approximately 31 inches during tests, which keeps the turbine exhaust sparger outlet submerged by 12 inches of water.



Figure 3.5. Suppression chamber analog water level meter.

3.3. Steam Generator

One of the key pieces of equipment in the facility is the steam generator, which plays the role of the reactor pressure vessel by supplying pressurized steam to the RCIC facility. The pressure vessel used for the steam generator is a Kennedy Tank and Manufacturing Company vessel with a maximum operating pressure of 135 psig at 350 °F. The vessel's total capacity is approximately 130-135 gallons. The steam generator resembles a 60-inch-tall vertical cylindrical vessel that is 24 inches in diameter, with a dome on the top and bottom that bring the total height to approximately 72 inches. The entire vessel is supported by 4 legs that hold the vessel approximately two feet off the floor. The cylindrical body of the steam generator is insulated by two inches of rigid mineral wool insulation while the top and bottom are insulated using multiple layers of fiberglass sheets that are fitted to the vessel's shape. The steam generator vessel can be seen in **Error! Reference source not found..**



Figure 3.6. Steam generator vessel.

There are several penetrations in the top and sides of the vessel for instrumentation, pressure relief valves, water return and steam outlet. Additionally, 6 penetrations in the sides of the vessel are fitted with flanges to admit electric heaters like the one shown in Figure 3.7. Heaters are shown as installed in Figure 3.8.



Figure 3.7. 50 kW heater prior to installation into the steam generator.

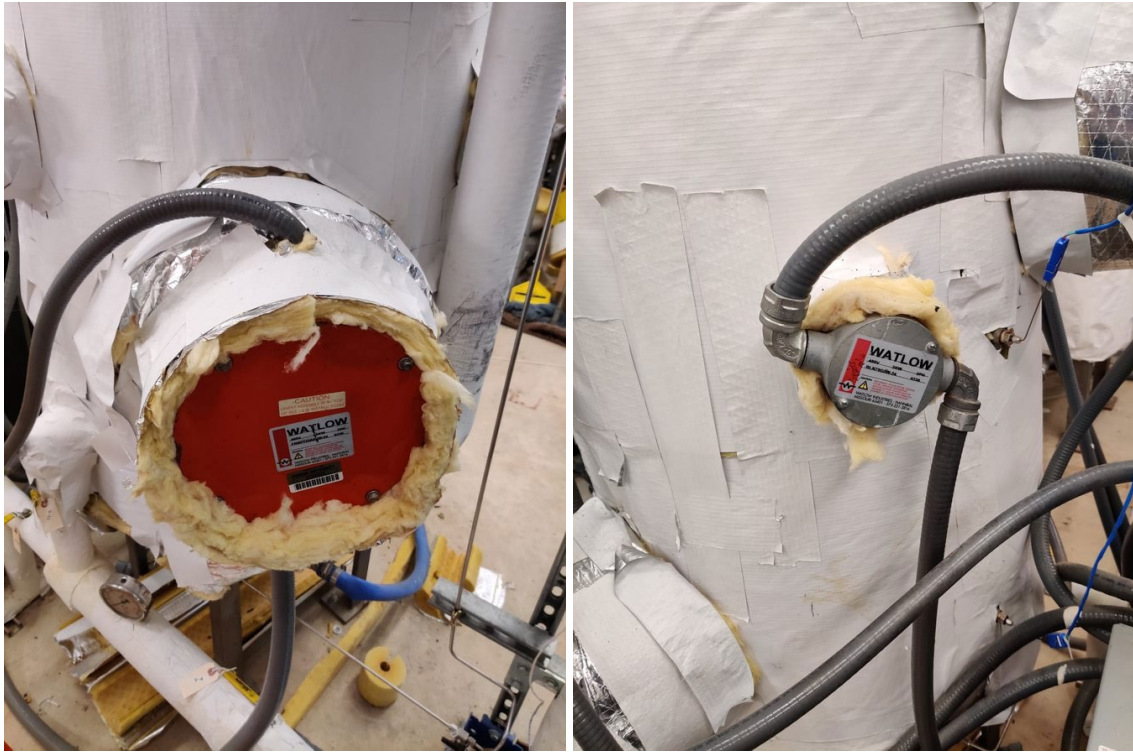


Figure 3.8. One of the 50kW heaters (Left) and one of the 2kW heaters (Right) on the steam generator.

Two of the heaters are each capable of producing either 25kW or 50kW. One heater has finer control, capable of producing 50 kW controlled to the nearest 6.25 kW. There are three smaller heaters, one of which produces 3 kW while the other two produce 2kW each. In total, the steam generator has the capacity to constantly produce 157 kW, controllable within 2 kW. The steam generator control board is shown in Figure 3.9.



Figure 3.9. Steam Generator Control Board.

As a backup to electronic water level measurements, a physical water level meter is attached to the side of the steam generator body, like the one installed on the suppression chamber analog. This water level meter functions using a magnetic float inside a stainless-steel pipe to follow the water level. A small orange shuttle indicator outside the pipe follows the magnetic float. This allows operators to visually check the water level without a sight-glass into the pressurized environment. The water level meter is shown in Figure 3.10.



Figure 3.10. Steam generator water level indicator.

3.4. ZS-1 Terry Turbine

One of the additions made to the facility for this work is a ZS-1 Terry turbine, which is a smaller scale turbine of the same design as the GS-series turbines used in the full-scale RCIC system. The wheel diameter for the ZS-1 is 18", compared to the 24" wheel used in the GS series turbines. In contrast to the GS-series turbines which employ multiple steam inlet nozzles, the ZS-1 used in this facility only has one inlet steam nozzle. While the RCIC turbine in a full-scale RCIC system would be coupled to a multi-stage pump, the ZS-1 turbine in this facility is coupled instead to a dynamometer which can be used to measure the torque provided by the turbine as well as control the turbine speed. The ZS-1 Terry turbine standard rotation rate is 3600 rpm, and the trip speed is 4100 rpm. The trip mechanism on this unit is damaged and does not reliably close the inlet steam valve at 4100 rpm every time. As a fail-safe, the process control system used in the facility is set to close the upstream main steam valve when the turbine rotational speed reaches 4000 rpm. While the turbine casing is generally leak-tight, when operated with downstream pressures in excess of 15 psig, steam has been seen to leak from the shaft seal condensate drainage lines. As a safety precaution, the condensate drainage lines are connected via high-temperature hose to a drum of water to condense any leaked steam. Before operation, the oil level in the turbine oil wells should be checked using the level indicators on the side of the casing. If the oil level is too low, damage to the shaft or bearing can occur, and if the oil level is too high, oil could spill out during the test due to thermal expansion and agitation. The ZS-1 turbine is shown as installed in the facility in Figure 3.11.

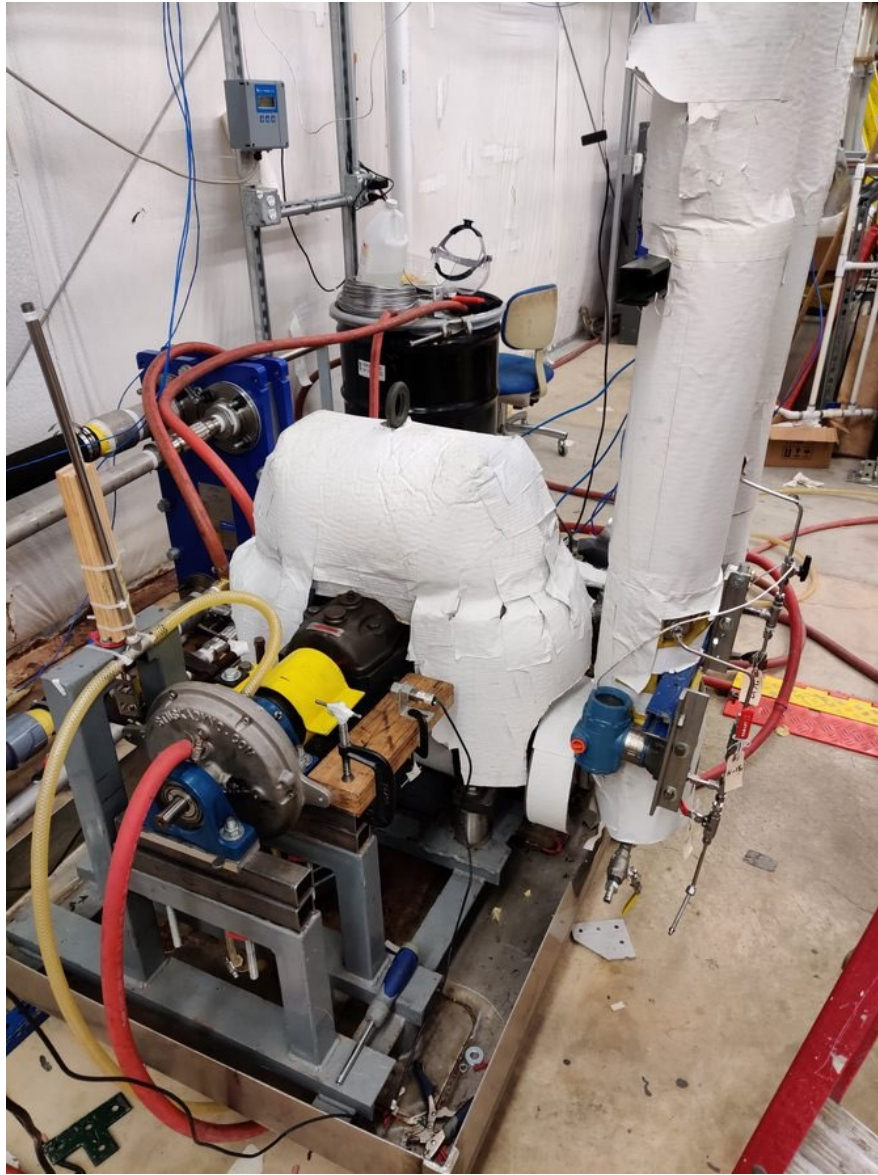


Figure 3.11. ZS-1 Terry Turbine with insulation coupled to dynamometer.

3.5. Flowmeters

This experimental facility is fitted with two flowmeters: One Foxboro 84W flowmeter for measurement of steam flow rates, and one Azbil (get model number) magnetic flowmeter for liquid flowrate measurement.

3.5.1. Foxboro Vortex Flowmeter

The flowrate of steam in the facility is measured by a Foxboro 84W vortex flowmeter with an accuracy of $\pm 1.0\%$ for steam readings [21]. Vortex flowmeters operate based on the Von Karman effect, whereby repeating vortices are produced by a liquid or gas flowing past a bluff body. In the case of the vortex flowmeter, this bluff body is the shedder bar. The repeating vortices cause oscillations in a small measuring element at a frequency that is directly proportional to the velocity of the flowing fluid. This velocity multiplied by the flow area of the meter gives the volumetric flowrate [22]. Additionally, by specifying the fluid parameters such as density and temperature, the Foxboro 84W can calculate the mass flow rate.

Each Foxboro 84W is calibrated with water to identify the proportionality constant specific to the device, referred to as the K-factor. Vortex flowmeters are resilient to degradation, such that regular use will not affect the K-factor of the device, meaning it does not need to be re-calibrated regularly in the absence of significant damage [23]. The device outputs a 4-20mA signal scaled from 0 to an upper-range value chosen by the user. Since the flowmeter is calibrated using water at room temperature, care must be taken when measuring flows at significantly higher temperatures due to thermal expansion of the shedder bar which affects the K-factor. While the device is

configured to account for this expansion using the inputted fluid temperature, in cases such as this experiment where the steam temperature can vary throughout the test, it is important to account for changing temperature in real time to minimize error. Since the device settings cannot be changed instantaneously in real time, the values received from the device need to be adjusted to account for the current temperature using Equation (3.1) where K_{ref} is the reference K-factor, α is the thermal expansion coefficient, T is the current temperature, and T_{ref} is the reference calibration temperature.

$$K = K_{ref} * (1 - 3 * \alpha * (T - T_{ref})) \quad (3.1)$$

3.5.2. Azbil Magnetic Flowmeter

Water flowrates throughout the facility are measured using Azbil MagneW 3000 PLUS electromagnetic flowmeter converters, model number MGG14C-MH4H-1B1N-YAH coupled to MGG180-015P21LS5AAA-XX-Y flow detectors [24]. The flow detector transmits a signal to the converter which interprets the signal into the desired flowrate units. The converter also outputs a 4-20mA signal that can be interpreted by the DAQ system for data logging. Azbil MagneW 3000 PLUS converters are powered by standard 100 to 120 VAC power supplies and are acceptable for use in ambient temperatures between -25 °C and 60 °C. An LCD screen displays the current flowrate in the desired units along with the percentage of the upper range value. Reading accuracy is dependent on the detector size, setting range velocity, and the current flow velocity. For detectors on a ½-inch line, the accuracy is defined by the ranges displayed in Table 3.1.

Table 3.1. Accuracy of Azbil MagneW 3000 PLUS converter in combination with a detector <Size 2.5 to 15 mm (0.1 to ½ inch)>. Information from [24]

V_s = Velocity of setting range

V _s (m/s)	Velocity during measurement ≥ V _s × 40%	Velocity during measurement ≤ V _s × 40%
1.0 ≤ V _s ≤ 10	±0.5 % of rate	±0.2% of V _s
0.1 ≤ V _s ≤ 1.0	±(0.1/V _s +0.4) % of rate	±0.4 (0.1/V _s + 0.4) % of V _s

The setting range for the flowmeters used in this facility is 15 GPM, which corresponds to a velocity of 4.8 meters-per-second. In all tests included in this work, the maximum flowrate recorded is less than 40% of the URV, so the accuracy in flowrate measurement for flowmeters in this work is ±0.2% of URV.

3.6. Control Valves

One significant improvement to the testing facility as part of this work is the inclusion of computer-controlled valves that allow for automatic control of steam and water flows in the facility. Two of these valves are used for this work, one of which controls the flow of steam from the steam generator into the main steam line, while the other controls the flowrate of water returning to the steam generator.

3.6.1. Main Steam Control Valve

The steam flow rate in the facility is controlled by a Masoneilan 88-21124 equal percentage air-to-open steam globe valve on a 1.5-inch pipe, pictured in Figure 3.12. The rated CV for the valve when fully open is 18; the CV curve is shown in Figure 3.13. The

valve actuator is linearly controlled by a 4-20mA signal and requires an air supply pressure of 55psig. The valve should not be operated with a supply pressure higher than 60 psig. The supply pressure can be adjusted with the attached pressure regulator to maintain a supply pressure of 55 psig despite a higher upstream air supply pressure.



Figure 3.12. Masoneilan 21124 Top-Guided Globe Valve, used to control steam flow rate.

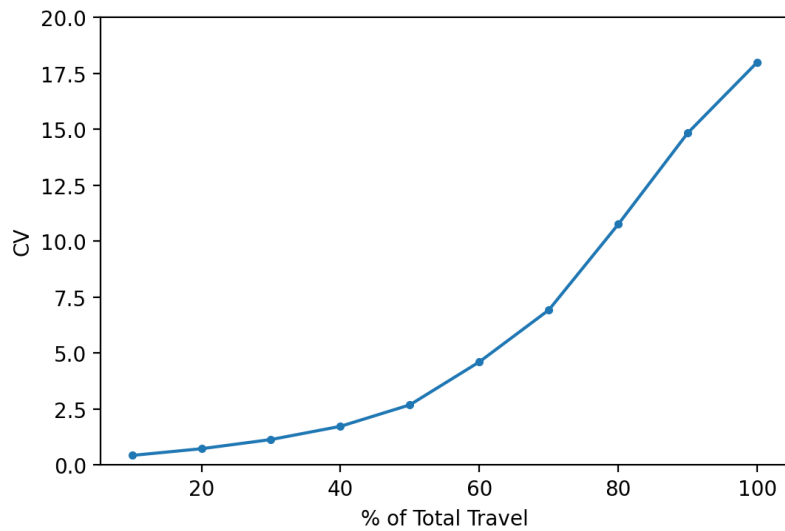


Figure 3.13. CV curve for equal-percentage Masoneilan 88-21124 globe valve. Data from [25].

3.6.2. Feedwater Control Valve

The flowrate of water returning to the steam generator from the suppression pool is controlled by a Fisher D041TV1 DN 25 GX equal percentage air-to-open globe valve with a 9.5 mm port diameter [26], pictured in Figure 3.14. The rated CV for the valve when fully open is 3.57 [27]; the CV curve is shown in Figure 3.15. The valve is operable in the temperature range $-20\text{ }^{\circ}\text{F}$ to $450\text{ }^{\circ}\text{F}$. Water temperatures in the line leading to this valve will be limited to $250\text{ }^{\circ}\text{F}$ by temperature limitations of the feedwater pump, so these temperature limitations will be no issue in this facility. The actuator can use air supply pressures up to 87 psig. The supply pressure can be adjusted with the attached pressure regulator to maintain a supply pressure below 87 psig despite a higher upstream air supply pressure.



Figure 3.14. Fisher D041TV1 DN25 GX air-to-open globe valve. Used to control the flowrate of water returning to the steam generator.

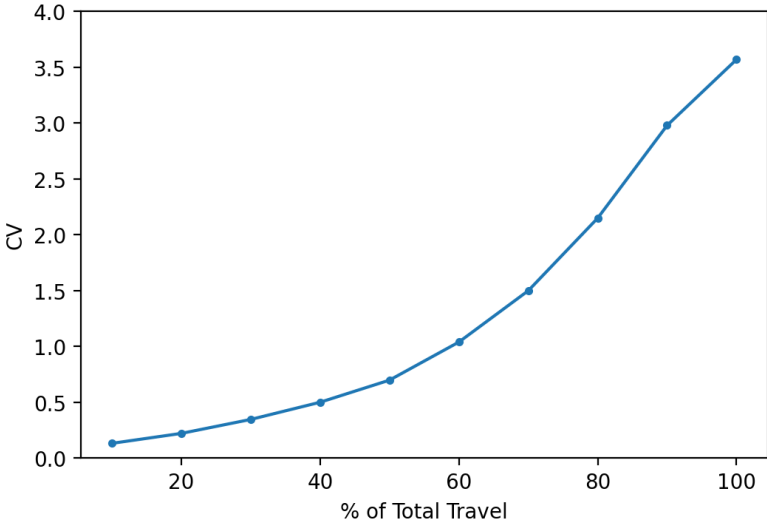


Figure 3.15. CV curve for Fisher D041TV1 DN 25 GX air-to-open globe valve. Data from [27]

3.7. Thermocouples

All thermocouples used in this experiment are Omega type T with special limits of error for accuracy of ± 0.5 °C. In total, 107 thermocouples are installed throughout the facility and are all connected to the data acquisition system via type T thermocouple extension wire from Omega. Any thermocouple whose reading will be used for data analysis is connected via extension wire specifically designed to meet special limits of error requirements. Other thermocouples which are present solely for operator guidance are connected via standard type T extension wire.

Of the 107 thermocouples, 72 are installed in the suppression pool and measure the temperature at various locations throughout it; 38 are spaced throughout the pool to monitor bulk temperature stratification in the vertical, lateral, and axial directions, 32 are tightly arranged near the turbine exhaust to monitor the development of a thermal plume throughout the test, 1 is installed inside the turbine exhaust line, about 4 inches from the outlet, and the final thermocouple in the suppression pool is in the airspace. These thermocouple locations are shown in Figure 3.16, Figure 3.17, and Figure 3.18 . Since the greatest level of thermal stratification is expected to exist in the vertical direction, the suppression pool is most finely instrumented vertically, with a thermocouple spacing of 4 inches. To monitor any axial stratification that may appear, an array of vertically spaced thermocouples is placed at three axial locations in the pool: near each head-weld and at the pool center. Additionally, a single thermocouple is placed on the tank centerline at intervals of 1 foot along the length of the pool. Lateral thermal stratification is not expected to be appreciable in this configuration, so each main thermocouple array

only measures the temperature at 3 lateral locations: on the centerline, and 1 foot to either side. A channel strut structure was fashioned of stainless steel which serves as an attachment point for a web of stainless-steel wire that is used to fix thermocouples in place.

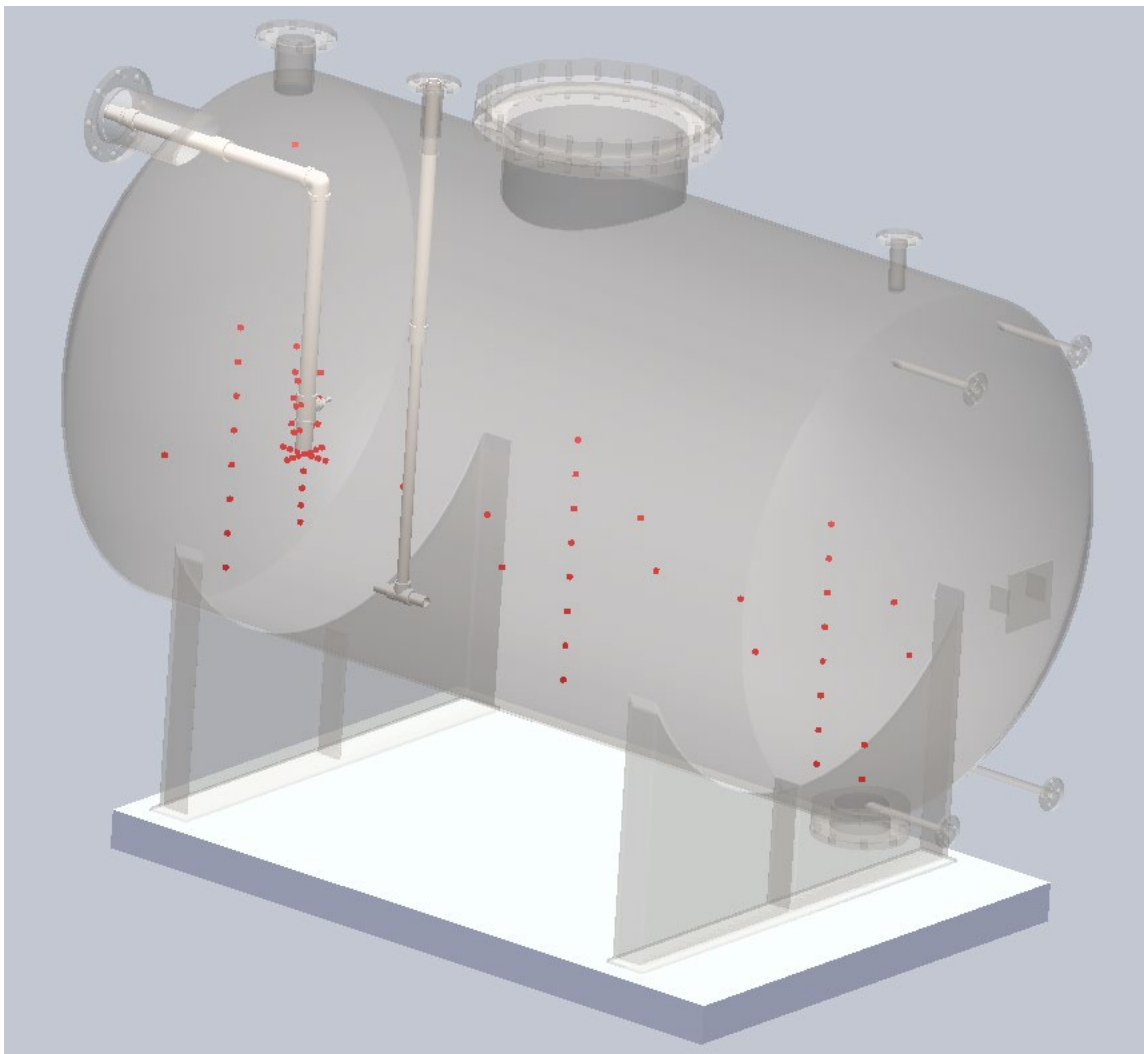


Figure 3.16. CAD model of the suppression chamber analog with thermocouple locations marked in red.

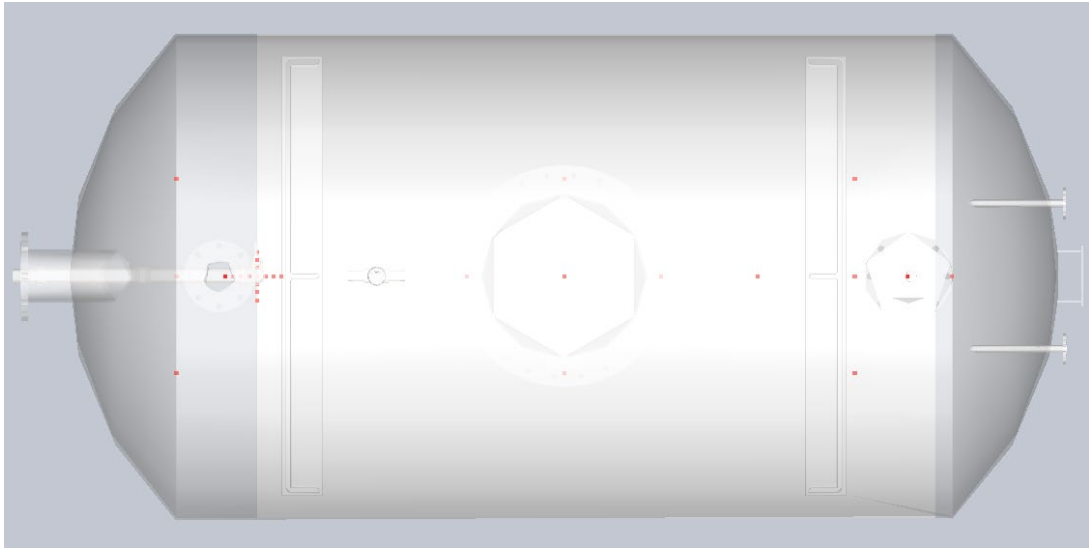


Figure 3.17. Top view of suppression chamber analog CAD model with thermocouple locations indicated in red.

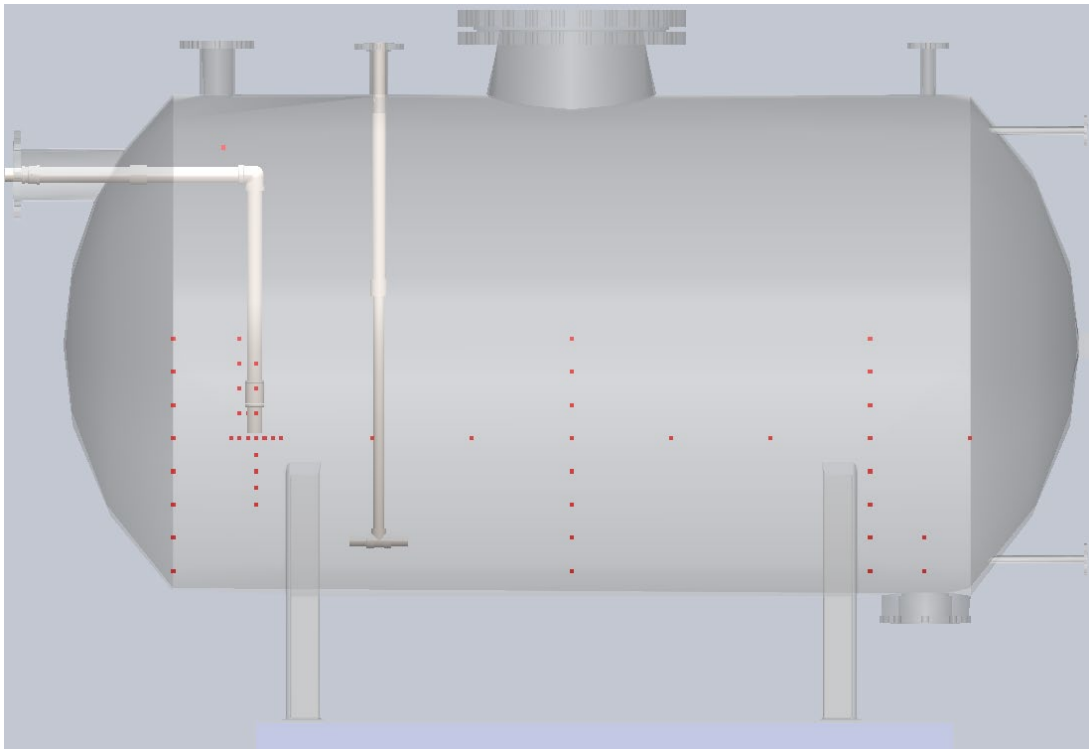


Figure 3.18. Side view of suppression chamber analog CAD model with thermocouples locations indicated in red.

3.8. Pressure Transmitters

Four different models of pressure transmitters are present in the facility. Emerson 3051CA absolute pressure transmitters measure the steam pressure at the inlet and outlet of the ZS-1 turbine, and the lab atmospheric pressure. Honeywell STA 940 absolute pressure transmitters monitor the steam generator pressure, main steam line pressure near the flow rate measurement site, and the suppression chamber pressure. Honeywell STD 924 differential pressure transmitters are used to monitor the water level in the steam generator and suppression chamber, as well as the differential pressure between the suppression chamber and the turbine exhaust line. Finally, Omega PX309-V150-GI pressure transmitters measure the pressure at the inlet and outlet of each pump in the facility. All pressure instrument calibrations were performed in-house with a Druck DPI 612. Each pressure transmitter except for the Omega PX309's is thermally isolated from the main process steam by a length of exposed steel tubing filled with water, which is assumed to remain at approximately room temperature. All four of the pressure instrument models used in this facility output a 4-20mA signal which is then converted back to a pressure reading based on the range of the instrument.

The uncertainty in pressure measurement of all pressure transmitters is dependent on the applied temperature, and for differential pressure transmitters the uncertainty is further dependent on the applied pressure. The lab temperature has been seen to deviate by up to $7^{\circ}C$ so this temperature deviation will be used to calculate the maximum expected uncertainty for each device. The reference uncertainty from the manufacturer is combined with the temperature and pressure effects with Equation (3.2) to produce an

overall uncertainty for the pressure instrument. Table 3.2 summarizes all pressure transmitters in the facility that are relevant to operations for this work.

$$u = \sqrt{u_{ref}^2 + u_{temp}^2 + u_{pressure}^2} \quad (3.2)$$

Table 3.2 Summary of pressure transmitters in the facility

Model	Serial No.	Location	Range	Accuracy
Emerson 3051CA2A22A 1AM4Q4HR7	108381	Turbine Outlet	0 – 150 psia	±0.082 psia
Emerson 3051CA2A22A 1AM4Q4HR7	108382	Turbine Inlet	0 – 150 psia	±0.082 psia
Emerson 3051CA1A22A 1AM4Q4HR7	108383	Open to atmosphere	0 – 30 psia	±0.016 psia
Honeywell STA 940	0149 10556305014	Steam Generator	12 – 150 psia	±0.173 psia
Honeywell STA 940	0150 10556305015	Main Steam Line	12 – 135 psia	±0.155 psia
Honeywell STA 940	0521C2696828001 001	Suppression chamber	12 – 110 psia	±0.126 psia
Honeywell STD 924	0414 C2537240003001	Suppression chamber Level Indicator	0 – 100 in H_2O	±0.108 in H_2O
Honeywell STD 924	0521- C2696828002001	Steam Generator Level Indicator	0 – 100 in H_2O	±0.109 in H_2O
Honeywell STD 924	0615- C2817149001001	Differential pressure between turbine outlet and suppression chamber	-20 – 400 in H_2O	±0.452 in H_2O
Omega PX309- V150-GI	100617D054	Feedwater pump inlet	-15 – 150 psig	±1.0%
Omega PX309- V150-GI	100617D052	Feedwater pump outlet	-15 – 150 psig	±1.0%

3.8.1. Emerson 3051CA

The Emerson 3051CA absolute pressure transmitter has a rated accuracy of $\pm 0.04\%$ span. One additional source of uncertainty for these Emerson pressure transmitters is the applied temperature effect which amounts to $\pm(0.025\% \text{ URL} + 0.125\% \text{ span})$ per 28°C deviation from reference temperature [28]. The 7°C temperature deviation observed in the laboratory gives a nominal ambient temperature effect of $\pm 0.00625\% \text{ URL} + 0.0313\% \text{ span}$). See Table 3.2 for calculated total uncertainty for each transmitter.

3.8.2. Honeywell STA 940

The Honeywell STA 940 absolute pressure transmitter of the ST3000 series 900 Honeywell smart transmitter family has a rated accuracy of $\pm 0.1\%$ of the greater of the calibrated span or upper range value. One additional source of error comes from ambient temperature effects which amounts to $\pm 0.25\% \text{ span}$ per 28°C deviation from reference temperature [29]. The 7°C temperature deviation observed in the laboratory gives a nominal ambient temperature effect of $\pm 0.0625\% \text{ span}$. See Table 3.2 for calculated total uncertainty for each transmitter.

3.8.3. Honeywell STD 924

The Honeywell STD 924 differential pressure transmitter of the ST3000 series 900 Honeywell smart transmitters has a rated accuracy of $\pm 0.075\%$ of the greater of the calibrated span or upper range value. This accuracy is also dependent on the applied temperature and pressure. The effect due to temperature is $\pm 0.3\%$ of span per 28°C deviation from reference temperature. Based on the maximum room temperature

deviation expected, the maximum uncertainty due to ambient temperature change is $\pm 0.075\%$ span. The effect due to applied pressure is $\pm 0.3\%$ span per 1000 psi [30]. For the transmitter installed to monitor the steam generator water level, the maximum applied pressure during tests is 80 psig, corresponding to an added uncertainty of $\pm 0.024\%$ span. The other two transmitters, which are connected to the suppression chamber, will be exposed to a maximum applied pressure of 60 psig, which corresponds to an added uncertainty of $\pm 0.018\%$. See Table 3.2 for calculated total uncertainty for each transmitter.

3.8.4. Omega PX309-V150-GI

The Omega PX309-V150-GI is a compound gage pressure instrument capable of measuring pressures ranging from -15 psig (full vacuum) to 150 psig and operates in temperatures ranging from -20 to 80°C. While liquid temperatures in this facility do exceed 80°C, each PX309 pressure transmitter is connected to the piping system via a length of bare stainless-steel $\frac{1}{4}$ " tubing which limits the amount of hot water that reaches the instrument. Due to the small flow diameter of the tubing, and the lack of bulk flow through the tubes, the water reaching the PX309 is sufficiently cool. The rated accuracy under calibration conditions is $\pm 0.25\%$ of the measured value, and the manufacturer provides an accuracy rating of $\pm 1.0\%$ of the measured value to compensate for any temperature effects inside the operating range. Since the PX309 transmitters will only be used for operator awareness during the experiment and their measurements will not be reflected in resulting data, this relatively large uncertainty compared to other transmitters

is acceptable. To protect the PX309 transmitters from potential water hammer damage, each transmitter is equipped with a pressure snubber to dampen rapid pressure waves.

3.9. Feedwater Pump

The pump used to return water from the suppression chamber to the steam generator is a Dayton 5UXF5 5-stage centrifugal pump, picture in Figure 3.19, and serves as an analog to the turbine-driven RCIC pump. It is coupled to a 0.75 hp electric motor powered by 115 VAC and has a maximum pressure boost of 93 psi [31]; the associated pump curve is shown in Figure 3.20. Since the motor speed is non-variable, the water flow rate will be controlled using a downstream throttling valve. Both the inlet and outlet are sized for $\frac{3}{4}$ -inch NPT pipe. The rated maximum operating temperature for the pump is $194^{\circ}F$ as delivered. This temperature limit is primarily due to the Buna-N mechanical seal included in the factory configuration. In this facility, the Buna-N seal has been replaced with a Viton seal which is rated to operate up to $250^{\circ}F$ for continuous operation. Testing has shown the pump operates effectively up to $250^{\circ}F$ with the Viton seal installed. The suction chamber and housing material of the pump are cast iron, while the impeller, bowl, and shaft are 304 stainless-steel. Since everything else in the system is made of 304 stainless-steel, the presence of cast iron in the pump presents a risk of corrosion over long operating periods at elevated temperatures. The pump should be checked for signs of corrosion regularly.

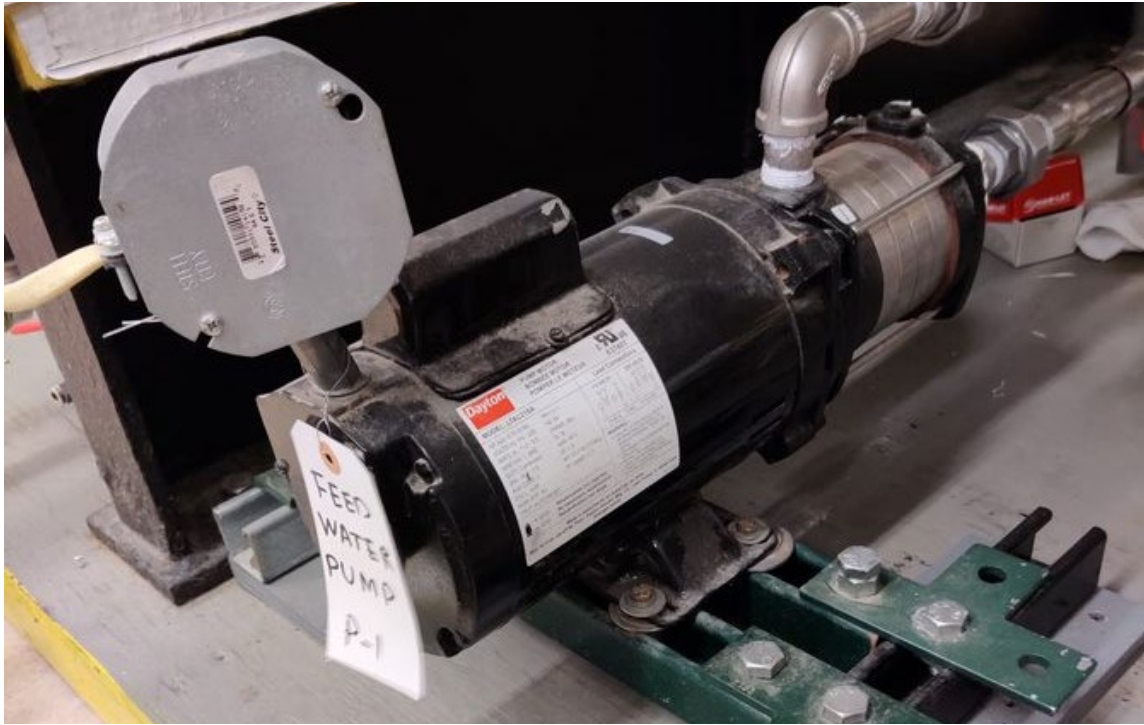


Figure 3.19. Feedwater Pump. Dayton 5UXF5 5-stage centrifugal pump coupled to an electric motor.

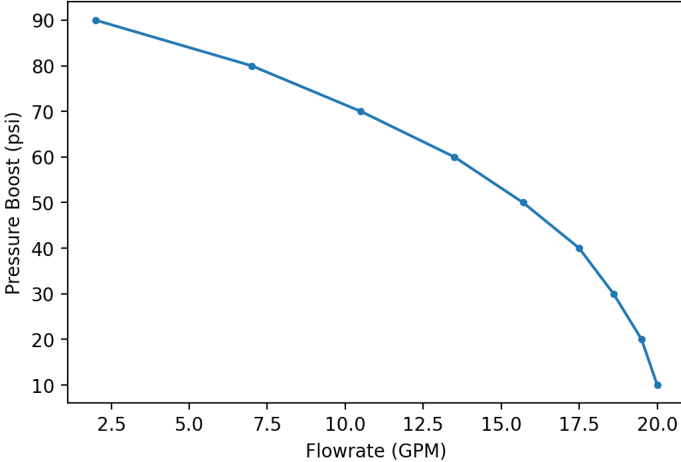


Figure 3.20. Pump Curve for Dayton UXF5 5-stage centrifugal pump. Data from [31].

3.10. Heat Rejection System

Tests for this work monitor the behavior of the water in the suppression chamber as the bulk temperature increases from near room temperature to near saturation conditions. Due to the insulation on the suppression chamber, allowing the suppression chamber to return to room temperature without active cooling would require a minimum of a week between tests for the water to cool. Additionally, some of the pressurized tests involve heating the water past its atmospheric pressure boiling point. To avoid releasing large amounts of steam, which is simultaneously a safety concern and a waste of deionized water inventory, the water must be cooled below 100°C before depressurizing the suppression chamber. To accelerate suppression chamber cooling and maintain the suppression chamber near room temperature during the system heat up, the Heat Rejection System (HRS) was designed and installed in the facility. The HRS consists of a plate heat exchanger, an induced draft cooling tower, two water pumps, over 150 feet of pipe, a considerable physical support structure, and instrumentation. While its actual performance depends on the outdoor temperature, it is designed to continually remove 120 kW of heat from the suppression chamber and can reduce the suppression chamber temperature from 100 °C to 40 °C in approximately 2 hours.

3.10.1. Heat Rejection System Heat Exchanger

The HRS utilizes a AQ3-MFG plate heat exchanger from Alfa Laval, pictured in Figure 3.21, to remove heat from the primary fluid in the suppression chamber. The heat exchanger is rated to operate from -20 to 350 °F at a maximum pressure of 150 psig. The total heat transfer area is 22.0 ft^2 . The heat exchanger has four flat-face flange

connections sized for 3-inch pipes. Flow is configured for counter-current heat exchange, with the hot, primary coolant flowing from top to bottom, and the cool, secondary coolant flowing from bottom to top.

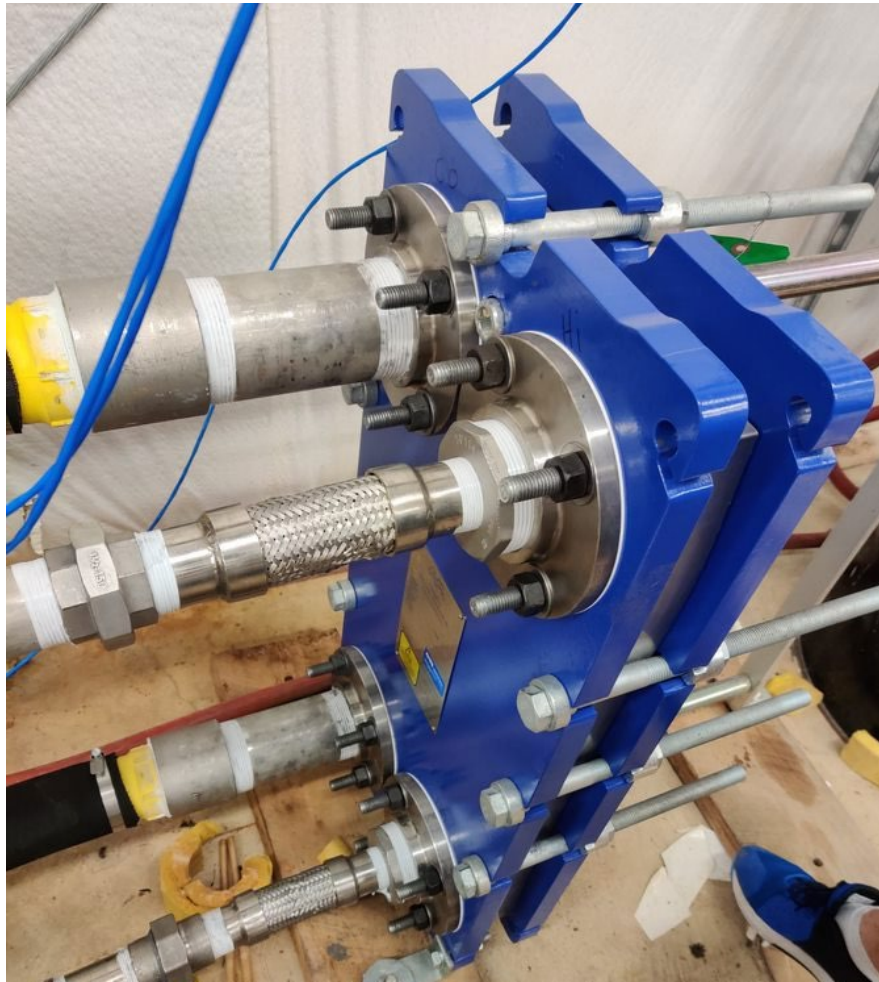


Figure 3.21. HRS Heat Exchanger.

3.10.2. Cooling Tower

To remove heat from the secondary coolant loop, water is pumped through a T-250 cooling tower purchased from Cooling Tower Systems. The T-250 is an induced draft cooling tower with a nominal cooling capacity of 50 tons at 148 GPM. The tower is elevated to allow the water basin to drain by gravity into the HRS water supply tank stored inside the building as shown in Figure 3.22.



Figure 3.22. HRS Cooling Tower.

3.10.3. Heat Rejection System Water Supply Tank

Since the heat rejection system is used discontinuously in this facility, sometimes with weeks passing between tests, a HRS water supply tank was requisitioned for storing cooling water indoors. Indoor storage limits the exposure to wildlife and plant growth during the Summer in addition to avoiding freezing during the Winter. The water supply tank is a 500-gallon HDPE horizontally mounted cylindrical tank, 4 ft. in diameter and 5 ft. in length, with a 20" lid centered on top of the tank. The tank has been modified by adding custom penetrations to meet system requirements. Figure 3.23 shows the tank as installed.



Figure 3.23. Photo of HRS Storage Tank as installed in facility.

The tank is filled with filtered tap water through a 1-inch NPT pipe entering through a 1 $\frac{1}{2}$ -inch penetration at the top of the tank. The flow of water is controlled automatically by a float valve which maintains a water level of approximately 30 inches, which corresponds to 350 gallons. A gate valve upstream of the water filter is available to slow or cut off the water supply if necessary. This configuration allows a maximum flow rate of 10 GPM. Water is drawn out of the storage tank through a 3-inch NPT bulkhead fitting near the bottom of the tank, where it can be routed either to the floor drain or the HRS primary-side pump. To avoid large debris ingress and vortex formation as the water is drawn out by the pump, a water suction manifold was fashioned from a 3-inch pipe with many $\frac{1}{2}$ -inch holes as shown in Figure 3.24. This manifold connects directly to the 3-inch NPT bulkhead.

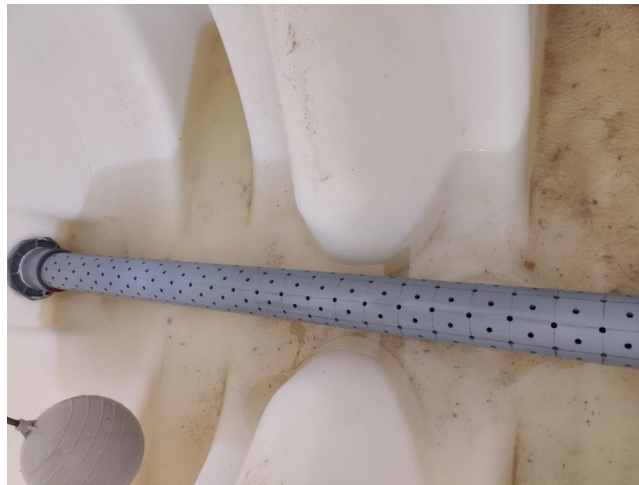


Figure 3.24. Water suction manifold.

Water is returned to the storage tank from the cooling tower through a 3-inch pipe which enters the tank through a penetration approximately 36” from the ground. This pipe has many $\frac{1}{2}$ -inch perforations on the bottom half which allows inlet water to rain down evenly into the storage tank instead of being dumped in a single location which could result in swirling inside the tank. Water swirling has the potential to allow air ingress to the HRS primary-side pump if water levels are low and flow rates are high. The water return line is supported by stainless steel channel strut that enters the tank through a 2-inch hole in the top of the tank as shown in Figure 3.25. Water from the water treatment system is admitted through a 1-inch NPT pipe entering through a $1\frac{1}{2}$ -inch penetration at the top of the tank, opposite the water fill line. One final penetration exists on the rounded face of the tank, at approximately 34” from the ground, and serves as an emergency drain line to limit the tank water level. This penetration is sized for a 1-inch pipe and leads directly to the floor drain manifold via a flexible hose.



Figure 3.25. Water return line from HRS cooling tower supported by stainless steel channel strut.

3.10.4. Heat Rejection System Water Treatment System

To avoid buildup of scaling and biomass in the HRS piping and equipment, the water needs to be treated. This is accomplished with a water treatment solution provided by Garrett Callahan ®. The controller, chemical storage tanks, pumps, and piping associated with the water treatment system can be seen in Figure 3.26. The amount of total dissolved solids in the cooling water is monitored by a conductivity meter, which triggers blowdown of water inventory if the conductivity exceeds its setpoint. New water from the supply line replenishes the inventory, diluting the dissolved solids. Additionally, anti-scaling and biocidal agents are injected based on a combination of a

timer and conductivity readings. The biocidal agent is considered a serious health hazard (3/4 on the hazard scale), while the anti-scaling agent is rated as a 1 on the hazard scale. One must exercise caution when handling either chemical tank, including the use of personal protective equipment and thorough washing of any exposed skin.



Figure 3.26. HRS Water Treatment System.

3.10.5. Heat Rejection System Primary-Side Pump

The coolant pump for the primary side of the HRS is a Liquiflo® 621- RS206G1 centrifugal pump, which is coupled to a 2 HP motor running on 208 VAC as pictured in Figure 3.27; the pump performance curves are shown in Figure 3.28. This pump's impeller size has been reduced to 4.5 in from the standard 5 in impeller, which gives it a maximum shutoff head of approximately 80 feet [32]. The suction and discharge ports are respectively sized for 1.5-inch NPT and 1-inch NPT threaded pipe. The pump housing material is 316 stainless-steel, with a graphoil gasket, which promotes durability during high temperature operation. Since the motor speed is invariable, the pump flow rate is controlled by adjusting a gate valve downstream of the pump discharge.

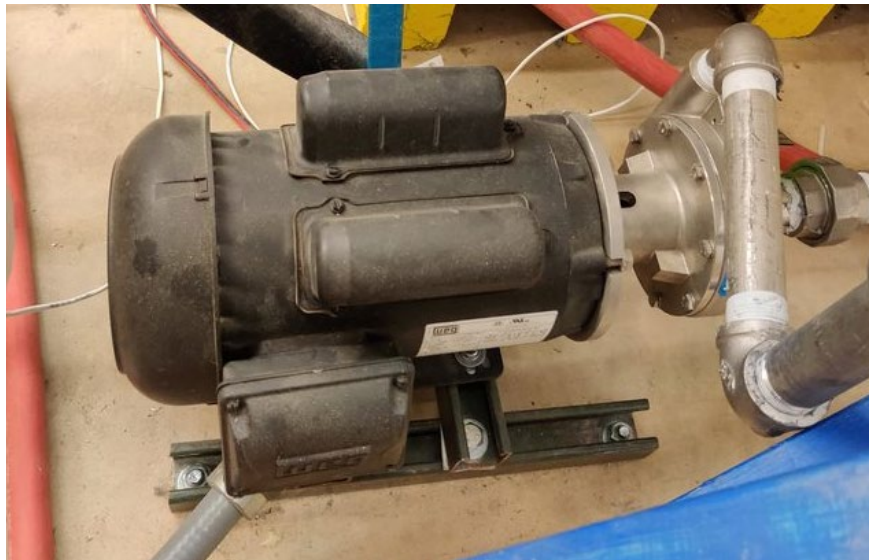


Figure 3.27. HRS Primary-side Pump.

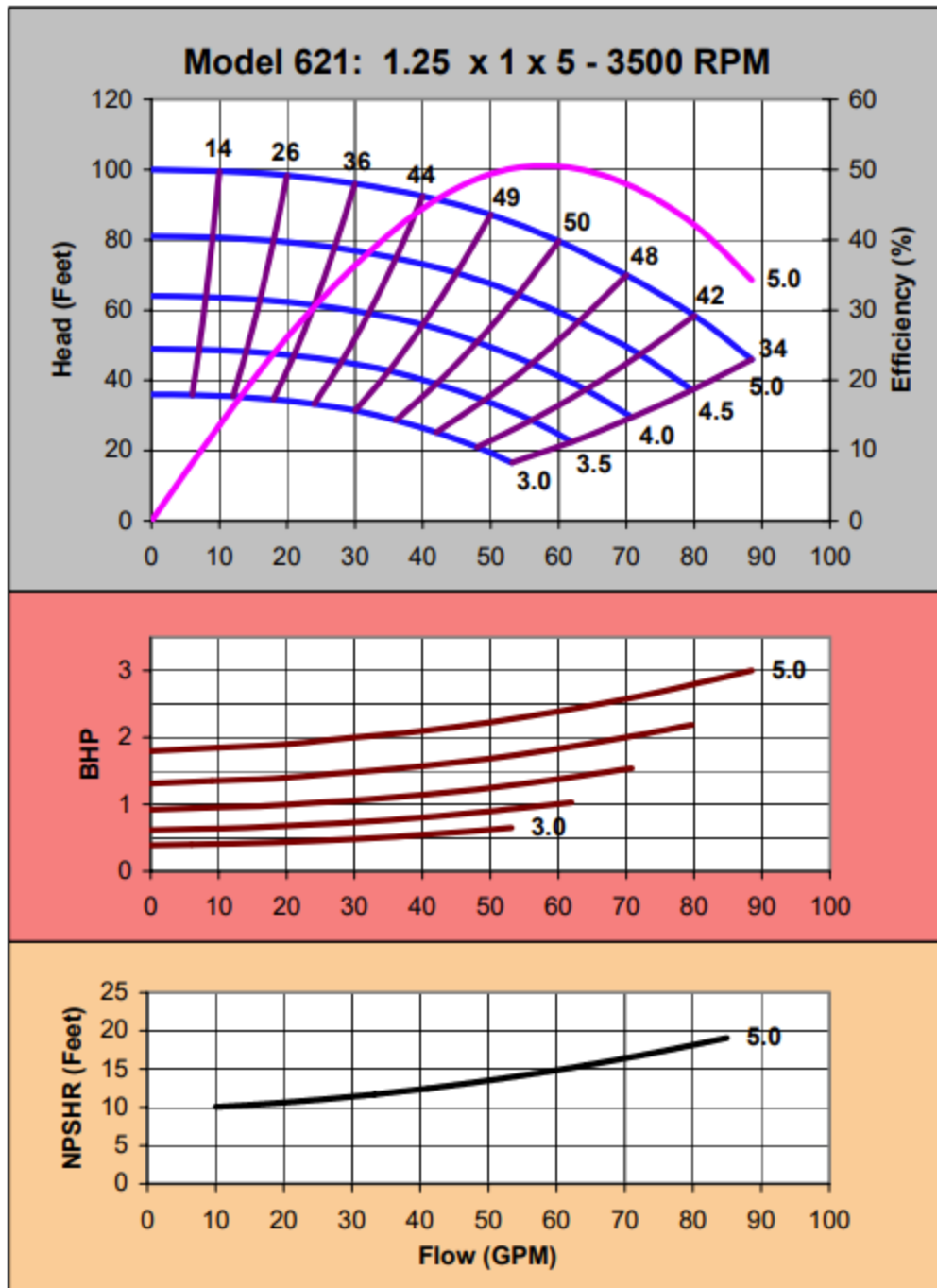


Figure 3.28. Performance Curves for Liquiflo® 621 Centrifugal Pump. Used as primary-side coolant pump. Reprinted from [33].

3.10.6. Heat Rejection System Secondary-Side Pump

The coolant pump for the secondary side of the HRS is a Dayton 12N813 self-priming centrifugal pump with a shutoff head of 88 feet [34], pictured in Figure 3.29. It is coupled to a 5 HP motor run on 208VAC; the pump performance curve is shown in Figure 3.30. Since the motor speed is non-variable, a throttling valve downstream must be used to control the water flow rate. It is capable of self-priming up to 20 feet of lift. Both the inlet and outlet are sized for 3-inch NPT pipe. The primary material in this pump is 304 stainless steel, which makes it ideal for pumping water to and from the cooling tower where contaminants can be introduced that would promote corrosion over time. The 12N813 has a Viton O-ring that is well-suited for long operation at elevated temperatures and is extremely chemically resistant, promoting its durability while exposed to unpurified water. This pump is rated to operate from $40^{\circ}F$ to $180^{\circ}F$. While it is rare for extended periods of cold weather in College Station, Texas, in cases where this occurs the water temperature should be checked before operating the pump.



Figure 3.29. HRS secondary-side coolant pump. Dayton 12N813 Self-Priming Centrifugal Pump.

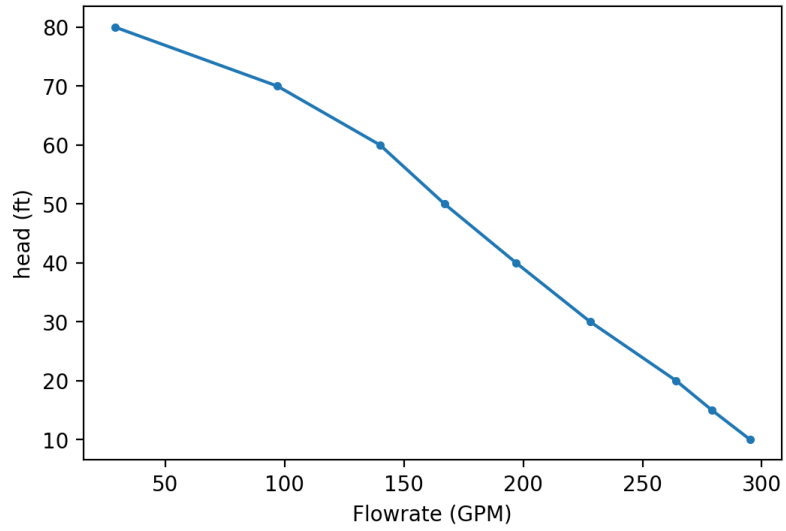


Figure 3.30 Pump curve for the Dayton 12N813 self-priming centrifugal pump. Data from [34].

3.10.7. Heat Rejection System Piping

The HRS piping is made up of two main sections. The HRS primary side piping handles hot water drawn from the suppression chamber, while the HRS secondary piping draws cooling water from the HRS water storage tank. The primary and secondary piping systems meet at the HRS heat exchanger as shown in Figure 3.31. Since the materials and setup differ greatly between the two sections, they will be discussed separately.



Figure 3.31. HRS piping connections to HRS heat exchanger.

3.10.7.1. Primary Side

Water for the primary side of the HRS is drawn directly from the suppression tank outlet by the HRS Primary Pump and passed through one side of the HRS heat exchanger. After passing through the heat exchanger, the cooled water returns to the suppression chamber where it is injected near the bottom of the tank. The momentum from this injection is sufficient to mix the suppression pool, maintaining a uniform pool temperature throughout cooldown. As shown in Figure 3.32, there is a globe valve installed downstream of the HRS Primary Pump which regulates the flow rate through the heat exchanger.

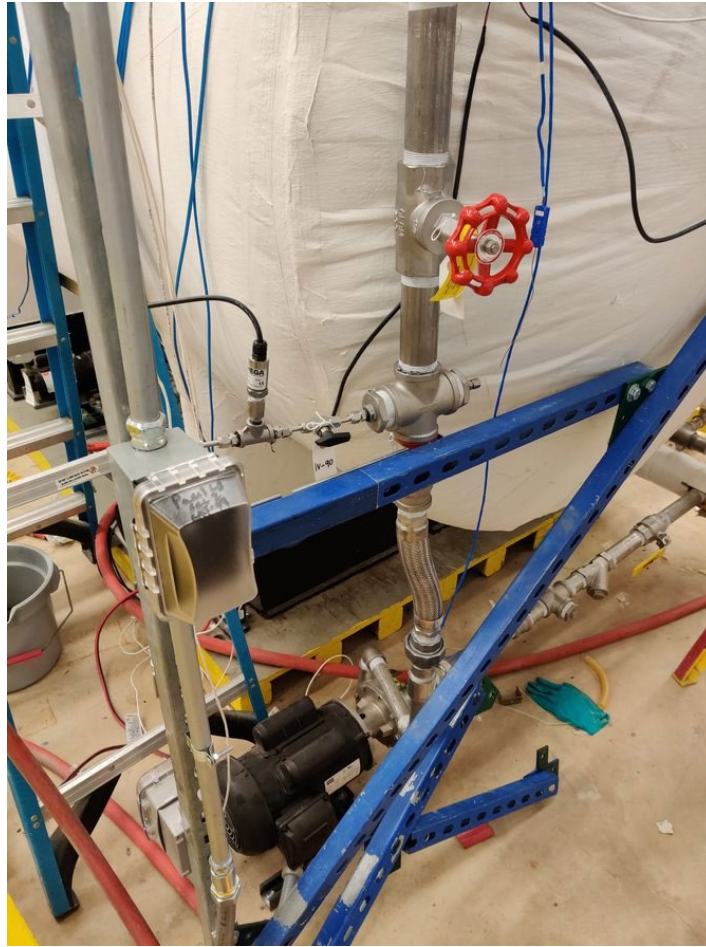


Figure 3.32. HRS Primary Side pump with piping. Red globe valve controls flow rate of primary coolant to the heat exchanger. Pump inlet comes from suppression tank.

Since the water in the suppression pool can potentially reach temperatures up to 120°C , the pipes in this section are required to be made of 304 stainless-steel. $1\frac{1}{2}$ inch pipe is used so that pressure drop in the pipe is not a limiting factor on the coolant flow rate through the heat exchanger.

3.10.7.2. Secondary Side

Routing cooling water from the HRS water storage tank, through the HRS secondary-side pump to the heat exchanger and back to the cooling tower was accomplished using 3-inch SCH80 CPVC pipe. The pipe size was chosen to minimize the pressure drop per unit length due to the significant distance between the HRS water storage tank and the HRS heat exchanger. While minimizing the distance traveled would be ideal, limitations on cooling tower installation locations and floor space availability made more convenient placement impossible. The 3-inch pipe also had the added convenience of matching the size of the connections on the cooling tower. CPVC was chosen over PVC to maximize durability during prolonged exposure to hot water (120 °F).

Water is drawn from the bottom of the HRS water storage tank through a bulkhead connection, where it can be directed either to the floor drain or to the HRS secondary pump (Figure 3.33). Before reaching the HRS secondary pump, water is routed through a strainer to filter out any large debris such as leaves or bugs that entered through the cooling tower (Figure 3.34). After the pump, water passes through a globe valve (Figure 3.35) which regulates the cooling water flow rate before traveling to the HRS heat exchanger.



Figure 3.33. HRS Tank outlet. 3-inch pipe with red ball valve leads to HRS secondary pump. 1.5-inch pipe with blue ball valve leads to floor drain.



Figure 3.34. HRS secondary-side piping. Water passes through the Y-strainer before entering the pump.



Figure 3.35. 3-inch pipes penetrating the wall route to the inlet and outlet of the HRS cooling tower. 3-inch pipe extending upward from the HRS secondary-side pump goes to the HRS heat exchanger and water treatment systems. Red globe valve controls the flow rate through the HRS piping system.

To minimize the footprint of the piping system, the piping is routed along the wall, elevated above all other equipment at approximately 20 ft above the floor at the highest point. According to common plumbing codes, suspended 3-inch CPVC piping has a maximum horizontal hanger spacing of 4 feet [35]. To achieve this, a support structure was fashioned from channel strut and fixed to the main structure's I-beams. This support structure consists of a series of 12 gage, back-to-back solid strut segments connected end to end, forming a central rail. Along the highest section of the structure, a length of 12 gage, slotted channel strut is affixed crosswise on top of the central rail

every 4 feet. Along the lower elevation section, a 6-foot length of 12 gage slotted channel strut descends from the central rail, and a cross piece is affixed at the bottom, identical to those used in the higher elevation section. A threaded rod descends from either side of each cross piece, where it connects to a pipe clamp which supports the pipe as shown in Figure 3.36. These threaded rods are effective in absorbing any shock experience in the piping system at startup and can adjust for a small amount of thermal expansion.



Figure 3.36. CAD model close-up of HRS pipe support structure.

The central rail is secured to the building's support beams via regularly spaced triangular supports that bear the weight of the support structure and piping, as shown in Figure 3.37.



Figure 3.37. Triangular supports bear the weight of the main support structure and fix it to the wall.



Figure 3.38. HRS elevated piping section #1.



Figure 3.39. HRS elevated piping section #2.

The HRS piping can be seen in Figure 3.38, Figure 3.39, Figure 3.40, Figure 3.41, Figure 3.42, and Figure 3.43. The same structure that supports the piping as a support for instrumentation wiring from the DAQ system to various instruments near the suppression pool, as shown in Figure 3.41.

Due to the significant temperature increase expected during operation, thermal expansion of the CPVC pipe needs to be accounted for. CPVC has a thermal expansion coefficient of 0.408 in./10°F/100 ft [36]. Based on an expected temperature increase from room temperature, 75°F, to 120°F, the pipe in this system can expand up to 1.836 in./100 ft. With a total length of approximately 200 feet, the pipes in the HRS could collectively expand by almost 4 inches, which could place strain on the joints and fittings if no accommodations were made. To account for this expansion, two different strategies were employed. First, additional changes in direction were incorporated in the form of elevation changes, arranged to meet commercial standards for thermal expansion as described by Charlotte Pipe and Foundry Company ® [36]. A second strategy employed is the incorporation of flexible hosing on the longest runs of pipe as shown in Figure 3.40. These lengths of high temperature hose aid in both mitigating the effects of thermal expansion, as well as the alignment of different piping segments to avoid placing pipes and fittings under tension.



Figure 3.40. HRS elevated piping section #3. Black flexible hose helps to account for thermal expansion.



Figure 3.41. HRS elevated piping section #4. Blue and White instrumentation wires run along the top of the pipe support structure.



Figure 3.42. HRS vertical piping section.



Figure 3.43. HRS piping. Red ball valves allow for heat exchanger bypass.

3.11. Data Acquisition System

The Data Acquisition System refers to the hardware and software used to record data, monitor operations, and control certain systems throughout the experiments. Data recorded includes measurements from all 107 thermocouples as well as 4-20 mA instruments including pressure transmitters, flowmeters, and a tachometer. Control valves throughout the facility are controlled by 4-20 mA signals as well.

3.11.1. Hardware

The primary hardware component in the Data Acquisition System used in these tests is a National Instruments PXIe-1075 with a NI PXIe-8821 embedded controller.

The PXIe-1075 chassis backplane has 18 PXI Express slots that each have up to 1 GB/s dedicated bandwidth. The high stability (± 25 ppm) internal 100 MHz reference clock for PXIe slots and 10 MHz reference clock for PXI slots allow for very accurate measurement timing [37]. The NI PXIe-8821 embedded controller has an Intel® Core™ i3 4110E processor (2.6 GHz dual-core processor), and a 320 GB hard drive, which makes this controller ideal for remote target IO applications such as LabVIEW RT [38]. The following modules are installed for instrumentation: 4 NI TB-4353 modules each with 32 channels for thermocouples, for a total thermocouple capacity of 128, 1 NI TB-4322 with 8 analog output channels for valve control, 1 NI TB-4302 with 32 filtered analog input channels configured for -10-10V signals, and 1 NI TB-4302C with 32 filtered analog input channels configured for 4-20mA signals. Figure 3.44 shows the DAQ chassis with all modules installed.



Figure 3.44. NI PXIe-1075 with modules installed.

3.11.2. Software

The software for the Data Acquisition System is partitioned into two sections. The primary software environment is 32-bit LabVIEW 2019 running under 64-bit Microsoft Windows 2010 Enterprise on a PC with an Intel® Xeon® CPU E3-1270 v6. This primary environment is where the user interacts with the facility by viewing lab conditions and adjusting control valve positions using the LabVIEW control panel. The primary environment handles most intermediate calculations and saves data to the hard drive. The secondary environment is a LabVIEW 2019 RT instance, housed on the PXIe-8821 embedded controller aboard the PXIe-1075. This environment performs all the direct interactions with instrumentation throughout the facility, converting thermocouple voltage differences and 4-20 mA signals into temperatures, pressures, and flow rates. LabVIEW 2019 RT implements precise timing loops to make sure data is collected from each data instrument at a consistent frequency, packaged into a single

array, and transmitted to the primary LabVIEW environment for processing and saving. The user interfaces with the DAQ system through the control panel on the primary LabVIEW VI. The control panel is separated into 4 sections which can be accessed by selecting the desired tab at the top of the VI. The sections are the main control panel, the suppression pool monitoring screen, the Heat Rejection System monitoring screen, and the PID settings screen. The main control panel is shown in Figure 3.45. This panel presents the user with system conditions throughout the facility and is where the user will spend most of their time while running an experiment. All control valves in the facility can be activated from this screen, and either controlled manually or placed in automatic mode where the valve will attempt to maintain a target condition. Additionally, data logging is initiated on this screen by specifying a target file name and directory, locking the choice in place by toggling the “write to file” button, and pressing the button marked “start recording”. At any time, the user can end the experiment by pressing the “End Run” button, which will close all control valves and stop data logging.

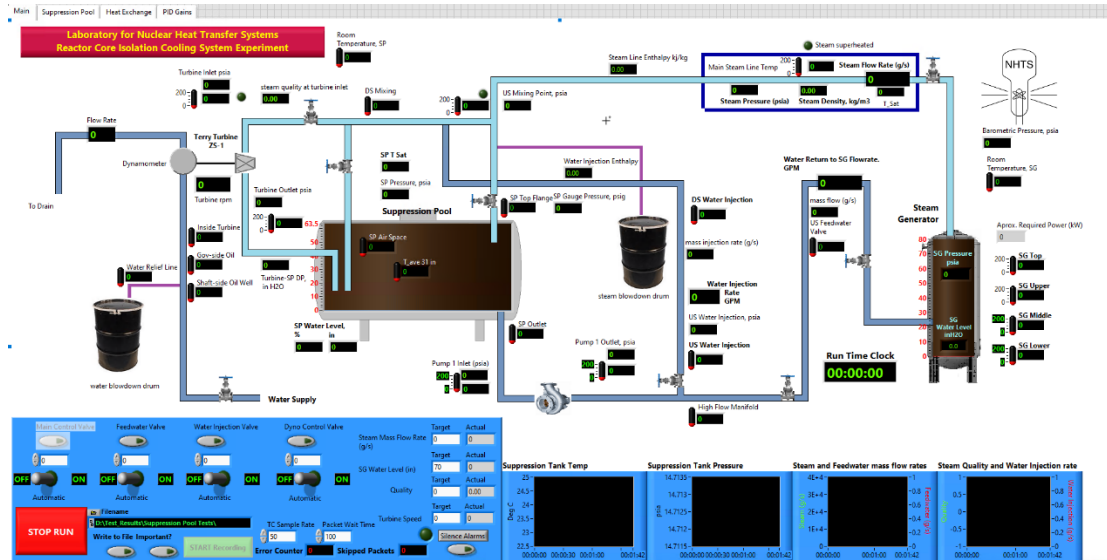


Figure 3.45. Main Control Panel on LabVIEW VI.

The second panel that is commonly watched during the experiment is the suppression pool monitoring panel, shown in Figure 3.46. This panel shows the detailed temperature distribution throughout the suppression pool including the temperature inside the turbine exhaust line, which is crucial for identifying when the facility warmup procedure is complete. This screen is also helpful for the user to recognize unexpected phenomena that can occur during the tests, such as hot or cold spots within the pool.

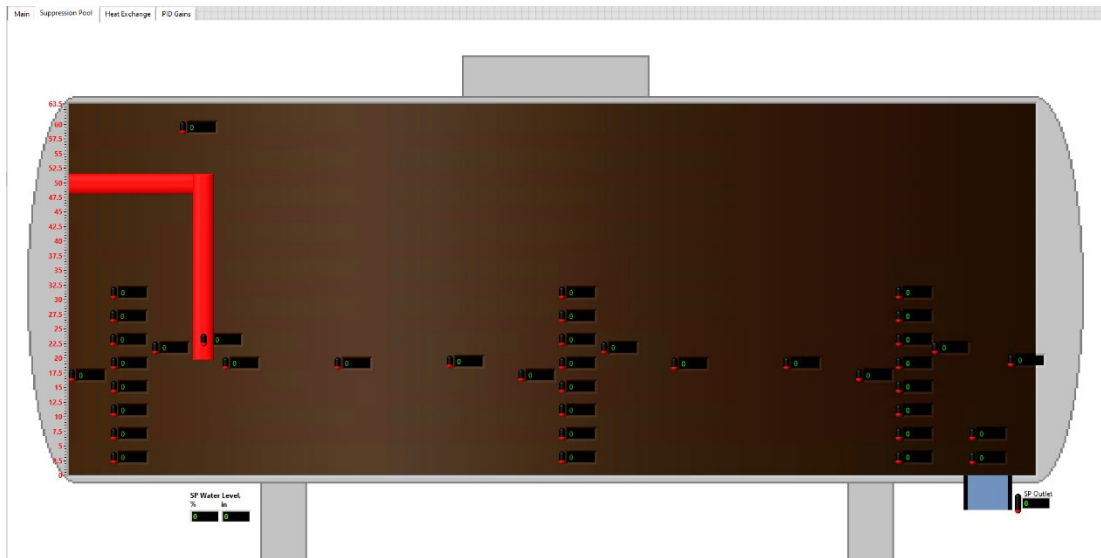


Figure 3.46. Suppression pool monitoring panel for LabVIEW VI.

The Heat Rejection System monitoring panel as shown in Figure 3.47 is typically only viewed during facility cooldown at the end of the test. Here the user can monitor the average tank temperature as well as the inlet and outlet temperatures for both the primary and secondary side of the HRS heat exchanger. This is particularly important after very high temperature tests since the water on the cold side of the heat exchanger can heat up overtime if the amount of heat removed from the suppression pool exceeds that removed by the cooling tower. Monitoring this screen helps the user to avoid approaching the maximum temperature limit for the cooling tower, which is 140 °F or 60 °C.

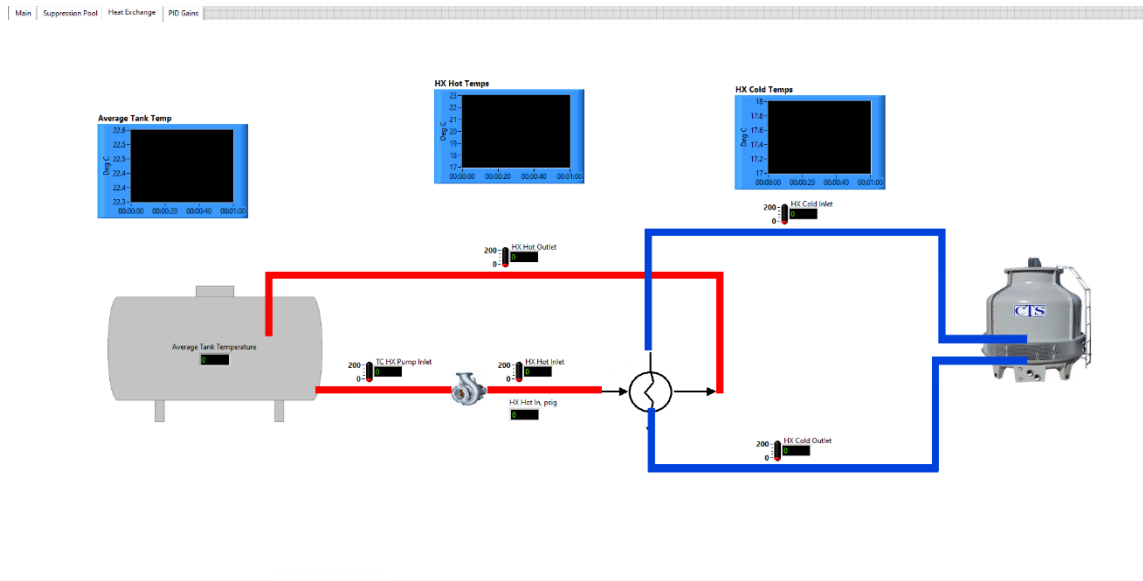


Figure 3.47. Heat Rejection System monitoring panel for LabVIEW VI.

Finally, the PID constant panel as shown in Figure 3.48 serves as an out-of-the-way location to store and edit the PID constants used in control logic throughout the facility. Typically, the user will not interact with this panel during an experiment, and is accessed more commonly while setting up control systems or re-tuning PID constants.

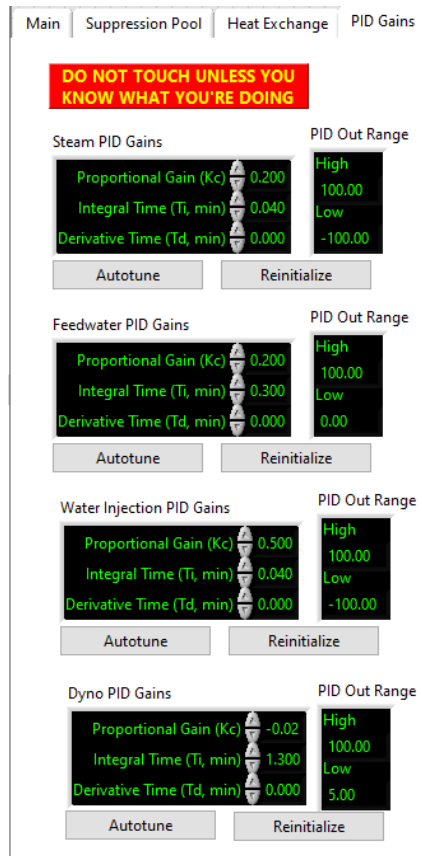


Figure 3.48. PID constants panel for LabVIEW VI.

The LabVIEW VI developed for this work was based on VIs produced for previous experiments performed in the Texas A&M Nuclear Heat Transfer Systems laboratory. Implementation of the dual environment interface of LabVIEW 2019 on the primary system and LabVIEW 2019 RT on the PXIe-8821 was adopted from ZS-1 and GS-2 Turbine Oil experiments, while the general data processing methods and user interface design stems from the previous study of thermal hydraulic behavior within the suppression chamber performed by Matthew Solom [19]. The data processing journey is very similar for each data point recorded. First, the electric signal is collected by the

LabVIEW RT VI where the mean and standard deviation of 10 readings are calculated. This helps to mitigate the effect of random noise in the data, as well as provide insight into the uncertainty in the reading. These values are then transmitted to the primary LabVIEW environment on the PC. This process is repeated 10x/second. In the case of temperature data, the DAQmx subroutine native to LabVIEW immediately converts the voltage signal into a temperature, so no further processing is required. For all other instruments, once the 4-20 mA signal has been transmitted to the PC, this must be converted into a meaningful value. The way this is done is by converting the mA signal into a percent of full range by linear interpolation ($20 \text{ mA} = 1$, $4 \text{ mA} = 0$). This percentage is then multiplied by the full range of the instrument in question and added to the lower range value of the device. This process requires proper calibration of all instruments or significant errors can occur. Once all signals are properly converted to useable data, the values are used for intermediate calculations and process control before being saved in a text file for permanent storage and post-processing analysis.

Introduction of improved hardware over previous configurations in the lab allow for a higher data recording frequency and more CPU-intensive on-line data processing and calculations. The most significant software contribution unique to this work is the implementation of process control logic, whereby the steam flow rate, steam generator water level, and steam quality (maintained at 100% for all tests presented in this work) can each be simultaneously controlled within approximately 1% of target values. Each of these control systems is based on PID control theory. The most important of these

control systems for this work is the steam mass flow rate control. To improve the response rate of the control system, an initial “guess” open fraction is calculated, after which the PID controller takes over for finer valve controls. This initial open fraction is calculated based on the valve CV curve and the pressure difference across the control valve. Choked flow is first checked for by comparing the pressure upstream and downstream of the control valve. If the ratio $\frac{P_{downstream}}{P_{upstream}}$ is less than 0.55, the flow is assumed to be choked. In this case, the desired valve CV is calculated from Equation (3.3). Alternatively, if flow is not choked, Equation (3.4) is used. Here, F_{target} refers to the desired steam volumetric flow rate in m^3/s , CV is the valve coefficient, P is the steam pressure, and $T_{superheat}$ is the degrees of steam superheat in $^{\circ}C$. The target mass flowrate is specified in g/s and converted to volumetric flowrate using the steam density.

$$CV = \left(\frac{F_{target}}{1.76 * P_{upstream}} \right) * (1 + 0.00065 * T_{superheat}) \quad (3.3)$$

$$CV = \left(\frac{F_{target}}{2.11 * \sqrt{P_{upstream}^2 - P_{downstream}^2}} \right) * (1 + 0.00065 * T_{superheat}) \quad (3.4)$$

Once the target CV is determined, it is converted to an open fraction using the steam valve CV curve as shown in Equation (3.5). This open fraction is added to the PID output as a self-adjusting offset. The combined use of a model-based offset value and a PID controller allows the PID to be better tuned for disturbance rejection instead of focusing on rapid setpoint changes.

$$Open\ Fraction = 19.588 * \ln(CV) + 26.826 \quad (3.5)$$

The steam generator water level controller is a feedforward PID control system, where instead of responding to change in water level, the feedwater flowrate is controlled to match the mass flowrate of steam leaving the steam generator. Deviation from the target water level is used to augment or diminish the target feedwater flowrate following Equation (3.6). Once the target flowrate is identified, the same procedure as used to control the steam flow rate is implemented to control the water flow rate into the steam generator. This procedure has been shown in practice to maintain the water level within 0.1 inches of the target water level.

$$m_{target} = m_{steam} * (1 - 0.1 * (h_{water} - h_{target})) \quad (3.6)$$

Steam quality control is achieved by injecting a controlled amount of water into the main steam line several meters before the turbine inlet, allowing the steam and water to mix. The steam quality controller uses the same method as the other controllers to control the mass flow rate of water injected, but the method of determining that flowrate is distinct. First, the desired steam quality is specified, after which the specific enthalpy of steam with that quality at the current temperature and pressure is calculated from Equation (3.7)

$$h_{mix} = h_{Sat\ Liquid} + Quality * (h_{Sat\ Vapor} - h_{Sat\ Liquid}) \quad (3.7)$$

Where the saturated liquid and vapor enthalpies of steam at the current temperature and pressure are determined from the IAPWS Industrial Formulation 1997 for the Thermodynamic Properties of Water and Steam [39]. The target water mass flow rate is

then calculated directly from Equation (3.8), where all enthalpies are determined by the IAPWS 97 formulation at current temperatures and pressures.

$$m_{water} = \frac{m_{steam} * (h_{steam} - h_{mix})}{h_{mix} - h_{water}} \quad (3.8)$$

3.12. Air Compressor

The facility utilizes a Quincy QT-15 air compressor (Figure 3.49) to supply air for control valves in addition to tests that utilize air in place of steam. The Quincy QT-15 can provide 175 psig of compressed air, which far exceeds the requirements of all control valves, the largest of which requires 87 psig to fully open.



Figure 3.49. Quincy Air Compressor.

One by-product of air compression is moisture generation. Especially in humid climates such as is found in College Station, Texas, a large amount of water can be present in the ambient air. This moisture is concentrated when the air is compressed and can condense as the air cools downstream. To combat this, a compressed air dryer (Figure 3.50) is used in tandem with the air compressor to reduce this water concentration and prevent water formation in compressed air line [40].



Figure 3.50. Quincy Compressed Air Dryer.

4. TESTING

4.1. Testing plan

For the first round of testing with this new facility, tests fall into one of two categories: Venting suppression pool tests and sealed suppression pool tests. In each case, steam is passed through the ZS-1 Terry turbine at a controlled mass flow rate. The temperature throughout the pool is measured until one of three end conditions occurs. These end conditions are: suppression pool pressure in excess of 60psig, an outlet water temperature exceeding 121° C, and a minimum suppression pool subcooling of 2° C. Each of these end conditions are motivated by lab safety, and adherence to equipment operating limits. Additionally, 60psig corresponds to the emergency operation limit for BWR Mark I containment, beyond which the containment would be vented in a controlled manner to avoid an uncontrolled containment failure.

4.2. Test Matrix

Seven tests were performed for this work, as summarized in Table 4.1. For the first two tests, the suppression pool was left open to the atmosphere, maintaining a constant atmospheric pressure in the suppression chamber. These two tests were performed to investigate the effect of changing the steam flow rate without the added effects due to a pressurized system. Additionally, these tests served as final shakedown tests for the facility to ensure all the equipment functioned as planned, and that the operating procedures were complete. After the two atmospheric pressure tests, two pressurized tests were performed at the same steam flow rates to observe the effects of

increasing tank pressure. These tests are a more accurate representation of what one would expect to see in a full-scale containment as the suppression tank pressure increases throughout an isolation event. A fifth test was performed with the same conditions as the first test, as a check for repeatability. Test #6 initiated the test by pressurizing the air space to 5 psig and then venting the air space in a controlled manner throughout the test to maintain a pressure of 5 psig. Finally, test #7 is an additional sealed-tank test performed using a lower steam mass flowrate.

Table 4.1. Test matrix

<u>Test #</u>	<u>Suppression Pool Pressure</u>	<u>Target Mass Flowrate(g/s)</u>
1	Venting	25
2	Venting	50
3	Sealed	25
4	Sealed	50
5	Venting	25
6	5 psig	25
7	Sealed	15

4.3. Operating Procedures

Procedures were developed to maximize operation safety and data quality, while attempting to replicate plant operation conditions as closely as possible. The procedures are split into several sections for ease of navigation. These sections are:

- Pre-startup
- Water Level Verification
- Warmup Mode
- Data Collection Mode
- Shutdown

See P&IDs in Appendix A for valve locations within the facility, and Table 4.2 for baseline valve positions.

Table 4.2 Default valve positions

<u>Valve</u>	<u>Position</u>	<u>Valve</u>	<u>Position</u>	<u>Valve</u>	<u>Position</u>
V-1	CLOSED	V-22	CLOSED	V-43	OPEN
V-2	OPEN	V-23	CLOSED	V-44	CLOSED
V-3	OPEN	V-24	CLOSED	V-45	CLOSED
V-4	OPEN	V-25	CLOSED	V-46	CLOSED
V-5	CLOSED	V-26	CLOSED	V-47	CLOSED
V-6	OPEN	V-27	OPEN	V-48	THROTTLE
V-7	CLOSED	V-28	CLOSED	V-49	CLOSED
V-8	CLOSED	V-29	CLOSED	V-50	CLOSED
V-9	CLOSED	V-30	OPEN	V-51	OPEN
V-10	CLOSED	V-31	CLOSED	V-52	CLOSED
V-11	OPEN	V-32	N/A	V-53	CLOSED
V-12	N/A	V-33	OPEN	V-54	OPEN
V-13	CLOSED	V-34	OPEN	V-55	OPEN
V-14	CLOSED	V-35	OPEN	V-56	CLOSED
V-15	CLOSED	V-36	CLOSED	V-57	CLOSED
V-16	CLOSED	V-37	CLOSED	V-58	CLOSED
V-17	CLOSED	V-38	OPEN	V-59	OPEN
V-18	CLOSED	V-39	CLOSED	V-60	OPEN
V-19	OPEN	V-40	CLOSED	V-61	CLOSED
V-20	OPEN	V-41	CLOSED	V-62	CLOSED
V-21	CLOSED	V-42	OPEN	V-63	CLOSED

Table 4.2 Continued.

<u>Valve</u>	<u>Position</u>	<u>Valve</u>	<u>Position</u>	<u>Valve</u>	<u>Position</u>
V-64	CLOSED	V-85	OPEN	V-106	OPEN
V-65	CLOSED	V-86	CLOSED	V-107	CLOSED
V-66	N/A	V-87	CLOSED	V-108	CLOSED
V-67	N/A	V-88	CLOSED	V-109	CLOSED
V-68	N/A	V-89	OPEN	V-110	OPEN
V-69	CLOSED	V-90	CLOSED	V-111	OPEN
V-70	OPEN	V-91	THROTTLE	V-112	OPEN
V-71	THROTTLE	V-92	CLOSED	V-113	CLOSED
V-72	CLOSED	V-93	THROTTLE	V-114	THROTTLE
V-73	THROTTLE	V-94	CLOSED	V-115	CLOSED
V-74	CLOSED	V-95	CLOSED	V-116	OPEN
V-75	CLOSED	V-96	CLOSED	V-117	OPEN
V-76	THROTTLE	V-97	CLOSED	V-118	OPEN
V-77	CLOSED	V-98	CLOSED	V-119	CLOSED
V-78	CLOSED	V-99	CLOSED	V-120	THROTTLE
V-79	OPEN	V-100	CLOSED	V-121	OPEN
V-80	CLOSED	V-101	CLOSED	V-122	OPEN
V-81	OPEN	V-102	CLOSED	V-123	OPEN
V-82	CLOSED	V-103	CLOSED	V-124	CLOSED
V-83	THROTTLE	V-104	OPEN	V-125	CLOSED
V-84	CLOSED	V-105	OPEN	V-126	OPEN

Table 4.2 Continued.

<u>Valve</u>	<u>Position</u>	<u>Valve</u>	<u>Position</u>	<u>Valve</u>	<u>Position</u>
V-127	OPEN	V-130	CLOSED	V-133	CLOSED
V-128	OPEN	V-131	OPEN	V-134	THROTTLE
V-129	OPEN	V-132	OPEN	V-135	CLOSED

4.3.1. Pre-startup procedures

- 1) Ensure all electrical instruments and cables are properly connected, and are not exposed to water/hot surfaces
- 2) Prepare RCIC turbine
 - Check that the ZS-1 turbine oil level in the oil wells is above the minimum level and below the maximum level, as marked on the turbine's oil cabinet.
 - Close turbine drainage valves V-36 and V-37, and instrumentation valve iV-13
 - Ensure the turbine's sealant drainage hoses are guided safely to the turbine catch drum, and the outlets are submerged in water.
- 3) Prepare pressure instrument lines
 - Ensure pressure instrument lines are filled with DI water for protection from steam.
- 4) Close V-3 (Steam Generator Blowdown Line)
- 5) Plug in and power on the DAQ chassis, DC power supply, and magnetic flowmeters.

6) Log into the Data Acquisition Computer and load up the following LabVIEW programs:

- Suppression_Pool_Stratification_Test.vi
- Suppression_Pool_Stratification_Test_RT.vi

4.3.2. Water Level Verification

Visually inspect the indicated water level on the steam generator and suppression pool magnetic float indicators. Make sure they are within operating bounds. The steam generator should be filled to at least 70 cm on the magnetic float indicator, but below 80 cm. The suppression pool should be filled to approximately 80 cm. Following are procedures to adjust these water levels before testing. Note that draining the suppression pool to the floor drain should be a last resort to conserve DI water.

To fill steam generator from suppression pool:

- 1) Power on feedwater pump
- 2) Use LabVIEW control panel to partially open V-18 (feedwater valve).
Adjust open ratio to maintain reasonable flow rate.
- 3) Once the desired level has been reached, close V-18 (feedwater valve)
- 4) Power off feedwater pump

To decrease steam generator water level:

- 1) Leave feedwater pump off
- 2) Open V-45, V-46, and V-8 to open both suppression pool and steam generator to the atmosphere.
- 3) Open V-21 to allow steam generator and suppression pool to equilibrate

- 4) Once the desired water level is reached, close V-21

To fill suppression pool:

- 1) Open V-58
- 2) Connect hose from tap water to the Culligan DI System inlet
- 3) Open valve on Culligan DI system outlet
- 4) Turn on tap water faucet
- 5) Once desired water level is reached, close V-58, turn off tap water faucet.

To decrease suppression pool water level:

Note: Floor drain should not be used while suppression pool water is hot.

- 1) Open V-57, which will admit water to the floor drain
- 2) Once desired water level is reached, close V-57

4.3.3. Warmup Mode

- 1) In LabVIEW control panel, enter the desired output data file location and name, including the date and “warmup”, and toggle “write to file” on.
- 2) Press the “Record” button on the LabVIEW control panel to start baseline recording
- 3) Check that the following valves are closed:
 - a) V-1 (Main Steam Line) via LabVIEW
 - b) V-24 (Main Air Line)
 - c) V-25 (Auxiliary Steam Line)
 - d) V-29 (CCFL Steam Admission Line)

- e) V-33 (Turbine Steam Admission Line)
 - f) V-38 (Turbine Exhaust Line)
 - g) V-43 (SRV Steam Admission Line)
 - h) V-106 (Water Injection Valve)
- 4) Open V-41 (Turbine Bypass Valve)
 - 5) Power on air compressor, which supplies air to all control valves. Make sure the air line has reached at least 60 psig before attempting to operate control valves.
 - 6) Power on HRS secondary loop circulation pump. While the HRS will not be in use during the test, the HRS secondary coolant line supplies water to the dynamometer to maintain turbine speeds at safe levels.
 - 7) Place a small bucket under the Steam Condensate Line outlet and make sure V-31 on the steam condensate line is partially open.
 - 8) Energize the steam generator electric heaters to full power (157 kW) until the steam generator pressure reaches the target pressure of 95 psia.
 - 9) Reduce heater power to 3 kW and adjust as needed to maintain pressure during warmup.
 - 10) Use LabVIEW control panel to power on V-1 (Main Steam Valve), and open to 5% to admit a slow flow rate of steam into the main steam line.
 - 11) Condensate should begin running out of the Steam Condensate Line momentarily. Eventually that condensate will be replaced by steam. When this happens, carefully close V-31 to contain the steam.

- 12) Once the Steam Condensate Line is closed, further open V-1 (Main Steam Valve) to 10%
- 13) Once the temperature along the entire main steam line reaches 100°C, open the following valves:
 - 14) V-33 (Turbine Steam Admission Line)
 - 15) V-38 (Turbine Exhaust Line)
- 16) Open V-60 to supply water to the dynamometer and use LabVIEW control panel to open dynamometer control valve to 50%.
- 17) Close V-41 (Turbine Bypass Valve)
- 18) At this point, condensate will begin to accumulate inside the ZS-1 turbine casing. Regularly purge this condensate by very carefully opening turbine drainage valves V-36 and V-37 until steam begins to flow, then close the valves.
- 19) Drain any new condensate in the main steam line by slowly cracking V-31 open to allow water to flow. Close when the flow becomes mostly steam. Do not open all the way. Caution: HOT!
- 20) Slowly increase the steam flow rate through the turbine by switching the steam control valve to automated control on the LabVIEW control panel and increase the target flow rate until the flow rate desired for the upcoming test is reached. The steam generator power will need to be increased to maintain pressure.
- 21) Power on the feedwater pump and use the LabVIEW control panel to automatically control the feedwater control valve. Set the desired water level in the steam generator. If the feedwater flow rate appears unstable, and the feedwater valve is

opening less than 10%, adjust the pump recirculation valve V-76 to reduce the available head until the flow rate stabilizes, and the feedwater valve is more than 10% open.

- 22) Open recirculation valves V-98 and V-99 at the front of the suppression pool to mix the pool to achieve an initially isothermal pool.
- 23) Continue warmup, continuing to collect accumulated condensate through V-31, V-36, and V-37, until the temperature at the Turbine Exhaust outlet reaches 100°C, signifying a steady flow of steam reaching the suppression pool.
- 24) Close recirculation valves V-98 and V-99 to cease active pool mixing.
- 25) Lower steam generator power to 3 kW
- 26) Use LabVIEW control panel to close V-1 (main steam valve)
- 27) Click “Stop” to stop recording baseline data.

4.3.4. Data Collection Mode

Data Collection should begin approximately 5 minutes after completion of the warmup procedure. This time allows the pool to settle after stopping the active mixing but does not allow so much time that the piping and other system components can cool too much before the tests begins.

For tests to be performed at atmospheric pressure:

- 1) Check that V-45, V-46, V-47, and V-49 are open to ensure atmospheric pressure conditions.
- 2) Set Steam Flow Rate

- a) Enter the desired target steam flow rate on the LabVIEW control panel. The Main Control Valve is programmed to automatically adjust the valve open ratio to meet the desired flow rate.
- 3) Set turbine speed
 - a) On LabVIEW control panel, set target turbine speed to 3000 rpm. The dynamometer control valve is programmed to adjust its open ratio to maintain this target turbine speed.
- 4) Feedwater control
 - a) Make sure V-81 is open
 - b) Set desired steam generator water level to 70 inches. The feedwater control valve is programmed to nominally match the feedwater rate to the steam mass flow rate and adjust to maintain the desired water level.
- 5) On LabVIEW control panel, enter the desired output data file location and name, including the date, steam mass flow rate, and “atmpressure”, and toggle “write to file” on.
- 6) On LabVIEW control panel, click “Start Recording” to begin test
- 7) Power on each control valve and set to automatic control.
- 8) Once flows have stabilized, push the button marked “important” to signal the start of the test data.
- 9) Monitor control panel throughout the test to ensure the following:
 - a) Steam generator pressure remains constant. Adjust steam generator heaters as necessary to maintain the steam generator pressure at approximately 95 psia.

Note: Too low of pressure will result in steam subcooling, while too high of pressure can result in backflow through the feedwater line. Safety logic is included to close the feedwater valve if backflow occurs, but it should still be avoided.

- b) Steam generator water level remains above 60 inches. The feedwater control valve logic should handle this, but it is good to verify with the orange indicator on the water level meter.

10) Continue test until the suppression pool surface water temperature reaches saturation.

Note: Since this is an unsealed test, there is no danger of rapidly increasing the pressure if saturation is reached. However, low-pressure steam will begin flowing out of V-46 in large quantities at this point.

11) Depress button on LabVIEW control panel marked “important” to signal end of test.

12) Go to Shut-down procedure.

For tests to be performed with a sealed suppression pool:

- 1) Close valves V-45, V-46, V-47, and V-49 to allow pressure to build inside suppression pool.
- 2) Set Steam Flow Rate
 - a) Enter the desired target steam flow rate on the LabVIEW control panel. The Main Control Valve is programmed to automatically adjust the valve open ratio to meet the desired flow rate.
- 3) Set turbine speed

- a) On LabVIEW control panel, set target turbine speed to 3000 rpm. The dynamometer control valve is programmed to adjust its open ratio to maintain this target turbine speed.
- 4) Feedwater control
 - a) Make sure V-81 is open
 - b) Set desired steam generator water level to 70 inches. The feedwater control valve is programmed to nominally match the feedwater rate to the steam mass flow rate and adjust to maintain the desired water level.
- 5) On LabVIEW control panel, enter the desired output data file location and name, including the date, steam mass flow rate, and “sealedpressure”, and toggle “write to file” on.
- 6) On LabVIEW control panel, click “Start Recording” to begin test
- 7) Power on each control valve and set to automatic control.
- 8) Once flows have stabilized, push the button marked “important” to signal the start of the test data.
- 9) Monitor control panel throughout the test to ensure the following:
 - a) Steam generator pressure remains constant. Adjust steam generator heaters as necessary to maintain the steam generator pressure at approximately 95 psia.

Note: Too low of pressure will result in steam subcooling, while too high of pressure can result in backflow through the feedwater line. Safety logic is included to close the feedwater valve if backflow occurs, but it should still be avoided.

- b) Steam generator water level remains above 60 inches. The feedwater control valve logic should handle this, but it is good to verify.
- 10) Continue test until one of the following three end criteria are met:
- a) Suppression Pool surface water temperature comes within 5°C of saturation.
Note: Operation near the saturation temperature in a sealed tank can lead to rapid suppression pool pressurization if steam is no longer fully condensed.
 - b) Suppression Pool pressure reaches 60 psig. This is the design pressure of suppression pools used in the Mark I BWR containment.
Note: The suppression pool is rated to operate up to 80 psig, so this end condition gives a considerable margin to ensure safety.
 - c) Feedwater pump inlet temperature reaches 121°C . This is the maximum operating temperature of the pump seal
- 11) Depress the button on LabVIEW control panel marked “important” to signal end of the test.
- 12) Go to Shut-Down procedure

4.3.5. Shut-down Procedure

After tests where the suppression pool has been pressurized, there is the potential for backflow into the turbine and steam line if care is not taken during shutdown. Once the turbine casing is full of water, it is essentially impossible to return it to the suppression pool, meaning the water will be wasted. In addition to the waste issue, pressurized water inside the turbine will leak out and flash to steam, posing a safety risk.

- 1) Do NOT close V-1 (main steam valve) immediately after testing ends.
- 2) Power off all heaters in the steam generator
- 3) Close V-18(Feedwater valve) using LabVIEW interface and power off feedwater pump (P-1)
- 4) Open V-41 and V-40, allowing steam to bypass the turbine
- 5) Close V-38 and V-33, isolating the turbine
- 6) Open iV-13, V-36, and V-37 to vent steam caught in turbine and allow condensate to drain. Leave open to prevent vacuum generation in the turbine as it cools.
- 7) Open V-1 fully to start blowdown from the steam generator
- 8) Start HRS.
 - a) Make sure V-51 is open to admit water to the HRS primary pump (P-4).
 - b) Adjust V-143 so that it is only slightly open
 - c) Power on HRS primary pump (P-4)
- 9) Monitor HRS, adjusting as necessary
 - a) On LabVIEW panel, the inlet and outlet water temperatures on both the primary and secondary side of the heat exchanger are plotted over time.
 - b) Adjust V-143 to adjust heat removal rate, making sure the secondary outlet temperature never exceeds 50°C
- 10) Once bulk pool temperature reaches 100°C , start suppression pool blowdown
 - a) Open V-45

- b) Slowly open V-47, checking to make sure water is not splashing out of the blowdown drum. Keep V-47 as open as possible while avoiding water splashing until suppression pool pressure has reduced to less than 1 psig.
 - c) Once suppression pool reaches 1 psig, slowly open V-46 to vent to the room. Leave open to prevent vacuum generation in the suppression chamber as the pool cools.
- 11) Once both the suppression pool and steam generator have depressurized to less than 1 psig, slowly open V-31 to allow condensate and any remaining steam to vent from the steam line. Leave open to prevent vacuum generation in the steam line as it cools.
 - 12) Close V-1 (main steam line) using LabVIEW interface.
 - 13) Open V-3 to expose steam generator to atmosphere. Leave open to prevent vacuum generation in steam generator as it cools.
 - 14) Continue operating HRS until the bulk suppression pool temperature is below 50°C .
If additional tests are planned for the following day, continue until 40°C .
 - 15) Turn off all pumps, the compressor, and cooling tower fan.
 - 16) On the LabVIEW panel, press the button marked “stop recording”, power off all control valves, and press “end run”

4.4. Results

4.4.1. Test #1

Test #1 is a venting pool test, with a nominal steam flow rate of 25 g/s. Thermal stratification began approximately 112 minutes after the start of the test and continued for 146 minutes. The bulk pool temperature at the onset of stratification was 49.0 °C, which corresponds to 51.0 °C of subcooling. While the temperature at lower elevations in the pool never flattens out entirely, suggesting a small amount of mixing occurred throughout the test, the violent mixing experienced earlier in the test that stopped stratification from developing ends at approximately 123 minutes, 11 minutes after stratification begins to develop. The maximum stratification was observed to be 28.1°C. This test was terminated due to the bulk pool temperature coming within 5 °C of the saturation temperature. Steam was observed exiting from the suppression pool through the vent piping, indicating the suppression pool was no longer successfully condensing the incoming steam. The average temperature of thermocouples at each monitored elevation in the pool is plotted in Figure 4.1 below. These average temperatures are calculated using every thermocouple located at the given elevation. At a minimum, each data point represents the averaged readings of 3 thermocouples.

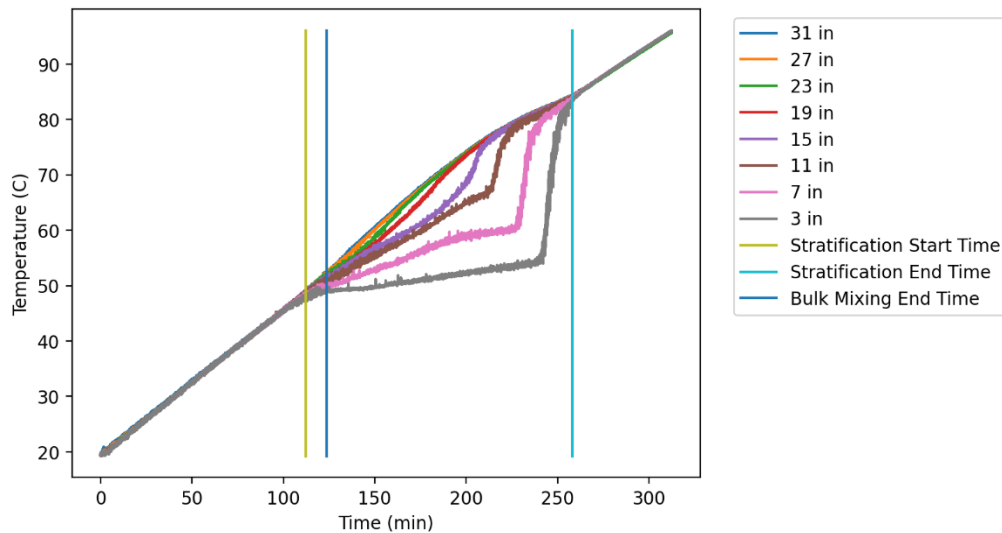


Figure 4.1. Average temperature at each monitored elevation within the suppression pool for test #1.

During this first test it was discovered that a single thermocouple at the lowest elevation measured in the pool, nearest the turbine exhaust, would repeatedly spike in temperature by a few degrees, making it a higher temperature than any of the thermocouples above it. This phenomenon ceased once thermal stratification began and never returned. This was the first indication that hot water expelled from the turbine exhaust line was traveling down to the bottom of the tank, promoting mixing within the pool. This theory was corroborated by plotting the temperature inside the turbine exhaust line, 3 inches from the exhaust line outlet, over time. As shown in Figure 4.2, the temperature inside the turbine exhaust line oscillates rapidly between the pool temperature at the exhaust outlet and the steam temperature. This indicates a fluctuating

water level inside the exhaust sparger as water was repeatedly expelled and readmitted into the turbine exhaust line. The open-ended sparger design directed the expelled water directly downward, resulting in extensive mixing. This chugging phenomenon is evident in each of the tests that have been performed and is caused by the low bulk pool temperature which leads to very rapid steam condensation inside the exhaust line.

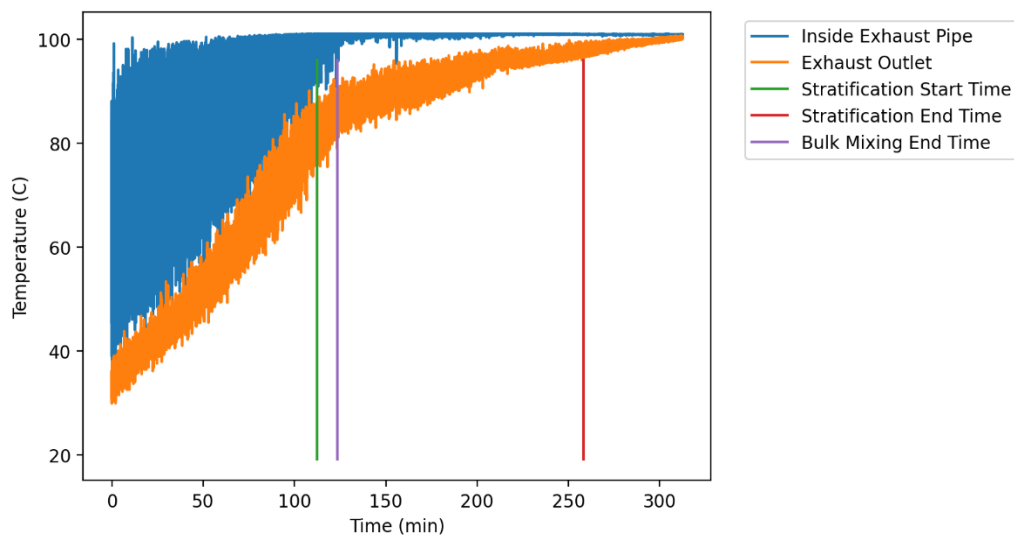


Figure 4.2. Plot of the temperature inside the turbine exhaust line, 4 inches from the outlet, and the water temperature at the outlet for test #1.

To investigate the possibility of axial temperature stratification, the temperature of the water at an elevation of 19 in from the bottom of the suppression chamber is plotted at every axial location measured. The data points in Figure 4.3 each represent the measurements from a single thermocouple, so temperature oscillations are more apparent

than the average temperatures reported for the vertical stratification plot in Figure 4.1. The greatest oscillations are observed for the thermocouples positioned 7 feet and 8 feet from the plate-side weld, respectively. These two thermocouples are the closest to the turbine exhaust sparger, so these oscillations are not surprising. For reference, these thermocouples are 2 inches and 10 inches from the turbine exhaust sparger outlet. Overall, no significant axial temperature stratification is apparent, except for in the immediate vicinity of the turbine sparger.

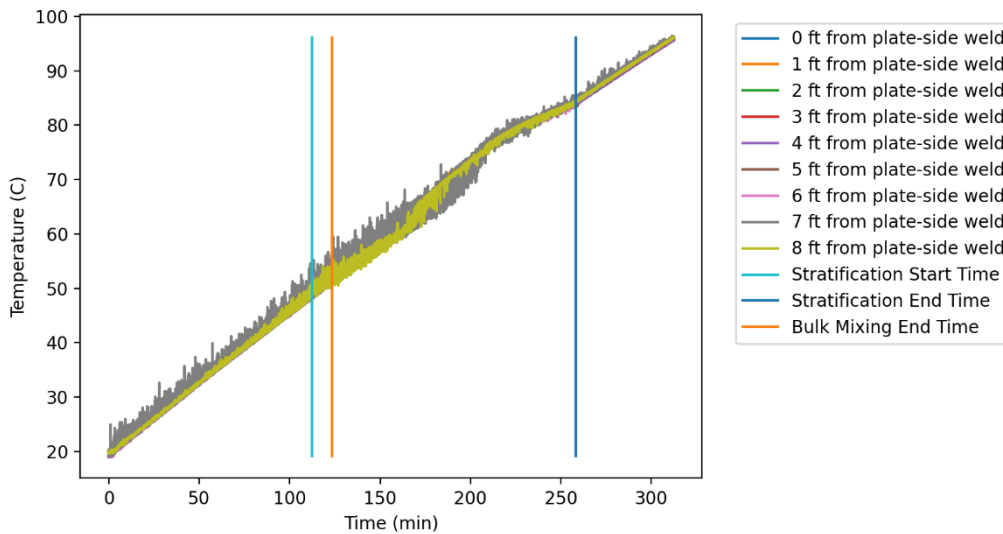


Figure 4.3 Plots of temperatures over time at each axial location measured within the suppression pool for Test #1.

As demonstrated in Figure 4.4, Figure 4.5, and Figure 4.6, there is no substantial temperature stratification when the lateral pool position is considered. A small amount of

variation is seen in Figure 4.4 which shows the lateral temperature profile at the turbine-side weld, 10 inches from the turbine exhaust sparger outlet. Here the temperature at the lateral middle is shown to be slightly higher for portions of the test. This makes sense since the other two thermocouples are significantly further away from the sparger. The amount of temperature stratification is very small relative to the vertical temperature stratification shown in Figure 4.1.

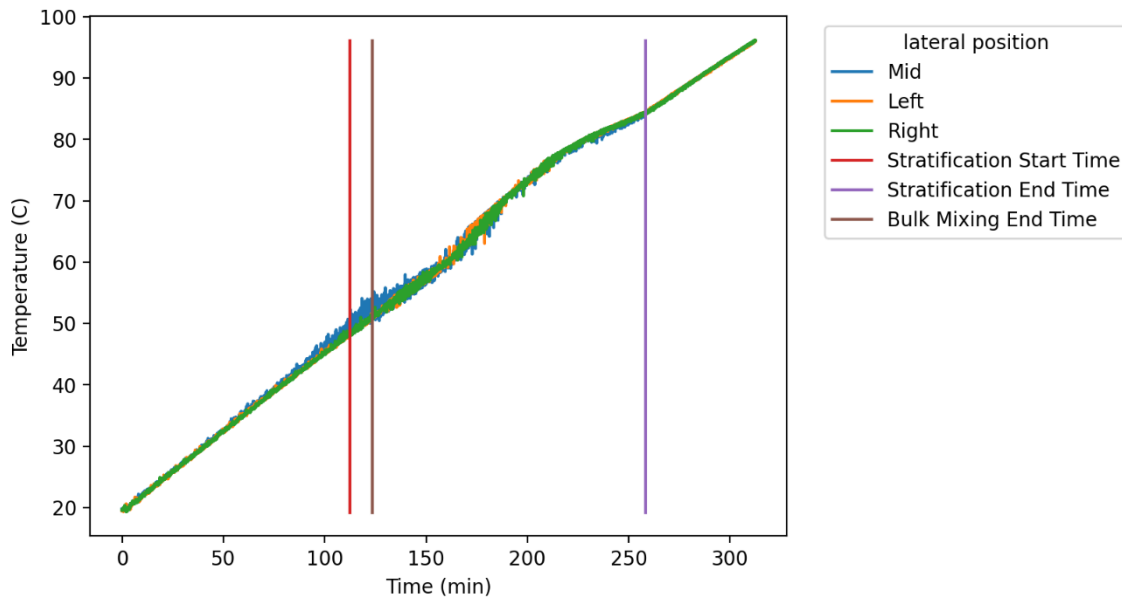


Figure 4.4. Plot of temperature measured at each lateral position at the turbine-side weld for test #1.

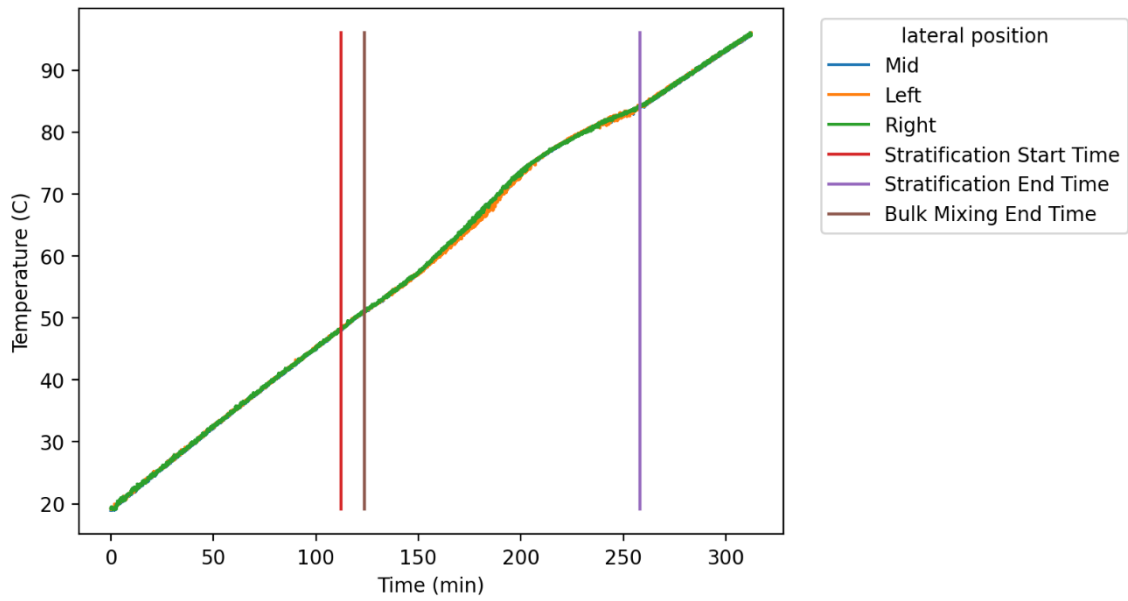


Figure 4.5. Plot of temperature measured at each lateral position at the center of the tank for test #1.

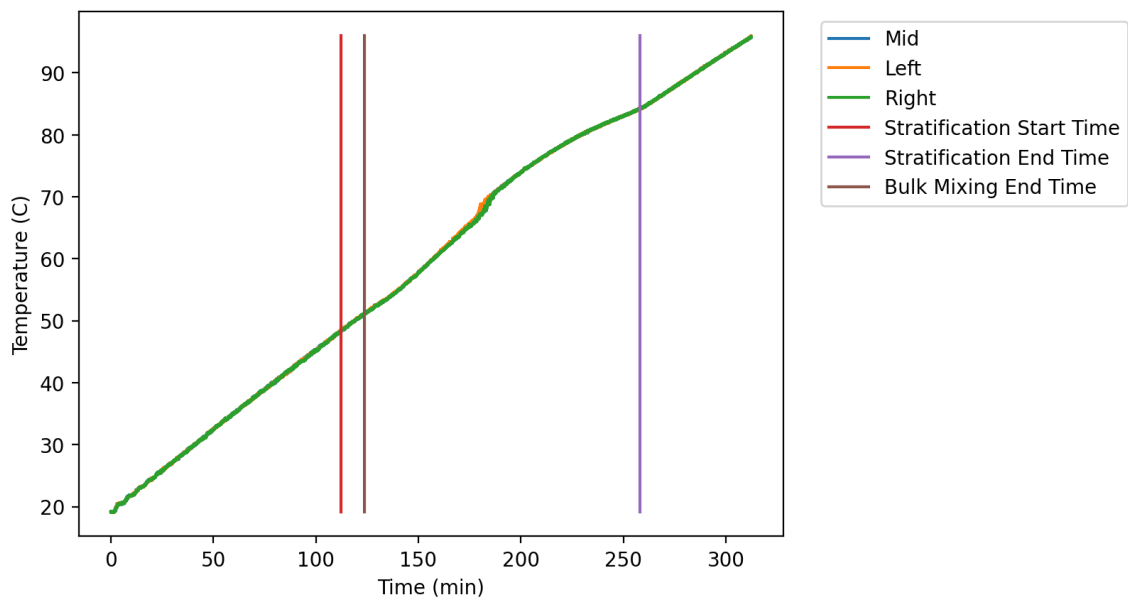


Figure 4.6. Plot of temperature measured at each lateral position at the plate-side weld for test #1.

Since the results for the lateral and axial temperature distributions as shown above are very similar for all tests, and are less significant than the vertical temperature distribution, only vertical stratification will be discussed for the remaining tests.

4.4.2. Test #2

Test #2 is a venting pool test with a nominal steam flow rate of 50 g/s. Thermal stratification began approximately 77.5 minutes after the start of the test and continued for 46 minutes. The bulk pool temperature at the onset of stratification was 68.6 °C, which corresponds to 31.5 °C of subcooling. In contrast to test #1, shortly after the onset of stratification bulk pool mixing is seen to cease entirely, as evident from the near-constant temperature measured at the bottom elevation in the pool as shown in Figure 4.7 below. The maximum stratification observed was 18.2 °C. The test was terminated due to the bulk pool temperature coming within 5 °C of the saturation temperature. Steam was observed exiting through the vent piping, indicating the steam was not being fully condensed.

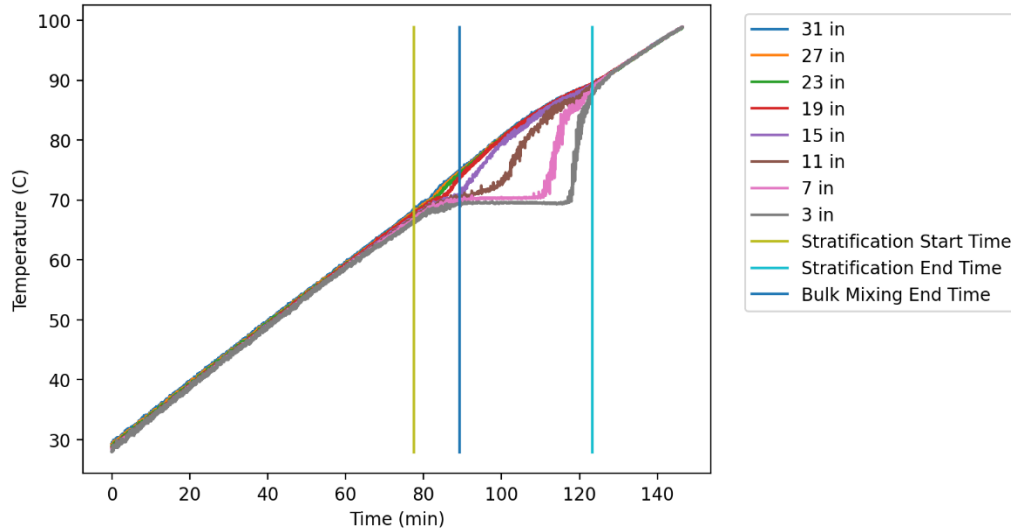


Figure 4.7. Average temperature at each monitored elevation within the suppression pool for test #2.

In test #2, the same temperature oscillation of the lowest thermocouple at the end of the tank nearest the exhaust line was observed as in test #1. Examination of the temperature inside the turbine exhaust line showed a different story than was observed in the lower flowrate test. In this test, minimal temperature oscillations were apparent early in the test but ceased far before the onset of thermal stratification, as shown in Figure 4.8. However, monitoring the exhaust outlet temperature shows that stratification did not begin until the exhaust outlet temperature first reached the steam temperature. Since the temperature oscillations which were observed in test #1 are not present in this test, it is possible any chugging that occurred simply did not travel far enough up the turbine

exhaust line to be detected by the thermocouple inside the pipe, due to the increased steam flow rate. The time that bulk pool mixing ended coincides with the time that the temperature at the turbine exhaust outlet stops oscillating and maintains at the steam temperature. When the turbine exhaust outlet temperature matches the steam temperature, no meaningful condensation can be expected. With no condensation occurring inside the turbine exhaust line, or immediately outside of it, non-condensed steam would rise toward the top of the pool until it encounters colder water, causing it to condense. Since the heat from the steam is imparted entirely to the upper portions of the pool in a steady manner, no bulk mixing is achieved in the suppression pool, allowing thermal stratification to develop.

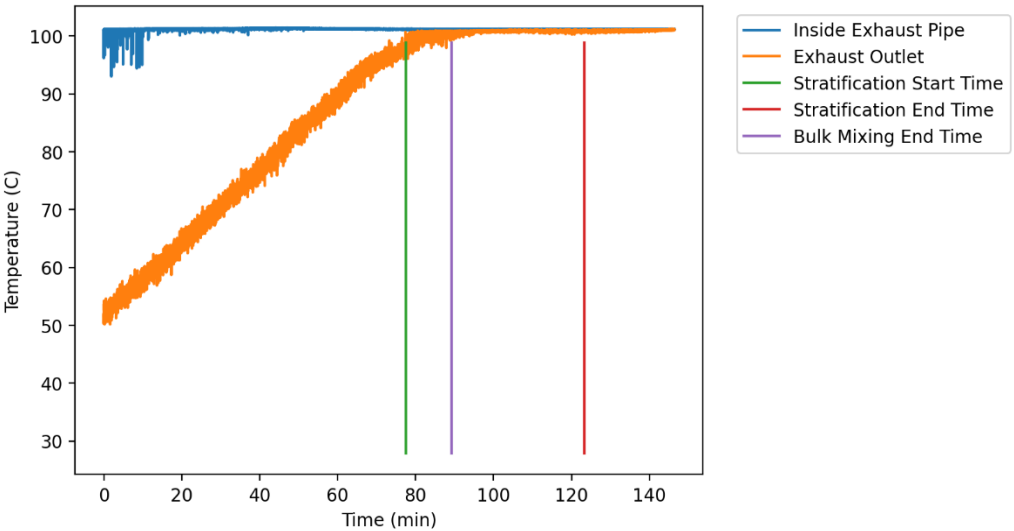


Figure 4.8. Plot of the temperature inside the turbine exhaust line, 4 inches from the outlet, and the water temperature at the outlet for test #2.

4.4.3. Test #3

Test #3 is a sealed pool test with a nominal steam flow rate of 25 g/s. Thermal stratification began approximately 127 minutes after the start of the test and continued until the test was terminated early, 172 minutes later. The bulk pool temperature at the onset of stratification was 51.8 °C, which corresponds to 53.4 °C of subcooling. The test was ended early due to steam leaks from the turbine casing. After the test, discussion with industry experts revealed that some amount of steam is expected to escape from the turbine casing during operation, so this will not result in the early termination of future sealed tank tests. The maximum stratification, which was observed at test termination, was 32.2 °C. The average temperature of thermocouples at each monitored elevation in the pool is plotted in Figure 4.9 below.

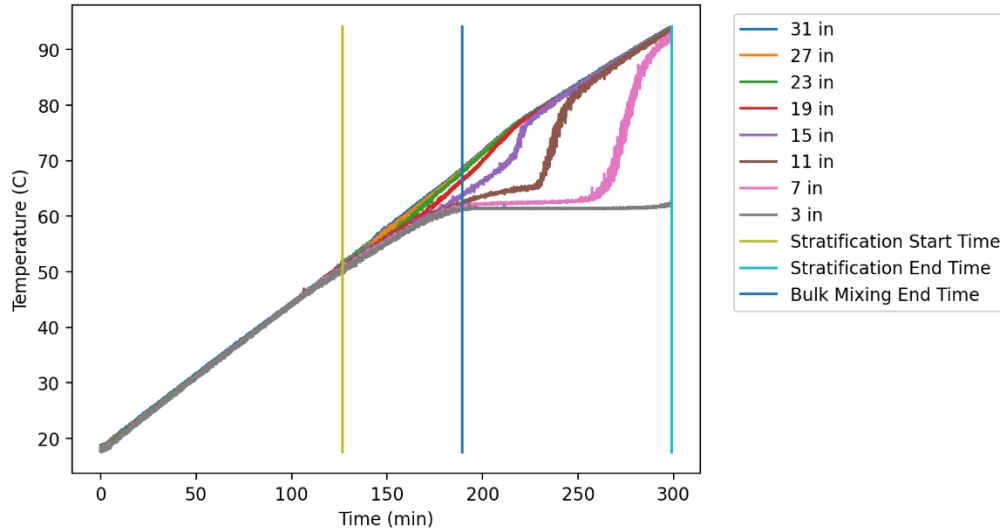


Figure 4.9. Average temperature at each monitored elevation within the suppression pool for test #3.

With the tank sealed, the pressure grew throughout the test until it reached a maximum of 30.0 psia at the time the test was terminated as shown in Figure 4.10. This pressure increase is expected despite full condensation of steam due to heating of non-condensable gases in the airspace of the tank, as well as increased partial pressure from water vapor as the surface water temperature increased.

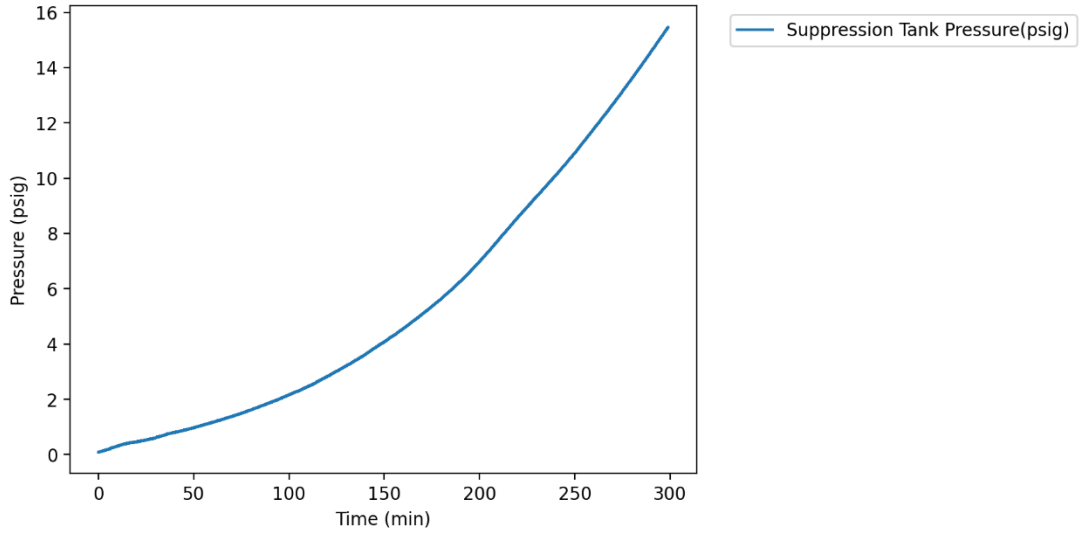


Figure 4.10. Plot of the pressure in the suppression tank during test #3.

This test follows the same trend as Test #1 with regards to chugging in the turbine exhaust line. As shown in Figure 4.11, the end of mixing coincides with the time large temperature oscillations cease in the turbine exhaust line.

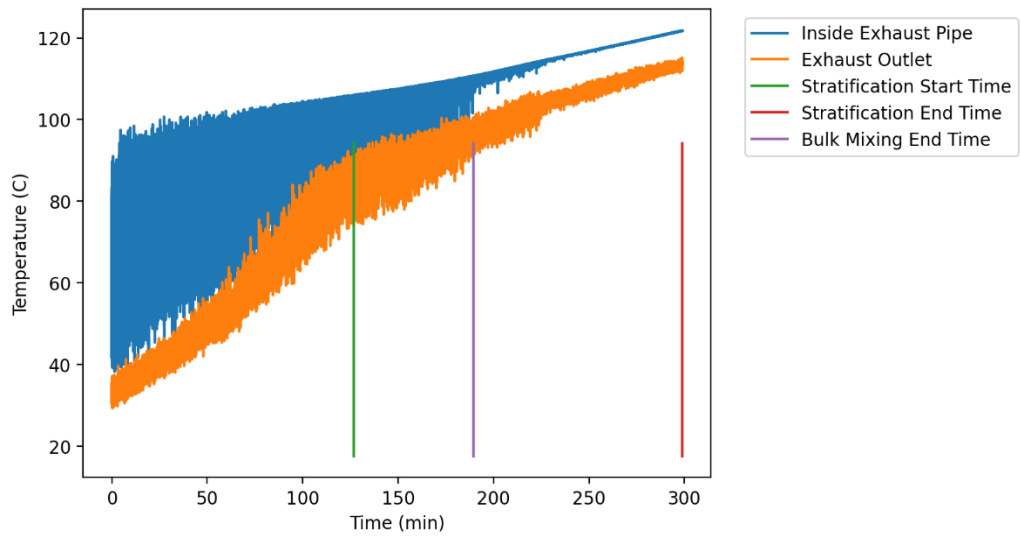


Figure 4.11. Plot of the temperature inside the turbine exhaust line, 4 inches from the outlet, and the water temperature at the outlet for test #3.

4.4.4. Test #4

Test #4 is a sealed pool test with a nominal steam flow rate of 50 g/s. Thermal stratification began approximately 63 minutes after the start of the test and continued for 112 minutes. The bulk pool temperature at the onset of stratification was 67.0 °C, which corresponds to 40.0 °C of subcooling. The maximum stratification observed was 40.9 °C. The test was terminated due to the tank outlet temperature reaching 121 °C, which is the maximum operating temperature of the feedwater pump. The average temperature of thermocouples at each monitored elevation in the pool is plotted in Figure 4.12 below.

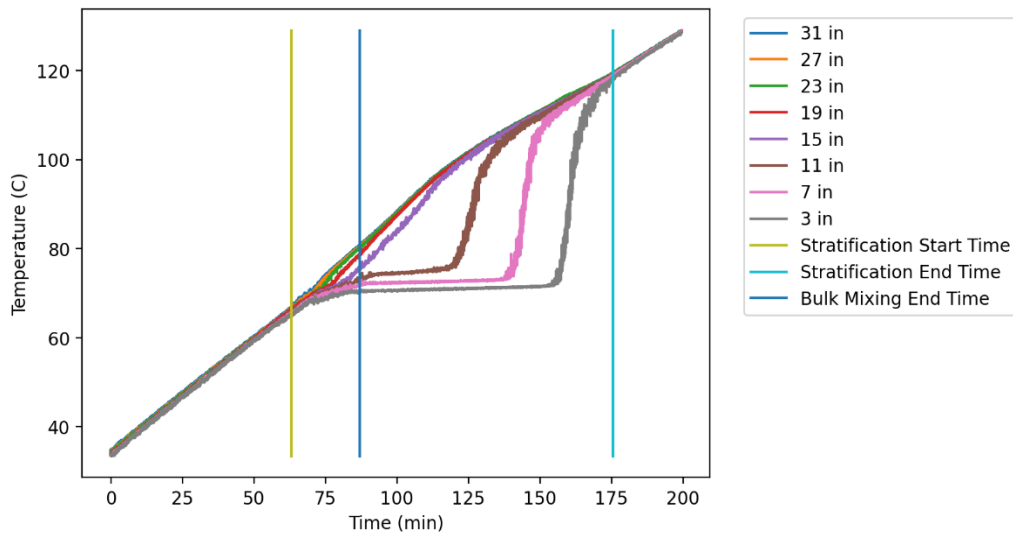


Figure 4.12. Average temperature at each monitored elevation within the suppression pool for test #4.

With the suppression tank sealed, the pressure grew throughout the test until it reached 57.1 psia at the end of the test, as shown in Figure 4.13. Like test #3, a slow, steady steam leak was observed for most of the test as suppression tank pressures rose. While this did not result in test termination, it is important to note that the steam leak was downstream of the vortex flowmeter measuring steam mass flowrate, meaning the actual mass flow rate of steam into the suppression tank is lower than the nominal steam flow rate upstream of the leak. As with the other tests, the temperature at the bottom of the tank near the turbine exhaust line was observed to oscillate while the pool warmed up until stratification began.

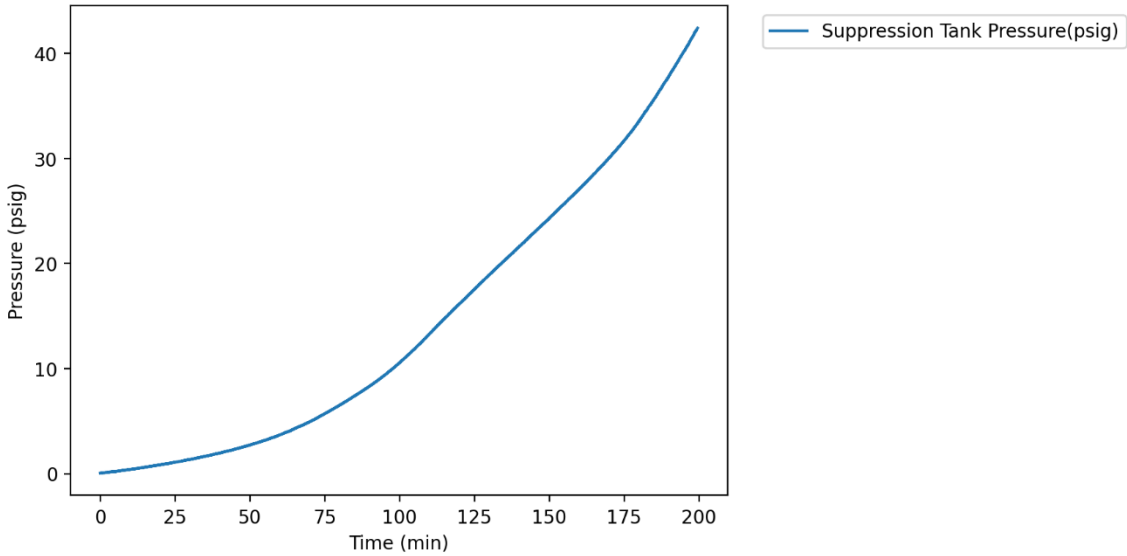


Figure 4.13. Plot of the pressure in the suppression tank during test #4.

As was seen during test #2, onset of thermal stratification coincided with the time the turbine exhaust outlet temperature first neared saturation. As shown in Figure 4.14, bulk mixing in the pool ceased at approximately the same time the turbine exhaust outlet temperature stabilized at saturation.

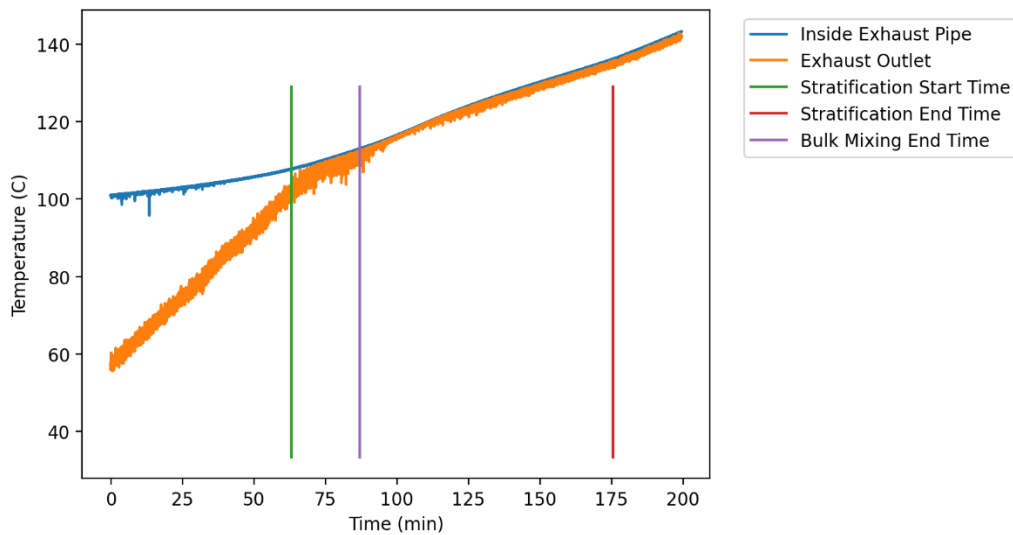


Figure 4.14. Plot of the temperature inside the turbine exhaust line, 4 inches from the outlet, and the water temperature at the outlet for test #4.

4.4.5. Test #5

Test #5 repeats the conditions of test #1, a venting pool test with a nominal steam flowrate of 25 g/s. There are two minor differences between the two tests. First, after test #1, additional insulation was installed in the piping connected to the suppression tank airspace. Second, the pool temperature at the start of the test was higher, which shortened the pre-stratification time of the test. Thermal stratification began approximately 63 minutes after the start of the test and continued for 142 minutes. The bulk pool temperature at the onset of stratification was 48.1 °C, which corresponds to 51.6 °C of subcooling. The maximum stratification observed was 26.2 °C. The test was terminated due to the bulk pool temperature approaching saturation temperature. The average temperature of thermocouples at each monitored elevation in the pool is plotted in Figure 4.15.

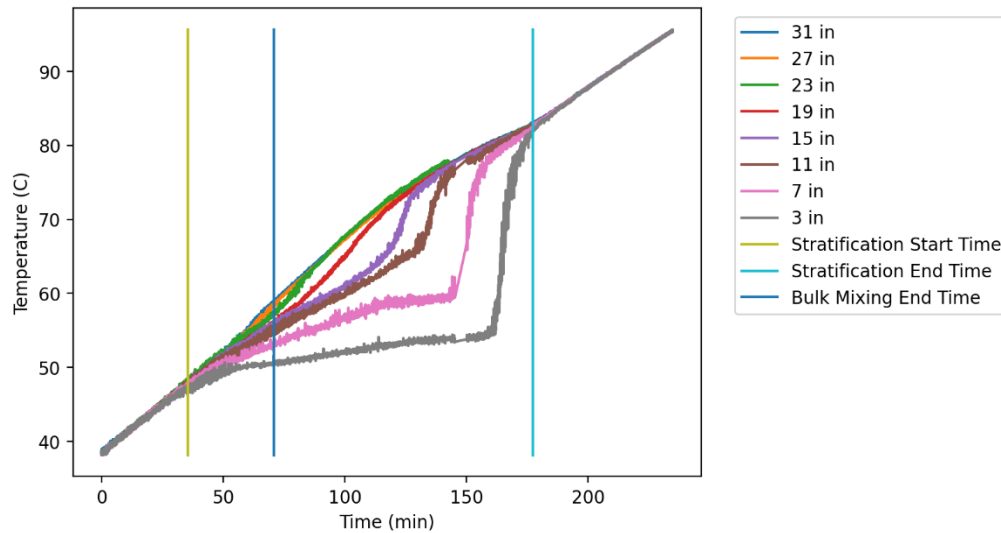


Figure 4.15. Average temperature at each monitored elevation within the suppression pool for test #5.

Comparison with results from test #1 suggests that there is no significant difference between the results of the two tests. The temperature of stratification onset differed by less than 1°C between the two tests; with a temperature uncertainty of 0.5°C for the thermocouples used in this facility, the two temperatures are statistically equal. The maximum stratification observed during the first test was approximately 2°C higher than the second test, which is a statistically significant difference. This slight difference is attributed to the change in insulation, and the difference in ambient conditions during the two tests, which play a direct role during the venting suppression pool tests. The barometric pressure during test #1 was 0.1 psi higher than during test #5, and the room temperature was 5°C lower during test #1.

4.4.6. Test #6

Test #6 is a little different from the other tests performed in this work. It is the only test where the suppression chamber was pre-pressurized before admitting steam, and the pressure was maintained constant throughout. This was accomplished by manually cracking a gate valve to allow air to vent from the chamber to counteract the increase in pressure caused by heating the air and water in the chamber. The nominal steam mass flowrate was 25 g/s. Thermal stratification began approximately 42 minutes after the start of the test and continued for 160 minutes. The bulk pool temperature at the onset of stratification was 50.7 °C, which corresponds to 57.9 °C of subcooling. The maximum stratification observed was 26.0 °C. The test was terminated due to the bulk pool temperature approaching saturation temperature. The average temperature of thermocouples at each monitored elevation in the pool is plotted in Figure 4.16.

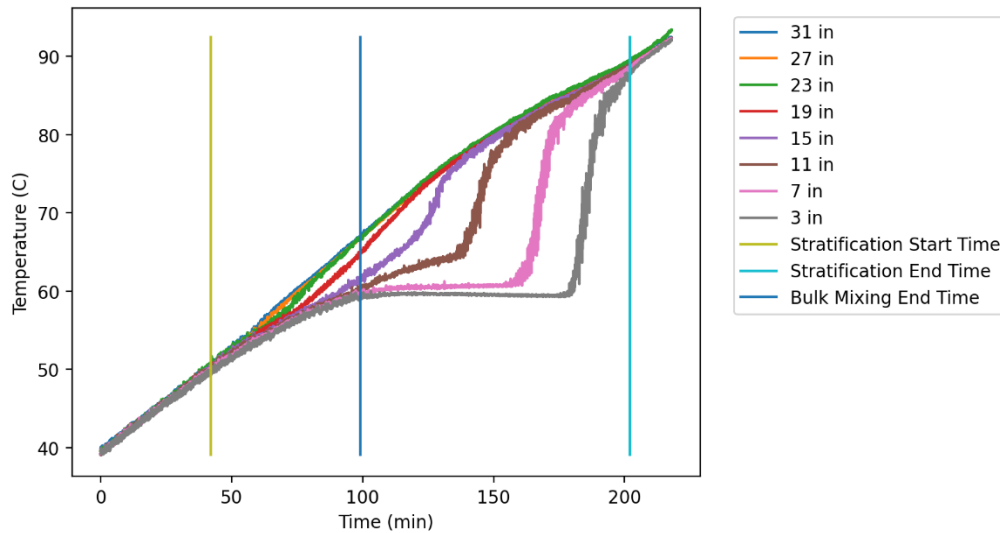


Figure 4.16. Average temperature at each monitored elevation within the suppression pool for test #6.

In contrast to tests #3 and #4, no significant steam leak was observed from the turbine casing since the pressure did not grow much beyond 5 psig as shown in Figure 4.17. Due to the crude pressure control method used, several pressure deviations can be seen. The largest of these occurs near the end of the test when the pressure drops to nearly 4 psig before rising to almost 6 psig. One result of this larger deviation was a change in suppression pool saturation temperature.

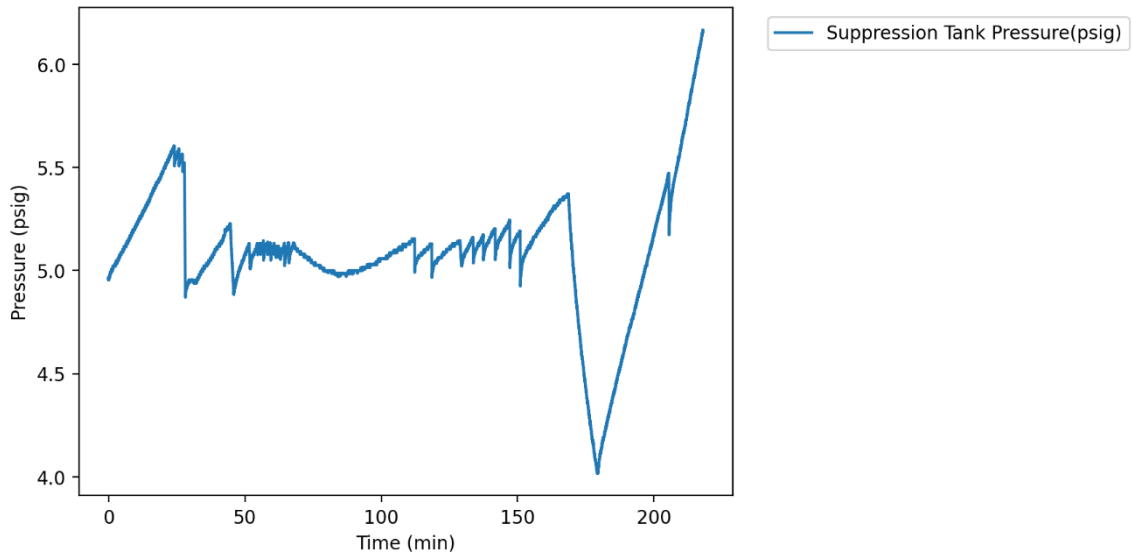


Figure 4.17. Plot of the pressure in the suppression tank during test #6.

As shown in Figure 4.18, bulk pool mixing ceased at approximately the same time the temperature inside the turbine exhaust line began to stabilize, signaling the end of chugging in the pipe. The sudden drop in suppression pool saturation temperature as the suppression chamber pressure fell to 4 psig can be observed in this figure as the saturated steam in the turbine exhaust line changes in temperature to match the new saturation temperature at around 10000 seconds.

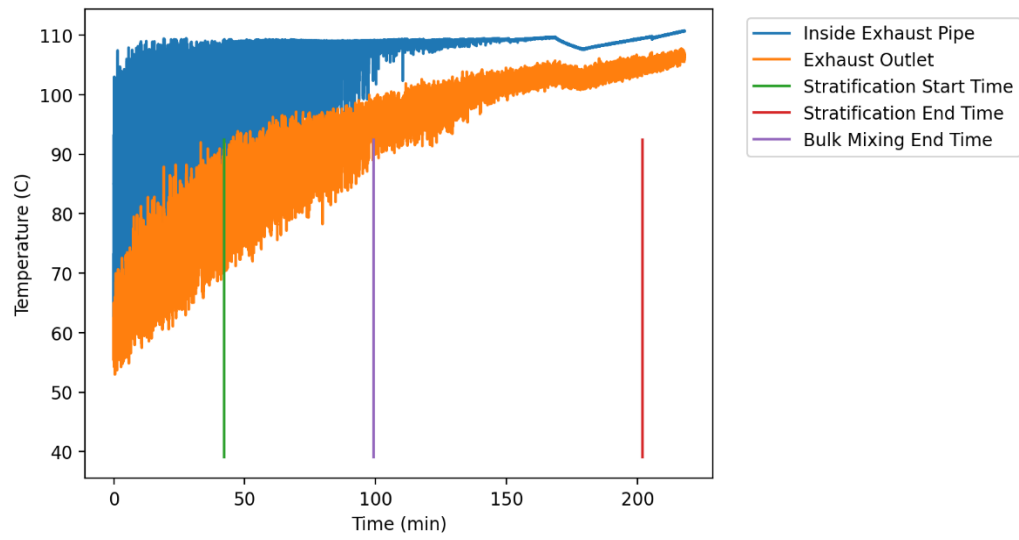


Figure 4.18. Plot of the temperature inside the turbine exhaust line, 4 inches from the outlet, and the water temperature at the outlet for test #6.

4.4.7. Test #7

Test #7 is a sealed tank test following the same procedures as tests #3 and #4, with a nominal steam flowrate of 15 g/s. Thermal stratification began approximately 161 minutes after the start of the test and continued for 308 minutes until the test was terminated. The bulk pool temperature at the onset of stratification was 53.9 °C, which corresponds to 51.3 °C of subcooling. The maximum stratification observed was 38.5 °C. The average temperature of thermocouples at each monitored elevation in the pool is plotted in Figure 4.19 below.

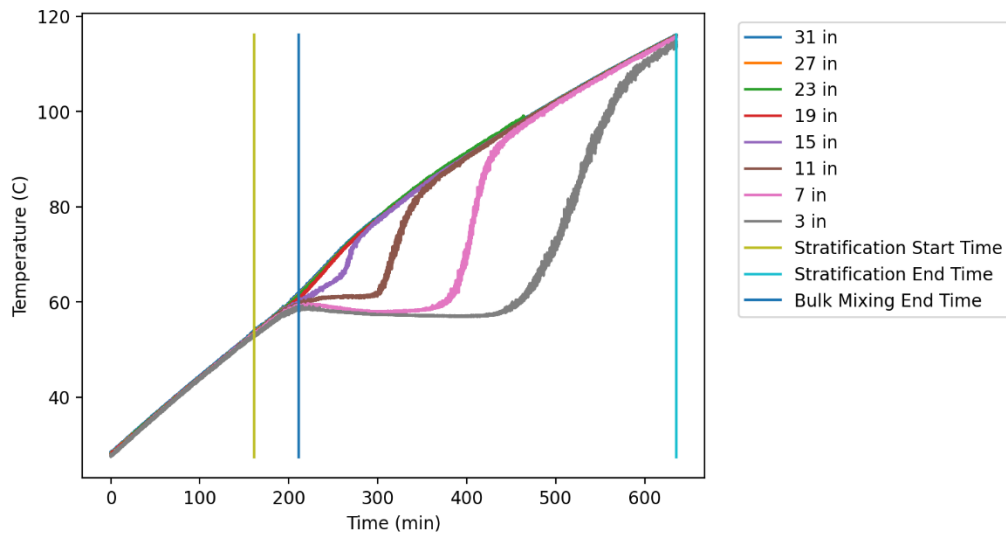


Figure 4.19. Average temperature at each monitored elevation within the suppression pool for test #7.

The test was terminated when it became clear the suppression pool would not reach complete thermal equilibrium since the amount of pool mixing was so small a cold pocket of water had collected at one end of the pool. Since the suppression pool is not set on a perfectly level surface, with the lower end facing away from the tank outlet, the coldest water in the tank was cooler than the water being pumped out of the tank, resulting in temperature oscillations in one thermocouple in the pool that kept the average temperature of the lowest set of thermocouples from reaching the same temperature as the rest of the pool. When thermal stratification closed within 2°C , the test was terminated. Figure 4.20 shows how the amount of thermal stratification began to level off at a value higher than was seen during the mixing period at the beginning of the test.

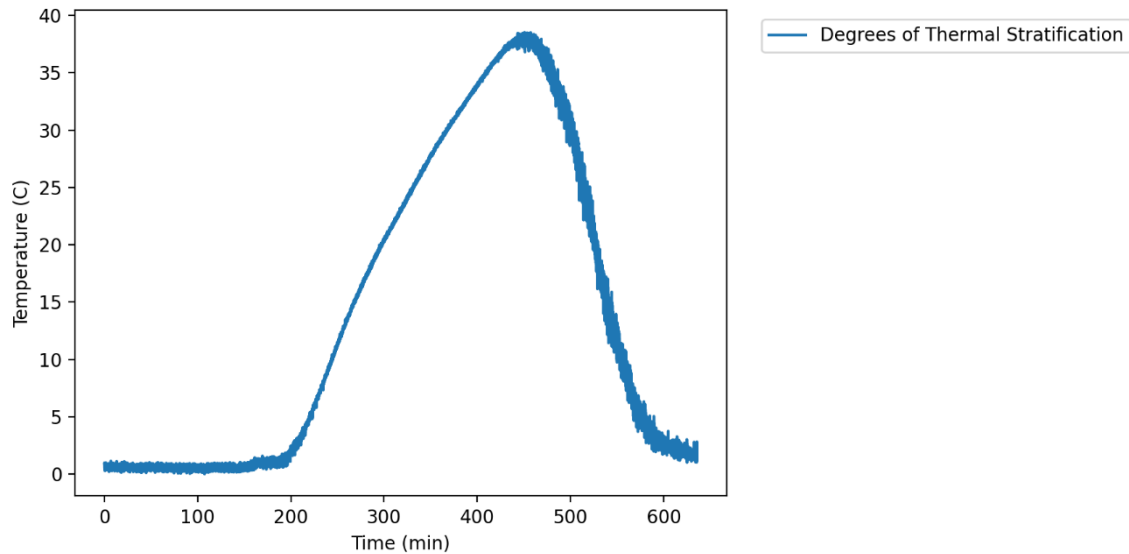


Figure 4.20. Degrees of thermal stratification from the highest elevation thermocouples to the lowest elevation thermocouples during test #7.

The suspected cause for the negligible mixing observed during test #7 is a combination of a low steam mass flowrate, and a high steam leakage rate. As shown in Figure 4.21, the suppression pool pressure was above 15 psig for approximately 4 hours at which point steam was already observed to leak from the turbine casing and through the seal drains. Enough steam had flowed through the seal drains that by half-way through the test, the seal drains collection tank began to overflow. The collection tank, a 55-gallon drum, was drained to about 2/3 of its capacity to avoid overflowing in the future. By the end of the test, the walls of the drum were too hot for operators to touch, and a steady flow of steam was rising from the opening in the top.

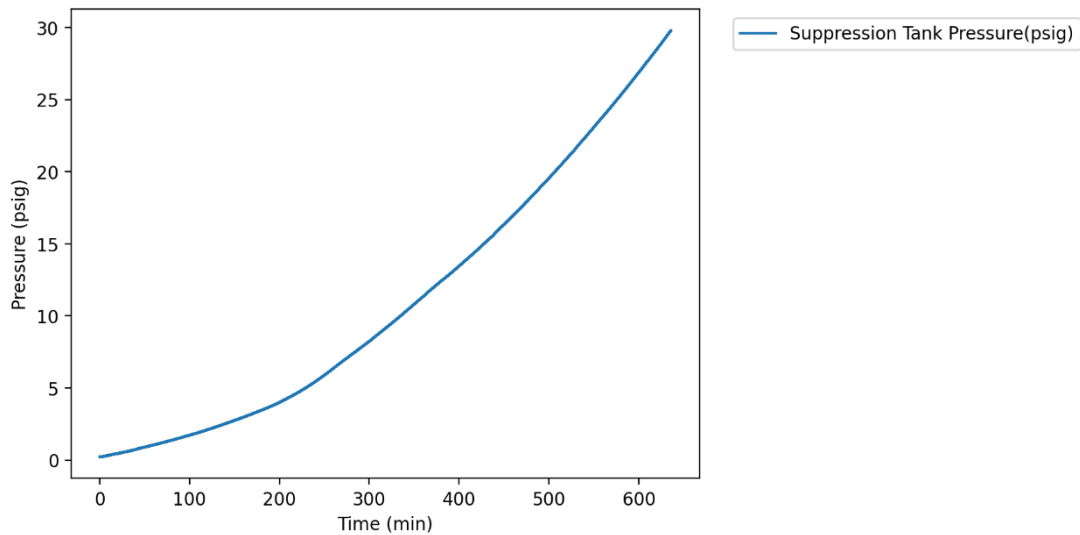


Figure 4.21. Plot of the pressure in the suppression tank during test #7.

While the amount of steam flowing into the suppression tank was certainly less than the nominal 15 g/s of steam flowing into the turbine, Figure 4.22 provides evidence that some amount of steam was still being injected into the pool since the temperature inside the turbine exhaust line stabilized to match the steam saturation temperature, and no evidence of chugging was observed after bulk pool mixing stopped. At the very least, steam was clearing the end of the sparger, but likely with no significant velocity. With such a small amount of steam being condensed, heat transfer from conduction through the pipe into the upper half of the suppression pool is expected to have had a larger effect than in previous tests.

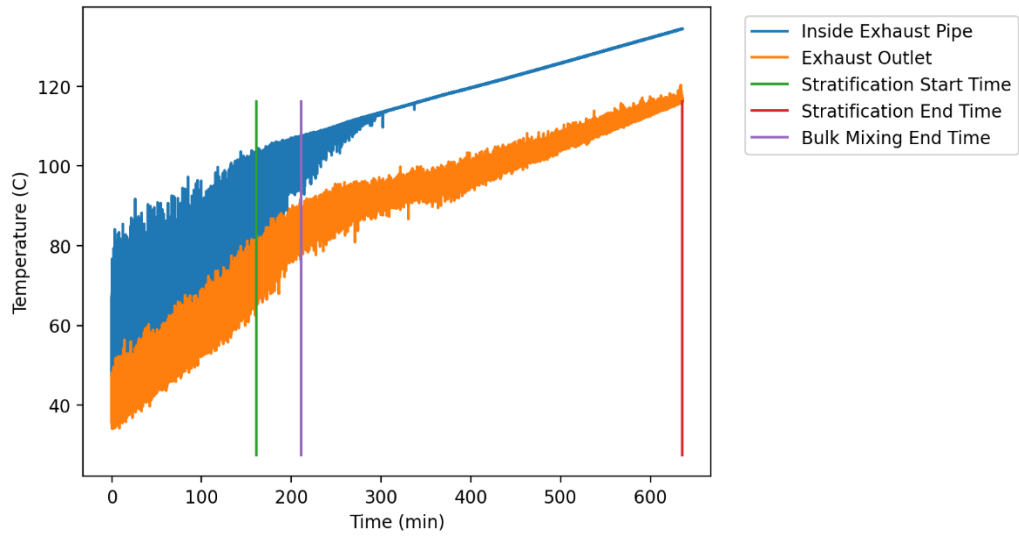


Figure 4.22. Plot of the temperature inside the turbine exhaust line, 4 inches from the outlet, and the water temperature at the outlet for test #7.

5. ANALYSIS

5.1. Goal of Analysis

There are two main goals of data analysis for this work. First is to quantify the effect of thermal stratification on RCIC system performance. The second goal is to identify conditions that maximize the effects of thermal stratification on RCIC system performance. In this case, RCIC system performance is defined as the system's ability to remove heat from the reactor core during an extended isolation event. This ability depends on three main factors: The duration that the RCIC system operates successfully, the rate that water is provided to the reactor pressure vessel, and the heat removed per mass of water. The relationship between these factors and the total heat removal is illustrated in (5.1).

$$Q = \int_{t_{initial}}^{t_{final}} \dot{m} \Delta h \quad (5.1)$$

Where Q is the total heat removed, \dot{m} is the mass flow rate of water returned to the reactor pressure vessel, and Δh is the change in enthalpy of the water from the time it leaves the suppression pool to when it has been boiled in the steam generator and reaches equilibrium with the rest of the steam in the reactor pressure vessel. Except for test #3, which was terminated prematurely due to a steam leak, all tests performed for this work operated long enough to pass the window of time where thermal stratification takes place. For this reason, the data gathered from these tests show no evidence that promoting thermal stratification in the suppression pool will affect the duration of RCIC

system operation. Similarly, the presence of thermal stratification in the suppression pool is not expected to have any effect on the ability of the RCIC pump to provide water to the reactor pressure vessel since the turbine speed is controlled automatically by the governor valve, which results in a controlled water flow rate back to the reactor pressure vessel. Thermal stratification does, however, directly impact the amount of heat a quantity of water will be able to remove from the reactor core. A large amount of stratification would minimize the water temperature near the bottom of the pool where the water is drawn from, while a uniform temperature field would result in a comparatively warmer temperature at the tank outlet. The potential effect of this difference will be discussed here.

5.2. Effect of Thermal Stratification on RCIC System Performance

To quantify the effect of thermal stratification on RCIC system performance, the amount of heat removed in these experiments will be compared with the theoretical amount of heat removed by water from a well-mixed pool with the same average temperature. The change in enthalpy, as called for in (5.1) will be calculated between the suppression chamber outlet and the steam generator. The enthalpy at each location will be calculated using the IAPWS Industrial Formulation 1997 for the Thermodynamic Properties of Water and Steam [39], which determines enthalpy as a function of temperature and pressure. To make comparisons between different tests relevant, a constant nominal enthalpy will be used for the steam generator to remove the effects of steam generator pressure deviations. This enthalpy is the enthalpy of saturated steam at 95 psia, which is the nominal steam generator operating pressure.

In contrast to the thermally stratified pool, where the water outlet is significantly cooler than the bulk pool temperature, outlet water temperature for a well-mixed pool should match the average pool temperature. While pool mixing helps to delay suppression chamber pressurization as the bulk pool approaches saturation temperature, thermal stratification ends in each of these experiments significantly before the hottest point in the pool approaches saturation temperature, so there should be no significant difference in pressure between the mixed and unmixed pools. For these reasons, enthalpy calculations for the theoretical mixed pool outlet water will use the average pool temperature and pressure from the corresponding stratified pool test. To best compare the mixed and unmixed pools, only the heat removed during the period of the test when thermal stratification is observed will be considered. As shown in Table 5.1, thermal stratification is expected to improve RCIC system performance by 2-6% over the stratification period.

Table 5.1. Effect of Thermal Stratification on RCIC System Heat Removal

Test	Actual Heat Removed (kJ)	Theoretical Heat Removed with Mixed Pool (kJ)	Relative Heat Removal Improvement (%)
1	556,000 ± 11.0%	539,000 ± 11.0%	3.01 ± 0.353
2	279,000 ± 6.7%	273,000 ± 6.7%	2.24 ± 0.193
3	640,000 ± 11.2%	624,000 ± 11.2%	2.55 ± 0.310
4	804,000 ± 5.7%	771,000 ± 5.7%	4.34 ± 0.277
5	549,000 ± 10.5%	533,000 ± 10.5%	2.97 ± 0.334
6	599,000 ± 11.2%	579,000 ± 11.2%	3.44 ± 0.403
7	1,100,000 ± 18.1%	1,040,000 ± 18.1%	5.94 ± 1.08

5.2.1. Error Analysis

Without enough test repetitions using the same test conditions, a full statistical analysis of the error is not possible with the data gathered in this work. However, determination of the total uncertainty in the data due to instrument uncertainties is possible. This was accomplished by the commonly used error propagation formula given in equation (5.2).

$$\sigma_u^2 = \left(\frac{\partial u}{\partial x}\right)^2 \sigma_x^2 + \left(\frac{\partial u}{\partial y}\right)^2 \sigma_y^2 + \left(\frac{\partial u}{\partial z}\right)^2 \sigma_z^2 + \dots \quad (5.2)$$

where

$$u = u(x, y, z, \dots)$$

Time is treated as an exact value in all uncertainty calculations performed for this work.

When calculating the uncertainty of values such as the steam specific enthalpy or density, direct calculation of derivatives as shown in equation (5.2) is infeasible due to the complexity of the IAPWS industrial formulation. In such cases, $\frac{\partial u}{\partial x}$ is linearly approximated near the measurement value using equation (5.3) which calculates the sensitivity of u to changes in each variable individually.

$$\frac{\partial u}{\partial x} \cong \frac{u\left(x + \frac{\sigma_x}{2}, y, z, \dots\right) - u\left(x - \frac{\sigma_x}{2}, y, z, \dots\right)}{\sigma_x} \quad (5.3)$$

5.2.2. Optimal Conditions to Maximize the Benefit of Thermal Stratification

To identify optimal conditions to maximize the benefit thermal stratification has on the RCIC system's performance, the results of each test will be compared to each other as a function of pressure, water flow rate, and degrees of thermal stratification. To account for differing test durations, the parameter of interest will be the change in average heat removal rate, instead of the total amount of heat removed as discussed previously. Average heat removal rate during the stratification period will be calculated using Equation (5.4)

$$q = \frac{\int_{t_{initial}}^{t_{final}} \dot{m} \Delta h}{t_{final} - t_{initial}} \quad (5.4)$$

which is simply the total heat removed during the stratification period divided by the duration of the stratification period. Table 5.2 presents the actual heat removal rate for each test, the theoretical heat removal rate with a mixed pool, and the difference between the two.

Table 5.2. Effect of Thermal Stratification on RCIC System Heat Removal Rate

Test	Actual Heat Removal Rate (kW)	Theoretical Heat Removal Rate with Mixed Pool (kW)	Heat Removal Rate Improvement (kW)
1	63.56 ± 11.0%	61.70 ± 11.0%	1.86 ± 0.073
2	101.48 ± 6.7%	99.25 ± 6.7%	2.23 ± 0.121
3	61.92 ± 11.2%	60.38 ± 11.2%	1.54 ± 0.072
4	119.33 ± 5.7%	114.36 ± 5.7%	4.97 ± 0.143
5	64.46 ± 10.5%	62.60 ± 10.5%	1.86 ± 0.074
6	62.37 ± 11.2%	60.30 ± 11.2%	2.07 ± 0.072
7	38.55 ± 18.1%	36.39 ± 18.1%	2.16 ± 0.045

As a first step, the heat rate improvement was plotted against pressure, water mass flowrate, and average degrees of thermal stratification, and overlaid with a linear fit as generated by the python `scipy.optimize.curve_fit` package.

As shown in Figure 5.1, the data does not appear to fit a linear trend in terms of pressure. The lowest heat removal rate improvement was observed for test #3, however it is possible this result was affected by early test termination due to steam leaks. The highest heat removal rate improvement was observed for test #4, during which the pressure was highest in the suppression chamber. Aside from the large increase at the high end of the pressure range, pressure does not appear to have any direct correlation with heat removal rate improvement.

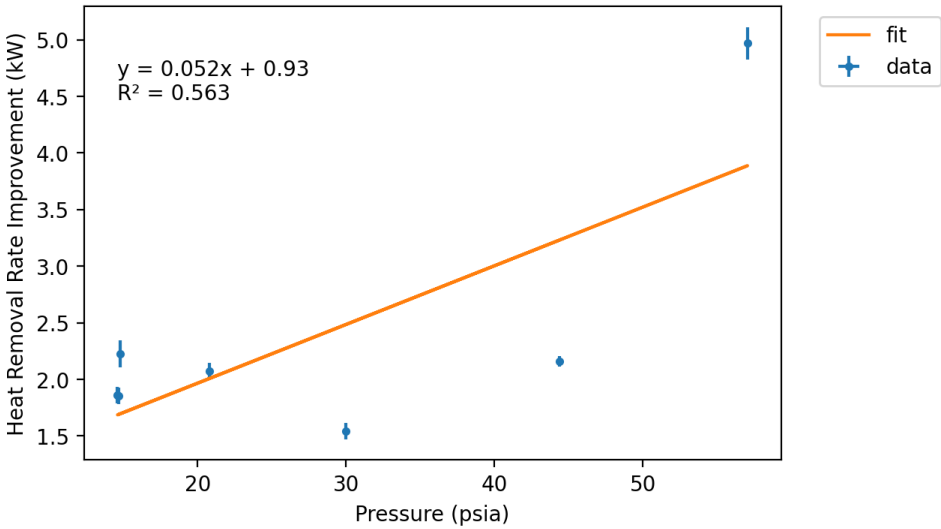


Figure 5.1. Plot of heat rate improvement as a function of suppression chamber pressure.

Likewise, as shown in Figure 5.2, the heat removal rate improvement does not appear to be directly correlated with the average degrees of thermal stratification. In fact, if the highest value is removed, the results would be essentially flat with respect to degrees of thermal stratification.

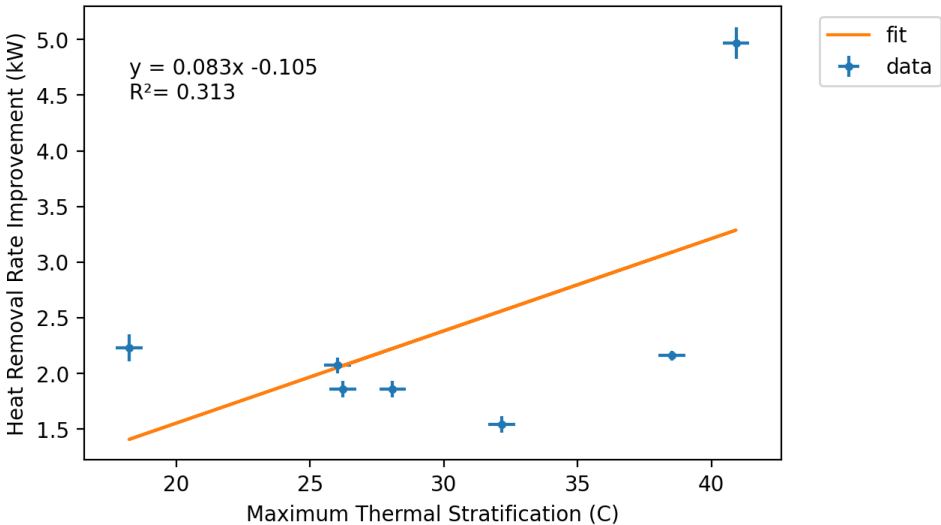


Figure 5.2. Plot of Heat Rate Improvement as a function of the average degrees of thermal stratification.

Figure 5.3 shows that the heat rate improvement does increase with increased water mass flow rate, but the test with the highest mass flow rate, test #2, showed significantly less improvement than test #4 which had the second highest flowrate. Clearly, none of these parameters has been shown to be a dominant factor in predicting the amount of heat removal rate improvement one should expect due to thermal stratification.

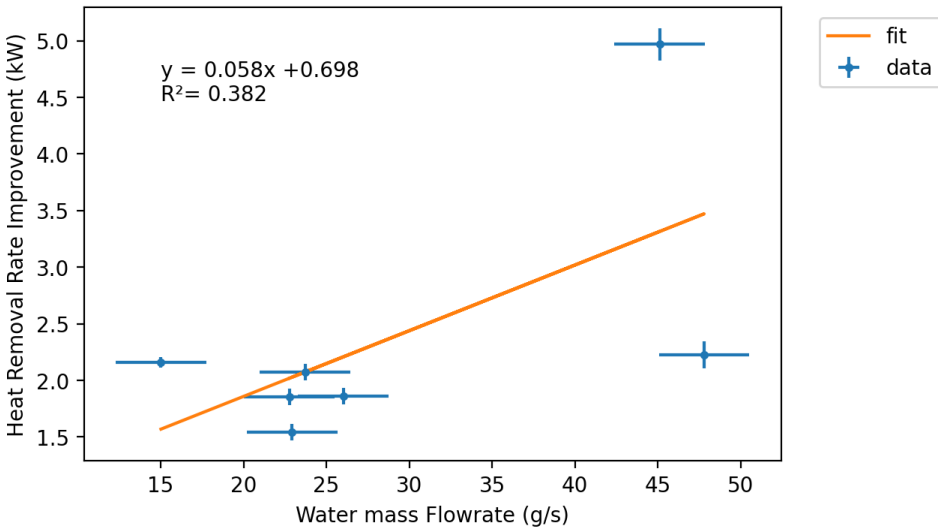


Figure 5.3. Plot of heat rate improvement as a function of water mass flowrate.

While the heat removal rate improvement does increase overall with increasing pressure, thermal stratification, and water mass flowrate, it is not strongly correlated with any of these variables separately. A combined variable is proposed to consider both the water mass flowrate and the average degrees of thermal stratification by plotting the heat removal rate improvement against the product of the mass flowrate and degrees of thermal stratification. The results of this comparison are shown in Figure 5.4, and suggest a strong correlation between heat removal rate improvement and the combined effects of water mass flowrate and degrees of thermal stratification. Optimal benefits from thermal stratification are expected to occur when thermal stratification is maximized at high water return flow rates. Further testing at intermediate flowrates will be required to explore the dataspace between the highest value and the lower values.

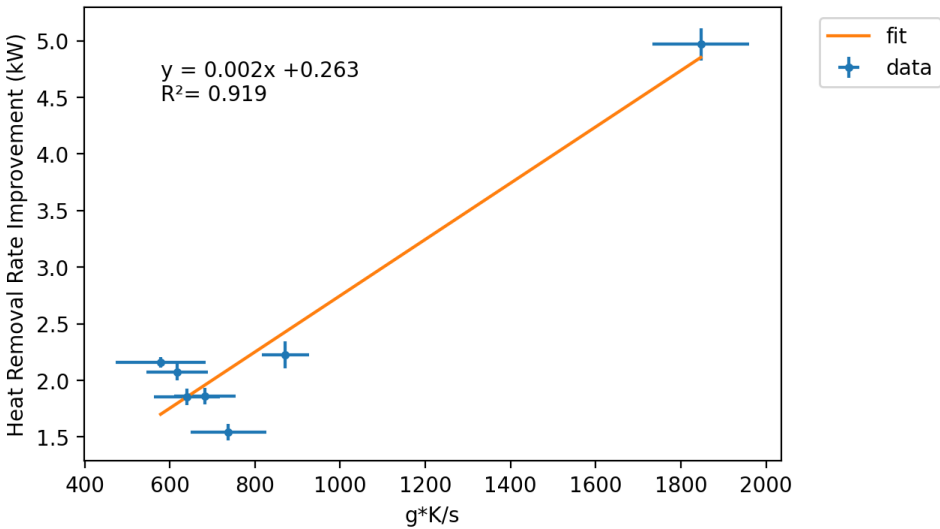


Figure 5.4. Heat Removal Rate Improvement as a function of a combined variable, mass flowrate \times degrees of thermal stratification.

5.2.3. Optimal conditions to promote thermal stratification

Since the performance of the RCIC system can be best improved by increasing both the water flow rate and extent of thermal stratification, a proposed strategy to maximize the effectiveness of the RCIC system is to induce thermal stratification when the water flow rate is maximized, and conditions allow the greatest amount of thermal stratification. This work considers two factors that can affect the amount of thermal stratification that exists in the suppression pool. These are the mass flowrate of steam, and the suppression chamber pressure. Table 5.3 shows the average steam mass flowrate, average suppression chamber pressure, and the maximum degrees of thermal stratification observed during each test. It can also be seen in Table 5.3 that the two tests performed with the highest steam mass flowrate did not experience thermal stratification until the pool was almost 20 °C hotter than the lower flowrate tests.

Table 5.3 Test conditions and maximum thermal stratification observed for each test

Test	Steam Flowrate (g/s)	Suppression Chamber Pressure (psia)	Maximum Thermal Stratification ($^{\circ}\text{C}$)	Temperature at onset of thermal stratification
1	$25.0 \pm 1\%$	14.71 ± 0.126	28.1 ± 0.5	49.0 ± 0.5
2	$50.0 \pm 1\%$	14.80 ± 0.126	18.2 ± 0.5	68.6 ± 0.5
3	$25.0 \pm 1\%$	29.98 ± 0.126	32.2 ± 0.5	51.8 ± 0.5
4	$50.0 \pm 1\%$	57.06 ± 0.126	40.9 ± 0.5	67.0 ± 0.5
5	$25.0 \pm 1\%$	14.61 ± 0.126	26.2 ± 0.5	48.1 ± 0.5
6	$25.0 \pm 1\%$	20.81 ± 0.126	26.0 ± 0.5	50.7 ± 0.5
7	$15.0 \pm 1\%$	44.40 ± 0.126	38.5 ± 0.5	53.9 ± 0.5

The steam flowrate directly influences the amount of thermal stratification since steam injection is the primary source of mixing in the pool. Contrary to this expectation, if all the data collected in this experiment is compared as a function of steam flow rate, there does not appear to be any correlation, as shown in Figure 5.5.

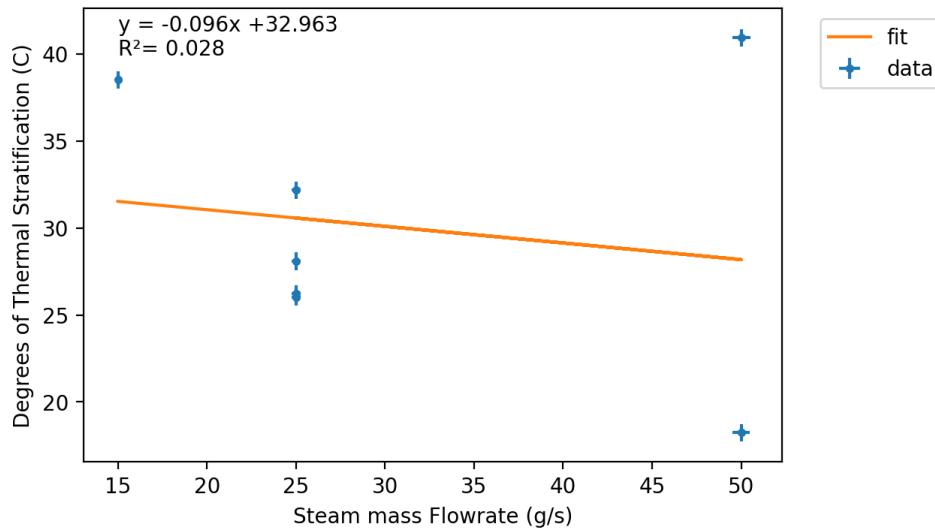


Figure 5.5. Plot of maximum thermal stratification as a function of steam mass flowrate.

There are two confounding factors that affect the results displayed in Figure 5.5. First, the effect of different suppression chamber pressures is not accounted for, meaning that any correlation between steam flowrate and thermal stratification could be lost in a stronger correlation with pressure. Second, due to steam leaks during pressurized tests, the exact flowrate of steam that is injected into the suppression pool is unknown. By considering only the data from tests performed at atmospheric pressure, each of the confounding factors can be circumvented during this preliminary analysis. As shown in Figure 5.6, if only the tests performed at atmospheric pressure are considered, an inverse relationship between the steam mass flowrate and the extent of thermal stratification is evident. Further testing at intermediate flowrates will be required to better characterize the relationship.

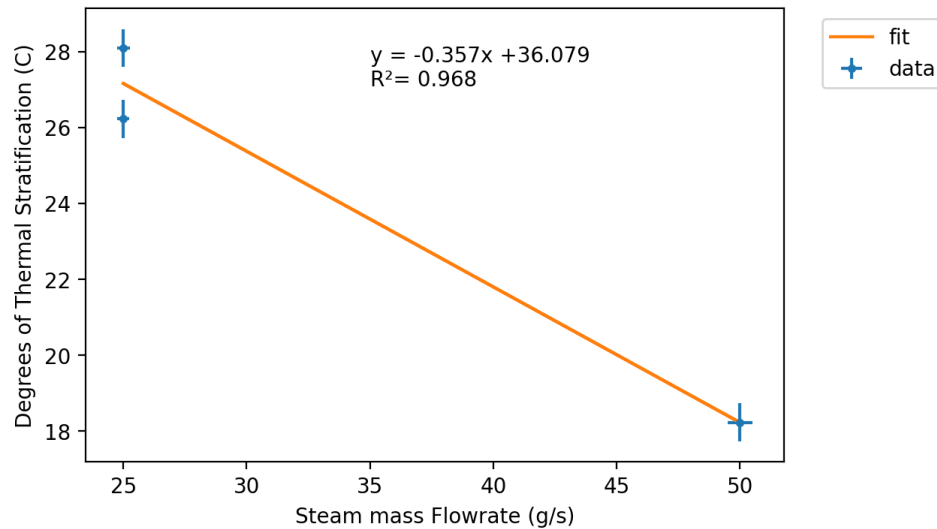


Figure 5.6. Plot of maximum thermal stratification as a function of steam mass flowrate for tests performed at atmospheric pressure.

The suppression chamber pressure influences thermal stratification since the saturation temperature of steam increases as a function of pressure. By maximizing the steam saturation temperature inside containment, the surface temperature limit increases, allowing for a greater temperature difference between the top and bottom of the water space inside the suppression pool. As demonstrated in Figure 5.7, the results from the experiments conducted for this work suggest a strong correlation between the suppression pool pressure and the degrees of thermal stratification observed. Visual inspection of Figure 5.7 suggests the relationship is non-linear, but since the steam mass flowrate is not constant across the tests a definitive statement about the exact nature of the correlation cannot be made. Further testing will be required to better characterize the relationship between suppression pool pressure and the extent of thermal stratification.

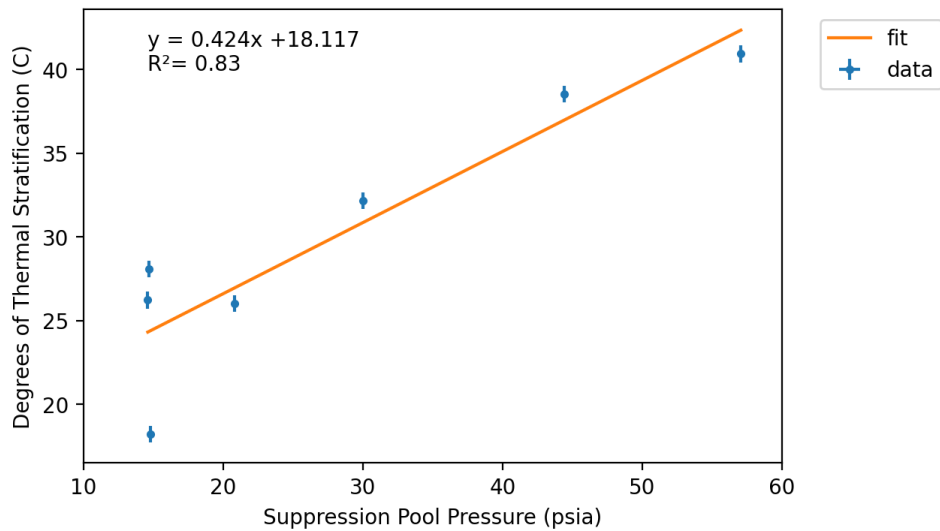


Figure 5.7. Plot of the maximum degrees of thermal stratification observed in the suppression pool as a function of suppression pool pressure.

5.3. Discussion of Reactor Safety Implications

The primary objective for the RCIC system is to maintain water inventory in the reactor pressure vessel such that the reactor core is never uncovered during an isolation event. If the reactor core becomes uncovered, fuel cladding oxidation can lead to rapid increases in fuel temperature that jeopardize fuel integrity as well as produce non-condensable gases including flammable hydrogen. In addition, increased fuel temperature exacerbates the problem of introducing water to the reactor pressure vessel since it will boil the water off more quickly. By maximizing the RCIC system's ability to remove the heat from the reactor, these dangers can be avoided. It has been shown that RCIC system performance is strongly influenced by the extent of thermal

stratification within the suppression pool. By maximizing the extent of thermal stratification during the earlier stages of RCIC system operation when reactor decay heat is highest, decay heat removal rate can be improved by as much as 5% compared to a well-mixed suppression pool.

The results of this work show that thermal stratification with the suppression pool is strongly dependent on the pressure within the suppression chamber, with maximum stratification occurring under high-pressure conditions. However, the entire purpose of the suppression pool is to keep containment pressure low by condensing steam released from the reactor pressure vessel so actively pressurizing the suppression chamber would be counterproductive. One potential strategy to take advantage of the effects of higher pressures would be to compartmentalize the suppression chamber airspace into a smaller, pressurized chamber which interfaces with a larger unpressurized chamber via a PRV. The smaller, pressurized chamber would provide conditions promoting thermal stratification in the suppression pool during the operation period where decay heats are highest, maximizing the RCIC system's performance when it is most necessary. Once the pressure in the smaller compartment exceeds some operational limit, the PRV would open, equalizing the pressure between the two compartments at a safe level for long-term operation. Another option to take advantage of initially high pressures without endangering containment integrity would be to pre-pressurize the entire containment and initiate a controlled vent procedure once the pressure rises to a certain upper limit before core damage has occurred.

An alternative strategy to maximize thermal stratification within the suppression pool without purposefully subjecting the suppression chamber to elevated pressures, is to employ a different turbine exhaust sparger design. One such design could be the perforated pipe design utilized in Fukushima Daiichi Unit 3 and other BWR power plants in the United States [6].

5.4. Scaling Discussion

While the experimental facility used for this work is not an exact model of the full-size RCIC system as found in BWR power plants, there is some basis for scalability as discussed in Matthew Solom's dissertation [19]. For instance, while the full-scale RCIC system is estimated to produce Mach numbers in the turbine exhaust sparger near to 0.1, tests performed in this work ranged in Mach number from 0.04 to 0.13. Similarly, while steam injection rates in a full-size plant are much higher than produced in this facility, the facility can produce mass fluxes comparable to the full-scale steam mass flux of approximately $39 \text{ kg/m}^2\text{s}$. Tests in this work produced steam mass fluxes ranging from $11.4 \text{ kg/m}^2\text{s}$ to $38.1 \text{ kg/m}^2\text{s}$. Similarity of steam injection velocities and mass fluxes gives confidence that steam injection conditions are comparable to the full-scale RCIC system.

Unfortunately, not every aspect of the facility scales so nicely. First, the shape of the suppression chamber analog used in this work differs from the toroidal suppression chamber shape used in the BWR Mark I containment. Depending on the specific BWR containment considered, suppression pool water volumes range from 75,000 cubic feet to 125,000 cubic feet, which correspond to a range of volume ratios from 1:750 –

1:1300. The turbine exhaust sparger diameter scales to 1:6.9 compared to the sparger used in Fukushima Unit 2 while the suppression chamber diameter scales to 1:5.9 [19].

Additionally, the ratio of liquid to gas volume in this facility's suppression chamber is not the same as in the real containment. The airspace in the real suppression chamber is connected to the entire drywell, and the suppression pool fills less than half the available volume. In this facility, the suppression chamber analog is filled slightly over halfway so that the sparger outlet could be submerged by at least one foot of water without reaching so far down into the suppression chamber that there is no space for stratification to develop. Further tests using different sparger submergence depths and water levels would be helpful to understand the effect of this difference.

Another factor that is not perfectly captured in these tests is the steam conditions prior to admittance by the steam governor valve. While the main steam valve in this facility allows for good control of steam flowrates, the steam generator pressure is far less than what would be produced in a true BWR reactor vessel. Since the suppression chamber pressure is the same for both facilities, the very high steam supply pressure of 2300 psi in the reactor vessel would result in much higher temperature steam being injected into the suppression pool than can be produced in this facility. Testing with alternative steam supply pressures could provide insight into the magnitude of this effect.

6. CONCLUSIONS

In this work, the development of thermal stratification within BWR containment suppression pools was investigated experimentally. Particularly, the benefit of thermal stratification to the overall performance of the RCIC system, whose purpose is to supply cooling water to the reactor pressure vessel during isolation events, was demonstrated. This work identified desirable operating conditions to maximize the benefits due to thermal stratification.

The formation of thermal stratification in the suppression pool is dependent on multiple factors including the existence of active mixing measures, the steam injection rate into the suppression pool, and the suppression chamber pressure. Active mixing, whether accomplished by injecting steam horizontally into the pool or recirculating pool water with pumps, was seen to be effective in ending thermal stratification promptly during facility shutdown procedures. High steam injection rates tended to correlate with lesser extents of thermal stratification due to the inherent mixing caused by exhausting large amounts of steam into the pool. This was particularly prevalent while suppression pool temperatures were low, resulting in condensation-induced chugging inside the turbine exhaust line, which mixed the pool very effectively. The largest amounts of thermal stratification were recorded in cases where the suppression pool pressure was high. Increased suppression pool pressures result in high water saturation temperatures, which increases the amount of local subcooling, assuring complete steam condensation. By maximizing the saturation temperature in the suppression pool, steam was condensed

by the subcooled water near the turbine exhaust outlet instead of traveling lower into the pool which would promote mixing.

Thermal stratification within the suppression pool is advantageous for RCIC system performance because it minimizes the temperature of water being pumped into the reactor pressure vessel. By decreasing the temperature of cooling water, the amount of decay heat removed from the reactor core by a given volume of water is maximized, in addition to protecting the RCIC pump from detrimental effects of high temperatures which could lead to premature RCIC system failure. In all cases tested in this work, thermal stratification in the suppression pool was shown to improve heat removal capacity by a minimum of 2% compared to a well-mixed pool, while tests with larger amounts of thermal stratification and higher water flowrates saw improvements as high as 6% relative to a well-mixed pool.

Since the largest amount of water is provided to the reactor pressure vessel during the early stages of core cooldown while decay heat is at a maximum, the potential benefits due to thermal stratification are greatest during early operation. Unfortunately, thermal stratification is less prominent during early stages of operation while the suppression pool pressure remains low. One possible strategy to capitalize on the benefits of thermal stratification early in operation is to utilize a RCIC turbine exhaust sparger design that promotes thermal stratification, unlike the open-ended pipe used in this work and in Fukushima Daiichi Unit 2. Another strategy that would take advantage of the effects of high pressure on thermal stratification development would be to

artificially increase the pressure inside the suppression chamber either through pre-pressurization with air or by constricting the airspace volume.

Further testing, particularly with alternative turbine exhaust sparger designs and additional pressure and steam flowrate conditions, would allow more definitive characterization of thermal stratification development in suppression pools. Testing with alternative turbine exhaust spargers would also aid in applying the results of this work to more BWR units throughout the United States in addition to those that utilize the open-ended pipe design. Additional testing will also be required to confirm behavior in full-scale RCIC systems.

6.1. Key Findings

The following are major findings from this work:

- RCIC system capacity to remove heat was determined to improve by 2-6% during the thermal stratification period.
- Higher suppression chamber pressure correlates to greater thermal stratification in suppression pools.
- The greatest opportunity to capitalize on the benefits from thermal stratification in suppression pools is in the early stages of RCIC system operation.

6.2. Future Work

Although this work adhered to a careful testing plan and robust set of operating procedures, the first work performed in any facility will lead to the discovery of potential ways to improve and expand upon preliminary investigations. The

following are suggested future efforts to further the investigation presented in this work:

- Test with additional steam flow rates.
- Repeat the controlled venting test using higher constant pressures.
- Account for steam leakage by either reinforcing turbine seals to avoid steam leakage or quantify the leak rate.
- Actively mix the suppression pool under each test condition to provide mixed-pool data instead of calculating approximate behavior.
- Replace the turbine exhaust sparger with other sparger designs to investigate the effect on thermal stratification.
- Change the amount of water in the pool to see the effect of sparger submergence depth
- Investigate the effect of changing the steam supply pressure

REFERENCES

- [1] National Police Agency of Japan, "National Police Agency," 10 March 2020.
[Online]. Available:
https://www.npa.go.jp/news/other/earthquake2011/pdf/higaijokyo_e.pdf.
[Accessed 13 March 2020].
- [2] Institute of Nuclear Power Operations, "Special Report on the Nuclear Accident at the Fukushima Daiichi Nuclear Power Station," November 2011. [Online].
Available: <https://www.nrc.gov/docs/ML1134/ML11347A454.pdf>. [Accessed 25 February 2021].
- [3] American Nuclear Society, "Fukushima Daiichi: ANS Committee Report," June 2012. [Online]. Available: http://fukushima.ans.org/report/Fukushima_report.pdf.
[Accessed 25 February 2021].
- [4] USNRC Technical Training Center, "Reactor Concepts Manual, Boiling Water Reactor (BWR) Systems," [Online]. Available: <https://www.nrc.gov/reading-rm/basic-ref/students/for-educators/03.pdf>. [Accessed 19 February 2021].
- [5] Tokyo Electric Power Company, "Unit 2 RCIC quencher," 30 October 2031. [Online]. Available: https://fdada.info/docs/pdf/Unit2_RCIC-quencher.pdf.
[Accessed 22 February 2021].

- [6] Tokyo Electric Power Company, "Unit 3 RCIC Quencher," 30 October 2013. [Online]. Available: https://fdada.info/docs/pdf/Unit3_RCIC-quencher.pdf. [Accessed 22 February 2021].
- [7] U.S. Nuclear Regulatory Commission, "Suppression Pool Temperature Limits for BWR Containments," November 1981. [Online]. Available: <https://www.nrc.gov/docs/ML1321/ML13217A292.pdf>. [Accessed 22 February 2021].
- [8] USNRC Technical Training Center, "Boiling Water Reactor GE BWR/4 Technology Advance Manual," [Online]. Available: <https://www.nrc.gov/docs/ML0230/ML023010606.pdf>. [Accessed 22 February 2021].
- [9] US NRC, "U.S. boiling-water reactors with "Mark 1" and "Mark 2" containments," 27 July 2020. [Online]. Available: <https://www.nrc.gov/reactors/operating/ops-experience/japan/us-boiling-water-reactors.html>. [Accessed 22 February 2021].
- [10] US NRC, "List of Power Reactor Units," 27 August 2020. [Online]. Available: <https://www.nrc.gov/reactors/operating/list-power-reactor-units.html>. [Accessed 22 February 2021].
- [11] World Nuclear Association, "Fukushima Daiichi Accident," January 2021. [Online]. Available: <https://world-nuclear.org/information-library/safety-and->

- security/safety-of-plants/fukushima-daiichi-accident.aspx. [Accessed 22 February 2021].
- [12] J. Vandervort, G. Lukasik, B. Ayyildiz, M. Solom, A. Delgado, K. V. Kirkland and A. Patil, "Performance evaluation of a Terry GS-2 steam impulse turbine with air-water mixtures," *Applied Thermal Engineering*, vol. 191, no. 116636, 2021.
- [13] A. Patil, Y. Wang, M. Solom, A. Alfandi, S. Sunday, K. V. Kirkland and G. Morrison, "Two-phase operation of a Terry steam turbine using air and water mixtures as working fluids," *Applied Thermal Engineering*, vol. 165, no. 114567, 2020.
- [14] Terry Steam Turbine Company, *Emergency Feedwater Pump Turbine Vendor Manual 00036-000*, 2010.
- [15] T. P. Freyman, "Effect of Oil Temperature on GS-2 Terry Turbine Bearing Performance and Condition. Master's thesis, Texas A&M University," 2020. [Online]. Available: <https://hdl.handle.net/1969.1/193047>. [Accessed 24 May 2021].
- [16] D. J. Peck, "Turbine Oil Degradation and Its Effects on Performance of a Terry Turbine in Nuclear Applications. Master's thesis, Texas A&M University," 2019. [Online]. Available: <https://hdl.handle.net/1969.1/187526>. [Accessed 24 May 2021].

- [17] G. B. Green, "Effect of Degraded Oil on Terry Turbine Bearing Performance at High Temperature. Master's thesis, Texas A&M University," 2020. [Online]. Available: <https://hdl.handle.net/1969.1/191651>. [Accessed 24 May 2021].
- [18] United States Nuclear Regulatory Commission, "Enclosure 2 BWR MARK I AND MARK II REGULATORY HISTORY," 26 November 2012. [Online]. Available: <https://www.nrc.gov/docs/ML1232/ML12326A344.pdf>. [Accessed 25 February 2021].
- [19] M. A. Solom, "Experimental Study on Suppression Chamber Thermal-Hydraulic Behavior for Long-Term Reactor Core Isolation Cooling System Operation," May 2016. [Online]. Available: <https://hdl.handle.net/1969.1/157135>. [Accessed 13 April 2021].
- [20] M. Solom and K. V. Kirkland, "Experimental Investigation of BWR Suppression Pool Stratification during RCIC System Operation," *Nuclear Engineering and Design*, vol. 310, pp. 564-569, 2016.
- [21] Foxboro, "Foxboro 84 Series Intelligent Vortex Flowmeter," December 2015. [Online]. Available: https://download.schneider-electric.com/files?p_enDocType=Data+Bulletin&p_File_Name=FD-DS-F-008.pdf&p_Doc_Ref=FD-DS-F-008. [Accessed 4 February 2021].
- [22] Emerson Electric Co., "Vortex Flow Measurement," 2021. [Online]. Available: <https://www.emerson.com/en-us/automation/measurement-instrumentation/flow-measurement/about-vortex>. [Accessed 4 February 2021].

- [23] J. Cote, *Personal Communication: Case# 75378277*, 2020.
- [24] Azbil, "MagneW PLUS+ Electromagnetic Flowmeter Converter Model MGG14C," September 2020. [Online]. Available: <https://www.azbil.com/products/factory/download/catalog-spec/SS2-MGG410-0100-11.pdf>. [Accessed 21 May 2021].
- [25] GE Oil & Gas, "Masoneilan 21000 Series Complete Line of Rugged, Top Guided, Globe Valves with Lo-dB and Anti-Cavitation Capabilities," February 2016. [Online]. Available: <https://www.valvenco.com/content/files/21000-series-globe-valve-spec-data-gea19371d.pdf>. [Accessed 21 May 2021].
- [26] Fisher, "Fisher GX Control Valve and Actuator System," May 2019. [Online]. Available: <https://www.emerson.com/documents/automation/product-bulletin-fisher-gx-control-valve-actuator-system-en-135196.pdf>. [Accessed 21 May 2021].
- [27] Emerson Process Management, "Fisher Catalog 12," June 2014. [Online]. Available: <https://www.emerson.com/documents/automation/product-data-sheet-catalog-12-section-1-sept-2017-fisher-en-122394.pdf>. [Accessed 21 May 2021].
- [28] Emerson, "Rosemount 3051 Pressure Transmitter," December 2020. [Online]. Available: <https://www.emerson.com/documents/automation/product-data-sheet-rosemount-3051-pressure-products-en-73134.pdf>. [Accessed 5 February 2021].
- [29] Honeywell, "St 3000 Smart transmitter Series 900 Absolute Pressure Models Specifications 34-ST-03-66 February 2012," February 2012. [Online]. Available:

- <https://www.honeywellprocess.com/library/marketing/tech-specs/34-ST-03-66.pdf>. [Accessed 5 February 2021].
- [30] Honeywell, "ST 3000 Smart Pressure Transmitter Series 900 Differential Pressure Models Specifications 34-ST-03-65, January 2013," January 2013. [Online]. Available: <https://www.honeywellprocess.com/library/marketing/tech-specs/34-ST-03-65.pdf>. [Accessed 5 February 2021].
- [31] Dayton, "Dayton Horizontal Multistage Pressure Booster Pumps," [Online]. Available: <https://www.grainger.com/ec/pdf/Dayton-Horz-Multistage-Booster-Pump-OIPM.pdf>. [Accessed 12 May 2021].
- [32] Liquiflo Chemical Processing Pumps, "Centry-Series, Mechanically-Sealed, Close-Coupled, Centrifugal Pumps Models 621 & 622 - Sealed," [Online]. Available: <http://www.liquiflo.com/v2/manual/IOM-Centry-621&622-Sealed.pdf>. [Accessed 17 May 2021].
- [33] Liquiflo, "Centry-Series Performance Curves Model 621," [Online]. Available: http://www.liquiflo.com/v2/files/pdf/perf_centry/PerformCurves-621-1750&3500.pdf. [Accessed 17 May 2021].
- [34] Dayton, "Dayton Self-Priming Centrifugal Pumps," [Online]. Available: https://www.grainger.com/ec/pdf/12N810_1.pdf. [Accessed 12 May 2021].
- [35] Charlotte Pipe and Foundry Company, "Horizontal and Vertical Support," [Online]. Available:

- https://www.charlottepipe.com/Documents/PL_Tech_Man/Horizontal_and_Vertical_Support.pdf. [Accessed 12 May 2021].
- [36] Charlotte Pipe and Foundry Company, "Expansion and Contraction of PVC Schedule 40, PVC Schedule 80, PVC PR 200 PVC PR 160," [Online]. Available: https://www.charlottepipe.com/TechTools/Content/expansion_calc_info.pdf. [Accessed 27 April 2021].
- [37] National Instruments, "PXI Express NI PXIe-1075 User Manual," January 2017. [Online]. Available: <https://www.ni.com/pdf/manuals/372537c.pdf>. [Accessed 17 May 2021].
- [38] National Instruments, "PXIe-8821 User Manual," [Online]. Available: <https://www.ni.com/pdf/manuals/376445b.pdf>. [Accessed 17 May 2021].
- [39] The International Association for the Properties of Water and Steam, "Revised Release on the IAPWS Industrial Formulation 1997 for the Thermodynamic Properties of Water and Steam," August 2207. [Online]. Available: <http://iapws.org/relguide/IF97-Rev.pdf>. [Accessed 6 May 2021].
- [40] Quincy Compressor, "QT and QTS Series Compressors," May 2019. [Online]. Available: <https://www.aircompressorsdirect.com/manuals/quincy-48a5eeb8eb03a4c766e4a821bee0a479.pdf>. [Accessed 17 May 2021].
- [41] J. Kelly and J. Hedengren, "a steady-state detection (SSD) algorithm to detect non-stationary drifts in processes," March 2013. [Online]. Available: <https://doi.org/10.1016/j.jprocont.2012.12.001>. [Accessed 25 May 2021].

- [42] Electric Power Research Institute, "Terry Turbine Maintenance Guide, AFW Application: Replace TR-105874 and TR-016909-R1," Palo Alto, CA, 2002. 1007460.
- [43] G. F. Knoll, Radiation Detection and Measurement. 3rd ed., Hoboken, NJ: John Wiley & Sons, Inc., 2000.

APPENDIX A

FACILITY P&ID

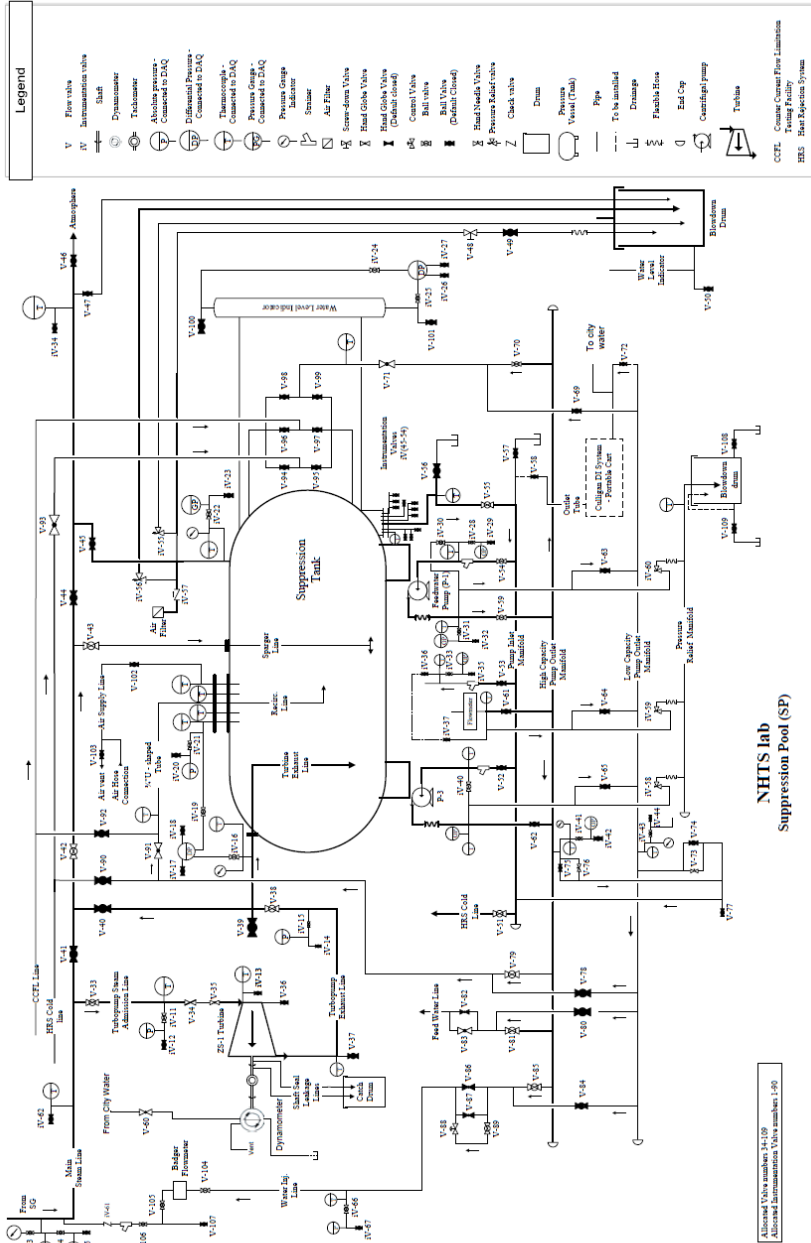


Figure A. 1. Facility P&ID Suppression Chamber

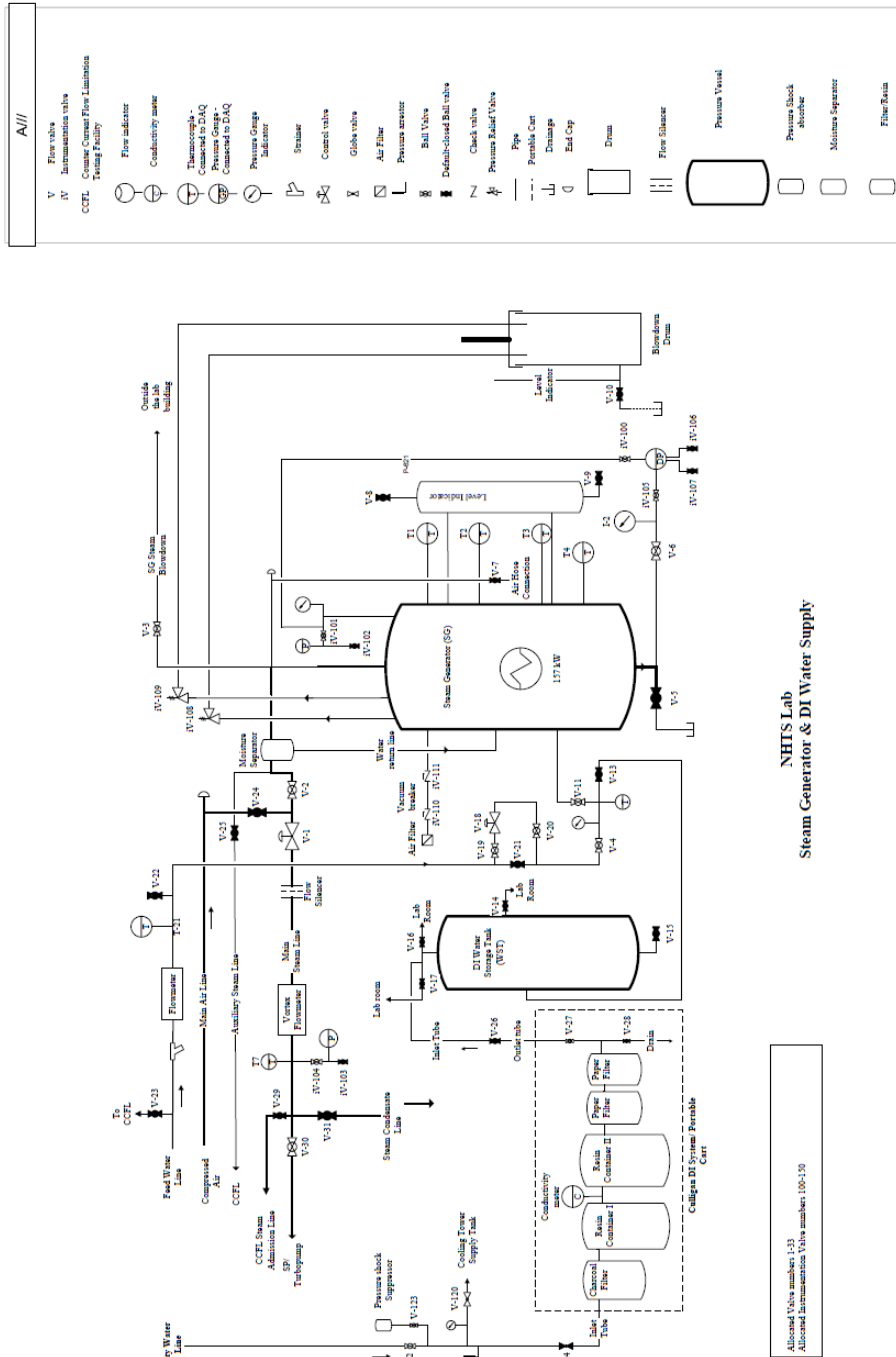


Figure A. 2. Facility P&ID - Steam Generator

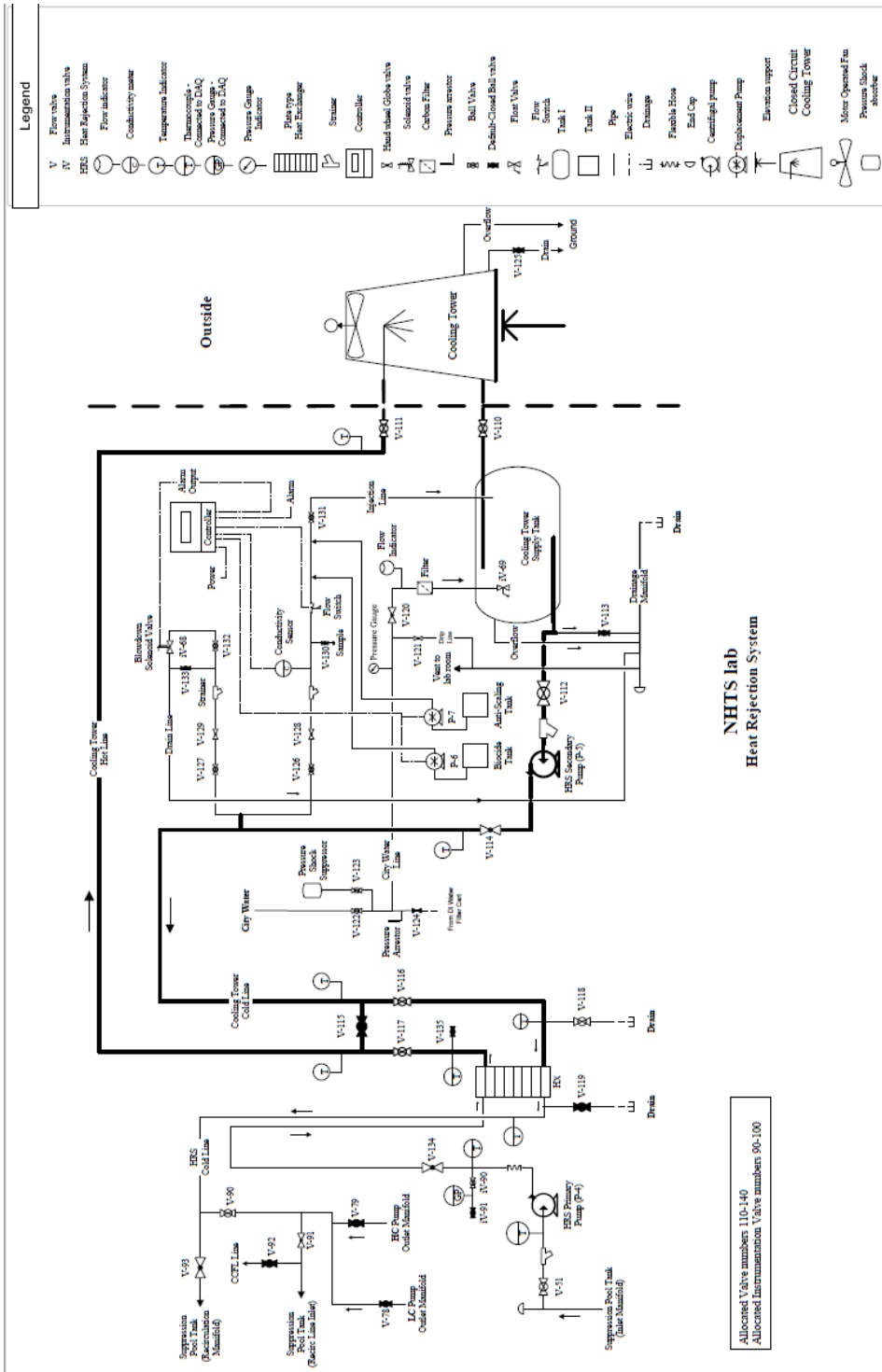


Figure A. 3. Facility P&ID Heat Rejection System

APPENDIX B

DATA PROCESSING SCRIPTS

Appendix B shows the python scripts used to process the raw data.

B.1 Guidelines

Five different python scripts are used in tandem to perform the data processing for this work, although the user need only interact with one of them. The scripts are “Master_Script.py”, “Read_Data.py”, “SteamProperties.py”, “search.py”, and “SteadyStateDetection.py”. All five scripts should be in the same directory for this to function correctly. Please reference the first few lines of each file to make sure all required packages are installed and available.

The main script that the user must run is entitled “Master_Script.py”. Upon running the script, the user will be prompted to choose a series of data files to include in the analysis. The file explorer UI default starting directory is the current working directory. To change this default directory, edit the “search.py” script on line 12 and set Home equal to the desired directory. Once the input files are selected, the user will be prompted to choose an output directory for all data results. The master script will then facilitate running all the desired data files in parallel to minimize computing time. By default, the script is set to utilize the maximum number of available CPU cores minus 1 simultaneously, and load in new data files as space becomes available. To change this, one can edit the master script at line 21 where it says “Cores=multiprocessing.cpu_count()-1” and set Cores equal to any desired number of

maximum CPU cores. Once all the cases have finished, Master_Script.py creates plots showing trends as seen in the analysis section of this work.

The master script file calls the file “read_data.py” which is responsible for the bulk of the data processing for each case. The script outputs a text file entitled readout.txt which includes some of the key information describing the onset and termination of stratification for each test, in addition to the extent of thermal stratification observed, the amount of heat removed, the theoretical amount of heat removed from a mixed pool, and the associated uncertainties. Several plots are saved as .png files, including some not included in the body of this thesis, that are considered useful in determining suppression pool behavior. The output from this script will be placed in a separate folder for each case with the title matching the name of the data input file.

“SteadyStateDetection.py” is called by “Read_Data.py” to determine when the lowest elevation thermocouple in the suppression pool reaches steady state. This script uses a Steady-State Detection Algorithm developed at Brigham Young University by Jeffrey Kelly [41] to identify when steady state is achieved. The algorithm was developed for use in industrial process control systems.

“SteamProperties.py” invokes the IAPWS Industrial Formulation 97 for the Thermodynamic Properties of Water and Steam [39] to calculate various properties of steam and water as a function of temperature and pressure. For this work, the density, specific enthalpy, and saturation temperature are calculated using “SteamProperties.py”

B.2 Python Scripts

B.2.1 Master Script.py

```
# -*- coding: utf-8 -*-  
"""
```

Created on Thu Dec 17 03:51:37 2020

Runfile to setup multiple simultaneous runs for Master's Thesis Analysis

```
@author: dkeeslin  
"""
```

```
import search  
import subprocess  
import time  
import multiprocessing  
import numpy as np  
import pandas as pd  
import matplotlib.pyplot as plt  
from scipy import optimize  
#%%
```

```
runfile='Read_Data.py'  
print('running ', runfile)
```

```
Cores=multiprocessing.cpu_count()-1 #leave one core alone for any other processes on  
the machine
```

```
inputpath= search.search_for_files()  
Outputpath = search.search_for_directory()  
runs = len(inputpath)  
print(runs,' total cases')  
filename=list(range(runs))  
OutputDir=list(range(runs))  
for i in range(runs):  
    filename[i]=inputpath[i].split('/')[-1]  
    OutputDir[i]= Outputpath +"\\" + filename[i]  
i=0  
running=0  
done_prev=0  
done = 0  
start_time=time.time()  
print('Progress')  
print('0 %')  
while i < runs:
```

```
globals()['case'+str(i+1)]= subprocess.Popen(["python",runfile,"-i",inputpath[i],'-o',OutputDir[i]])
```

```
print('case',i+1,'begun')  
running+=1
```

```
if running == Cores:  
    if done > 0:  
        print(round(done/runs*100),'%')  
        """"  
    while running ==Cores:  
        running = 0  
        for j in range(Cores):  
            complete=globals()['case'+str(i+1-j)].poll()  
            if complete == None:  
                running+=1  
            """"  
    while done <= done_prev:  
        done = 0  
        for k in range(i):  
            complete = globals()['case' +str(k+1)].poll()  
            if complete != None:  
                done+=1  
        if done > done_prev:  
            running -=1  
    i+=1  
    done_prev = done
```

```
while done < runs:  
    done =0  
    for k in range(i):  
        complete = globals()['case' +str(k+1)].poll()  
        if complete != None:  
            done+=1  
    if done > done_prev:  
        print(round(done/runs*100),'%')  
        done_prev = done  
    time.sleep(1)
```

```
globals()['case'+str(runs)].wait()  
#%>%
```

```

print('Do you want to run analysis on output data (y/[n])?')
#fit curves

def linear(x,a,b):
    return a*x+b

def quadratic(x,a,b,c):
    return a*x**2 +b*x+c

def poly3(x,a,b,c,d):
    return a*x**3 + b*x**2 +c*x +d

if 'OutputDir' not in globals():
    import search
    import subprocess
    import time
    import multiprocessing
    import numpy as np
    import pandas as pd
    import matplotlib.pyplot as plt
    from scipy import optimize
    inputpath= search.search_for_files()
    start_time=time.time()
    runs = len(inputpath)
    print(runs,' total cases')
    filename=list(range(runs))
    OutputDir=list(range(runs))
    for i in range(runs):
        filename[i]=inputpath[i].split('/')[-1]
        #OutputDir[i]= 'H:/Research/Python/Test/'+filename[i]
        OutputDir[i]= 'C:/Users/dkeeslin/Python/Output Files/'+filename[i]

x = input()
if x == 'y':
    water_massflow=np.zeros(len(OutputDir))
    u_water_massflow = np.zeros(len(OutputDir))
    steam_massflow=np.zeros(len(OutputDir))
    u_steam_massflow = np.zeros(len(OutputDir))
    P = np.zeros(len(OutputDir))
    u_P = np.zeros(len(OutputDir))
    T_strat = np.zeros(len(OutputDir))

```

```

u_T_strat = np.zeros(len(OutputDir))
heat_rem = np.zeros(len(OutputDir))
u_heat_rem = np.zeros(len(OutputDir))
heat_rem_mix = np.zeros(len(OutputDir))
u_heat_rem_mix = np.zeros(len(OutputDir))
heat_rem_improvement = np.zeros(len(OutputDir))
u_heat_rem_improvement = np.zeros(len(OutputDir))
heat_rem_rate = np.zeros(len(OutputDir))
u_heat_rem_rate = np.zeros(len(OutputDir))
heat_rem_rate_mix = np.zeros(len(OutputDir))
u_heat_rem_rate_mix = np.zeros(len(OutputDir))
heat_rate_improvement = np.zeros(len(OutputDir))
u_heat_rate_improvement = np.zeros(len(OutputDir))
for i in range (len(OutputDir)):
    data=pd.read_csv(OutputDir[i]+'\\output_'+filename[i]+'.csv')
    water_massflow[i]=data['Nominal Water Mass Flow Rate (g/s)']
    u_water_massflow[i] = data['U_massflow']
    steam_massflow[i]=data['Nominal Steam Mass Flow Rate (g/s)']
    u_steam_massflow[i]=data['U_steam_massflow']
    #P[i]=data['Average Pressure (psia)']
    P[i]=data['Maximum Pressure (psia)']
    u_P[i]= data['U_Pressure']
    T_strat[i]=data['Maximum Degrees of Stratification (C)']
    u_T_strat[i]=data['U_T_strat']
    heat_rem[i]=data['Heat Removed (kJ)']
    u_heat_rem[i]=data['U_heat removed']
    heat_rem_mix[i]=data['Theoretical Heat Removed for Mixed Pool (kJ)']
    heat_rem_improvement[i] = data['Heat Removal Improvement (kJ)']
    u_heat_rem_improvement[i] = data['U_heat removal improvement (kJ)']
    u_heat_rem_mix[i]=data['U_heat removed mixed']
    heat_rem_rate[i]=data['Heat Removal Rate (kW)']
    u_heat_rem_rate[i]=data['U_Heat removal']
    heat_rem_rate_mix[i]=data['Theoretical Heat Removal Rate for Mixed Pool (kW)']
    u_heat_rem_rate_mix[i] = data['U_heat removal Theoretical']
    heat_rate_improvement[i] = data['Heat Removal Rate Improvement (kW)']
    u_heat_rate_improvement[i] = data['U_heat removal rate improvement']

    u_heat_rem_improvement =
    (heat_rem_improvement/heat_rem_mix*100)*((u_heat_rem_improvement/heat_rem_im
    provement)**2+(u_heat_rem_mix/heat_rem_mix)**2)**0.5
    heat_rem_improvement = (heat_rem_improvement)/heat_rem_mix*100

#linear P

```

```

a , b= optimize.curve_fit(linear, P,heat_rate_improvement)[0]
P_lin=a*P+b
SSEtot=np.sum((heat_rate_improvement-np.average(heat_rate_improvement))**2)
SSEres=np.sum((P_lin - heat_rate_improvement)**2)
R_squared=1-(SSEres/SSEtot)

```

```

if b < 0:

```

```

    regress_text = "y = " +str(round(a,3))+ "x "+str(round(b,3))+"\n" +
    +u"R\u00B2= "+str(round(R_squared,3))

```

```

else:

```

```

    regress_text = "y = " +str(round(a,3))+ "x + "+str(round(b,3))+"\n" +
    +u"R\u00B2= "+str(round(R_squared,3))

```

```

plt.figure('Pressure_linear',dpi=200)
#plt.plot(P,heat_rate_improvement,"*")
plt.errorbar(P,heat_rate_improvement,u_heat_rate_improvement,u_P,'!',label='data')
plt.plot(P,P_lin,label='fit')
plt.legend(loc='upper left',bbox_to_anchor=(1.04,1))
plt.text(min(P),max(heat_rate_improvement)-0.5,regress_text)
plt.xlabel('Pressure (psia)')
plt.ylabel('Heat Removal Rate Improvement (kW)')
#plt.title('Pressure Correlation')
plt.show()

```

```

#thermal stratification linear

```

```

a , b= optimize.curve_fit(linear, T_strat,heat_rate_improvement)[0]
T_strat_lin=a*T_strat +b
SSEtot=np.sum((heat_rate_improvement-np.average(heat_rate_improvement))**2)
SSEres=np.sum((T_strat_lin - heat_rate_improvement)**2)
R_squared=1-(SSEres/SSEtot)

```

```

regress_text = "y = " +str(round(a,3))+ "x "+str(round(b,3))+"\n" +
    +u"R\u00B2= "+str(round(R_squared,3))

```

```

plt.figure('T_strat_Linear',dpi=200)
#plt.plot(P,heat_rate_improvement,"*")

```

```

plt.errorbar(T_strat,heat_rate_improvement,u_heat_rate_improvement,u_T_strat,'!',label
='data')

```

```

plt.plot(T_strat,T_strat_lin,label='fit')
plt.legend(loc='upper left',bbox_to_anchor=(1.04,1))
plt.text(min(T_strat),max(heat_rate_improvement)-0.5,regress_text)

```



```

plt.xlabel('Maximum Thermal Stratification (C)')
plt.ylabel('Heat Removal Rate Improvement (kW)')
#plt.title('Thermal Stratification Correlation')
plt.show()
#only plot massflows for pressurized tests

A=np.where(P >0)[0]

#mass flow
a , b= optimize.curve_fit(linear, [water_massflow[i] for i in
A],[heat_rate_improvement[i] for i in A])[0]
massflow_lin=a*np.asarray([water_massflow[i] for i in A]) +b
SSEtot=np.sum(([heat_rate_improvement[i] for i in A]-
np.average([heat_rate_improvement[i] for i in A]))**2)
SSEres=np.sum((massflow_lin - [heat_rate_improvement[i] for i in A])**2)
R_squared=1-(SSEres/SSEtot)

regress_text = "y = " +str(round(a,3))+ "x "+str(round(b,3))+ "\n" \
+u"R\u00B2= "+str(round(R_squared,3))

plt.figure('massflow_linear',dpi=200)
#plt.plot(P,heat_rate_improvement,"*")
plt.errorbar([water_massflow[i] for i in A],[heat_rate_improvement[i] for i in
A],[u_heat_rate_improvement[i] for i in A],[u_water_massflow[i] for i in
A],',',label='data')
plt.plot([water_massflow[i] for i in A],massflow_lin,label='fit')
plt.legend(loc='upper left',bbox_to_anchor=(1.04,1))
plt.text(min([water_massflow[i] for i in A]),max([heat_rate_improvement[i] for i in
A])-0.5,regress_text)
plt.xlabel('Water mass Flowrate (g/s)')
plt.ylabel('Heat Removal Rate Improvement (kW)')
#plt.title('Water Flowrate Correlation')
plt.show()
#quadratic fit

a , b,c= optimize.curve_fit(quadratic, [water_massflow[i] for i in
A],[heat_rate_improvement[i] for i in A])[0]

massflow_quad=quadratic(np.linspace(20,50,100),a,b,c)

```

```

SSEtot=np.sum([(heat_rate_improvement[i] for i in A]-
np.average([heat_rate_improvement[i] for i in A]))**2)
SSEres=np.sum((quadratic(np.asarray([water_massflow[i] for i in A]),a,b,c) -
[heat_rate_improvement[i] for i in A])**2)
R_squared=1-(SSEres/SSEtot)

regress_text = "y = " +str(round(a,3))+ "x\u00B2 "+str(round(b,3))+ "x
+"+str(round(c,3))+ "\n\
+u"R\u00B2= "+str(round(R_squared,3))

plt.figure('massflow_quadratic',dpi=200)
#plt.plot(P,heat_rate_improvement,"*")
plt.errorbar([water_massflow[i] for i in A],[heat_rate_improvement[i] for i in
A],[u_heat_rate_improvement[i] for i in A],[u_water_massflow[i] for i in
A],',',label='data')
plt.plot([i for i in np.linspace(20,50,100)],massflow_quad,label='fit')
plt.legend(loc='upper left',bbox_to_anchor=(1.04,1))
plt.text(min([water_massflow[i] for i in A]),max([heat_rate_improvement[i] for i in
A])-0.5,regress_text)
plt.xlabel('Water mass Flowrate (g/s)')
plt.ylabel('Heat Removal Rate Improvement (kW)')
#plt.title('Water Flowrate Correlation')
plt.show()
#combined thermal stratification and flowrate

combined=water_massflow*T_strat
u_combined =
combined*np.sqrt(((u_water_massflow/water_massflow)**2)+((u_T_strat/T_strat)**2))

a , b = optimize.curve_fit(linear,combined,heat_rate_improvement)[0]
combined_lin=linear(np.linspace(min(combined),max(combined),101),a,b)
SSEtot=np.sum((heat_rate_improvement-np.average(heat_rate_improvement))**2)
SSEres=np.sum((linear(np.asarray(combined),a,b) - heat_rate_improvement)**2)
R_squared=1-(SSEres/SSEtot)

regress_text = "y = " +str(round(a,3))+ "x "+str(round(b,3))+ "\n\
+u"R\u00B2= "+str(round(R_squared,3))

plt.figure('combined_linear',dpi=200)

plt.errorbar(combined,heat_rate_improvement,u_heat_rate_improvement,u_combined,',',
label='data')

```

```

plt.plot([i for i in
np.linspace(min(combined),max(combined),101)],combined_lin,label='fit')
plt.legend(loc='upper left',bbox_to_anchor=(1.04,1))
plt.text(min(combined),max(heat_rate_improvement)-0.5,regress_text)
plt.xlabel('g*K/s')
plt.ylabel('Heat Removal Rate Improvement (kW)')
#plt.title('Combined Correlation')
plt.show()
# correlation between pressure and thermal stratification
B =np.where(steam_massflow<60)[0]

a , b = optimize.curve_fit(linear,[P[i] for i in B],[T_strat[i] for i in B])[0]
corr_lin = linear(np.linspace(min([P[i] for i in B]),max([P[i] for i in B]),101),a,b)
SSEtot=np.sum((([T_strat[i] for i in B] - np.average([T_strat[i] for i in B]))**2)
SSEres=np.sum((linear(np.asarray([P[i] for i in B]),a,b) - [T_strat[i] for i in B])**2)
R_squared=1-(SSEres/SSEtot)

regress_text = "y = " +str(round(a,3))+ "x "+str(round(b,3))+ "\n" \
+u"R\u00B2= "+str(round(R_squared,3))

plt.figure('Pressure_T_strat',dpi=200)
plt.errorbar([P[i] for i in B],[T_strat[i] for i in B],[u_T_strat[i] for i in B],[u_P[i] for i
in B],',',label='data')
plt.plot([i for i in np.linspace(min([P[i] for i in B]),max([P[i] for i in
B]),101)],corr_lin,label='fit')
plt.legend(loc='upper left',bbox_to_anchor=(1.04,1))
plt.text(min([P[i] for i in B]),max([T_strat[i] for i in B])-1.0,regress_text)
plt.xlabel('Suppression Pool Pressure (psia)')
plt.ylabel('Degrees of Thermal Stratification (C)')
plt.xlim(10,60)
#plt.title('Pressure-T_strat Correlation')
plt.show()
# correlation between steam flowrate and thermal stratification
#pressurized tests
A=np.where(P >0)[0]

#mass flow
a , b= optimize.curve_fit(linear, [steam_massflow[i] for i in A],[T_strat[i] for i in
A])[0]
massflow_lin=a*np.asarray([steam_massflow[i] for i in A]) +b
SSEtot=np.sum((([T_strat[i] for i in A]-np.average([T_strat[i] for i in A]))**2)
SSEres=np.sum((massflow_lin - [T_strat[i] for i in A])**2)
R_squared=1-(SSEres/SSEtot)

```

```

regress_text = "y = " +str(round(a,3))+ "x "+str(round(b,3))+ "\n" \
+u"R\u00B2= "+str(round(R_squared,3))

plt.figure('Steamflow _ T_strat pressurized',dpi=200)
#plt.plot(P,heat_rate_improvement,"*")
plt.errorbar([steam_massflow[i] for i in A],[T_strat[i] for i in A],[u_T_strat[i] for i in
A],[u_steam_massflow[i] for i in A],',',label='data')
plt.plot([steam_massflow[i] for i in A],massflow_lin,label='fit')
plt.legend(loc='upper left',bbox_to_anchor=(1.04,1))
plt.text(min([steam_massflow[i] for i in A])+10,max([T_strat[i] for i in A])-
1.0,regress_text)
plt.xlabel('Steam mass Flowrate (g/s)')
plt.ylabel('Degrees of Thermal Stratification (C)')
#plt.title('Water Flowrate Correlation')
plt.show()
#atmospheric tests tests
A=np.where(P <16)[0]

#mass flow
a , b= optimize.curve_fit(linear, [steam_massflow[i] for i in A],[T_strat[i] for i in
A])[0]
massflow_lin=a*np.asarray([steam_massflow[i] for i in A]) +b
SSEtot=np.sum((([T_strat[i] for i in A]-np.average([T_strat[i] for i in A]))**2)
SSEres=np.sum((massflow_lin - [T_strat[i] for i in A])**2)
R_squared=1-(SSEres/SSEtot)

regress_text = "y = " +str(round(a,3))+ "x "+str(round(b,3))+ "\n" \
+u"R\u00B2= "+str(round(R_squared,3))

plt.figure('Steamflow _ T_strat atmospheric',dpi=200)
#plt.plot(P,heat_rate_improvement,"*")
plt.errorbar([steam_massflow[i] for i in A],[T_strat[i] for i in A],[u_T_strat[i] for i in
A],[u_steam_massflow[i] for i in A],',',label='data')
plt.plot([steam_massflow[i] for i in A],massflow_lin,label='fit')
plt.legend(loc='upper left',bbox_to_anchor=(1.04,1))
plt.text(min([steam_massflow[i] for i in A])+10,max([T_strat[i] for i in A])-
1.0,regress_text)
plt.xlabel('Steam mass Flowrate (g/s)')

```

```

plt.ylabel('Degrees of Thermal Stratification (C)')
plt.title('Water Flowrate Correlation')
plt.show()

```

```

Processing_Time=time.time()-start_time
print('Run Time=',round(Processing_Time,0),'Seconds')

```

B.2.2 Read_Data.py

```

import numpy as np
import pandas as pd
import matplotlib.pyplot as plt
import os,sys,getopt
import time
import search
import SteamProperties as SteamProp
from SteadyStateDetection import SSD
from scipy import stats
#%%
start_time=time.time()
def main(argv):
    inputfile=""
    outputdir=""
    try:
        opts, args = getopt.getopt(argv,"hi:o:",["ifile=","odir=""])
    except getopt.GetoptError:
        print ('get opt error')
        sys.exit(2)
    for opt, arg in opts:
        if opt == '-h':
            print (' getopt error')
            sys.exit()
        elif opt in ("-i", "--ifile"):
            inputfile= arg
        elif opt in ("-o", "--odir"):
            outputdir= arg
    return inputfile,outputdir

if __name__ == "__main__":
    inputfile,outputdir=main(sys.argv[1:])
    filename=inputfile.split('/')[ -1].split('.')[0]

if inputfile == "":

```

```

inputfile= search.search_for_file()
filename=inputfile.split('/')[-1].split('.')[0]
#outputdir= 'C:/Users/dkeeslin/Python/Output Files/'+filename
outputdir= search.search_for_directory()
search.clean_directory(outputdir)
try:
    os.makedirs(outputdir)
except OSError:
    print ("%s directory already exists. Replacing current directory" % outputdir)
else:
    print ("Successfully created the directory %s" % outputdir)
#%/%

rawdata=pd.read_csv(inputfile,delimiter='\t')
data=rawdata[rawdata['Important?']!= 0]
rows=data.shape[0]
Time=(data['Time (s)']-data['Time (s)'].iloc[0]).round(1)
#%/% Average of each elevation
subdirectory='Vertical Temperature Comparison'
try:
    os.makedirs(outputdir+'\\'+subdirectory)
except OSError:
    print ("%s directory already exists. Replacing current directory" % subdirectory)
else:
    print ("Successfully created the directory %s" % subdirectory)

TC=np.zeros(rows)
for i in [11,25,38]:
    col='TC '+str(i)
    TC=(TC+ data[col])
TC_31_ave=TC/3

TC=np.zeros(rows)
for i in [10,24,37]:
    col='TC '+str(i)
    TC=(TC+ data[col])
TC_27_ave=TC/3

TC=np.zeros(rows)
for i in [9,23,36]:
    col='TC '+str(i)
    TC=(TC+ data[col])
TC_23_ave=TC/3

```

```

TC=np.zeros(rows)
for i in [1,2,3,4,14,15,16,17,18,26,27,28,29,30,31]:
    col='TC '+str(i)
    TC=(TC+ data[col])
TC_19_ave=TC/15

TC=np.zeros(rows)
for i in [5,19,32]:
    col='TC '+str(i)
    TC=(TC+ data[col])
TC_15_ave=TC/3

TC=np.zeros(rows)
for i in [6,20,33]:
    col='TC '+str(i)
    TC=(TC+ data[col])
TC_11_ave=TC/3

TC=np.zeros(rows)
for i in [7,21,34]:
    col='TC '+str(i)
    TC=(TC+ data[col])
TC_7_ave=TC/3

TC=np.zeros(rows)
for i in [8,22,35]:
    col='TC '+str(i)
    TC=(TC+ data[col])
TC_3_ave=(TC/3)

plt.figure(dpi=200)
for i in [31,27,23,19,15,11,7,3]:
    plt.plot(Time/60,globals()['TC_'+str(i)+'_ave'],label=str(i)+' in')

for i in range(rows):
    if data['TC Tank Outlet'].iloc[i] < 0.0:
        data['TC Tank Outlet'].iloc[i]=0

# overall average
TC_ave=((TC_3_ave+TC_7_ave+TC_11_ave+TC_15_ave+TC_19_ave+TC_23_ave+TC_27_ave+TC_31_ave)/8).values

#%%%

```

```

T_strat=TC_31_ave-TC_3_ave

if rows < 360000:
    check=max(T_strat[0:(rows//10)])
else:
    check=max(T_strat[0:36000])
strat_start = [i for i in range(len(T_strat)) if sum(T_strat.iloc[max(0,i-100):i])/(i-max(-
1,i-100)) > check][0]

strat_end = [i for i in range(len(T_strat)) if T_strat.iloc[i]> check][-1]
i = 0
SS = False
n=12000
if n %2 ==1:
    n+=1
t_crit=stats.t.ppf(1-0.025,n)

while not SS and i<(strat_end-strat_start):

    SS,ratio = SSD(np.asarray(TC_3_ave.iloc[strat_start+i-
int(n/2):strat_start+i+int(n/2)]),t_crit,int(n))
    if SS:
        mix_stop = i +strat_start-int(n/2)
        if ratio <0.2:
            i+=600
        elif ratio < 0.5:
            i+=100
        elif ratio < 0.7:
            i+=20
        elif ratio < 0.9:
            i+=10
        else:
            i+=1
    if 'mix_stop' in globals():
        pass
    else:
        print('Did not reach steady state')

#%%%

def plot_strat():

```



```
plt.plot([Time.iloc[strat_start]/60,Time.iloc[strat_start]/60],[min(TC_3_ave),max(TC_31_ave)],label='Stratification Start Time')
```

```
plt.plot([Time.iloc[strat_end]/60,Time.iloc[strat_end]/60],[min(TC_3_ave),max(TC_31_ave)],label='Stratification End Time')  
if 'mix_stop' in globals():
```

```
plt.plot([Time.iloc[mix_stop]/60,Time.iloc[mix_stop]/60],[min(TC_3_ave),max(TC_31_ave)],label='Bulk Mixing End Time')
```

```
#%%
```

```
save_file_name=filename+' Comparison of average temperature as a function of elevation.png'
```

```
plt.ylabel('Temperature (C)')
```

```
plt.xlabel('Time (min)')
```

```
#plt.title('Comparison of average temperature at different elevations')
```

```
#plt.plot(Time,data['TC Tank Outlet'],label='Tank Outlet')
```

```
plot_strat()
```

```
lgd=plt.legend(loc='upper left',bbox_to_anchor=(1.04,1))
```

```
plt.savefig(outputdir+'\\'+subdirectory+'\\'+save_file_name,bbox_extra_artists=(lgd,),bbox_inches='tight',dpi=200)
```

```
plt.figure(dpi=200)
```

```
save_file_name=filename+' Degrees of Thermal Stratification.png'
```

```
plt.ylabel('Temperature (C)')
```

```
plt.xlabel('Time (min)')
```

```
#plt.title('Degrees of Thermal Stratification')
```

```
plt.plot(Time/60,T_strat,label='Degrees of Thermal Stratification')
```

```
lgd=plt.legend(loc='upper left',bbox_to_anchor=(1.04,1))
```

```
plt.savefig(outputdir+'\\'+subdirectory+'\\'+save_file_name,bbox_extra_artists=(lgd,),bbox_inches='tight',dpi=200)
```

```
plt.figure(dpi=200)
```

```
save_file_name=filename+'Average Suppression Pool Temperature.png'
```

```
plt.ylabel('Temperature (C)')
```

```
plt.xlabel('Time (min)')
```

```
#plt.title('Average Suppression Pool Temperature')
```

```
plt.plot(Time/60,TC_ave, label='Average Suppression Pool Temperature')
```

```
lgd=plt.legend(loc='upper left',bbox_to_anchor=(1.04,1))
```

```
plt.savefig(outputdir+'\\'+subdirectory+'\\'+save_file_name,bbox_extra_artists=(lgd,),bbox_inches='tight',dpi=200)
```

```

plt.figure(dpi=200)
save_file_name=filename+'Tank Outlet versus average tank temperature.png'
plt.ylabel('Temperature (C)')
plt.xlabel('Time (min)')
#plt.title('Tank Outlet Temperature vs. Average Pool Temperature')
plt.plot(Time/60,TC_ave,label='Average Pool Temperature')
plt.plot(Time/60,data['TC Tank Outlet'],label='Tank Outlet Temperature')
lgd=plt.legend(loc='upper left',bbox_to_anchor=(1.04,1))
plt.savefig(outputdir+'\\'+subdirectory+'\\'+save_file_name,bbox_extra_artists=(lgd,),bbox_inches='tight',dpi=200)

```

```

#%%% Repeat of comparison of average temperature as a function of elevation in terms of
degrees of subcooling

```

```

T_SP_Sat=data['SP Saturation Temp']

```

```

TC_3_sub_ave=T_SP_Sat-TC_3_ave
TC_7_sub_ave=T_SP_Sat-TC_7_ave
TC_11_sub_ave=T_SP_Sat-TC_11_ave
TC_15_sub_ave=T_SP_Sat-TC_15_ave
TC_19_sub_ave=T_SP_Sat-TC_19_ave
TC_23_sub_ave=T_SP_Sat-TC_23_ave
TC_27_sub_ave=T_SP_Sat-TC_27_ave
TC_31_sub_ave=T_SP_Sat-TC_31_ave

```

```

plt.figure(dpi=200)
save_file_name=filename+' Comparison of average subcooling as a function of
elevation.png'
plt.ylabel('Degrees of Subcooling (C)')
plt.xlabel('Time (min)')
#plt.title('Comparison of average subcooling at different elevations')
for i in [31,27,23,19,15,11,7,3]:
    plt.plot(Time/60,-globals()['TC_'+str(i)+'_sub_ave'],label=str(i)+' in')
lgd=plt.legend(loc='upper left',bbox_to_anchor=(1.04,1))
plt.savefig(outputdir+'\\'+subdirectory+'\\'+save_file_name,bbox_extra_artists=(lgd,),bbox_inches='tight',dpi=200)

```

```

#%%% Output Vertical DataFrame
save_file_name=filename+' processed data.csv'
Output_df=pd.DataFrame()

```

```

for i in [31,27,23,19,15,11,7,3]:
    Output_df['TC_'+str(i)+'_ave']=globals()['TC_'+str(i)+'_ave']
    Output_df['TC_'+str(i)+'_sub_ave']=globals()['TC_'+str(i)+'_sub_ave']
Output_df.to_csv(outputdir+'\\'+subdirectory+'\\'+save_file_name)
#%%% Comparison of average temperature as a function of axial position
subdirectory='Axial Temperature Comparison'
try:
    os.makedirs(outputdir+'\\'+subdirectory)
except OSError:
    print ("%s directory already exists. Replacing current directory" % subdirectory)
else:
    print ("Successfully created the directory %s" % subdirectory)

T_ax_0=data['TC 1']
T_ax_1=data['TC 2']
T_ax_2=data['TC 14']
T_ax_3=data['TC 15']
T_ax_4=data['TC 16']
T_ax_5=data['TC 26']
T_ax_6=data['TC 27']
T_ax_7=data['TC 28']
T_ax_8=data['TC 29']

plt.figure(dpi=200)
save_file_name=filename+' Comparison of average temperature at different axial
positions.png'
plt.ylabel('Temperature (C)')
plt.xlabel('Time (min)')
#plt.title('Comparison of average temperature at different axial positions')
for i in range(9):
    plt.plot(Time/60,globals()['T_ax_'+str(i)],label=str(i)+' ft')
plot_strat()
lgd=plt.legend(loc='upper left',bbox_to_anchor=(1.04,1))
plt.savefig(outputdir+'\\'+subdirectory+'\\'+save_file_name,bbox_extra_artists=(lgd,),bbo
x_inches='tight',dpi=200)

#%%% Repeat of comparison of average temperature as a function of axial position in
terms of degrees of subcooling

T_ax_0_sub=T_ax_0-T_SP_Sat
T_ax_1_sub=T_ax_1-T_SP_Sat
T_ax_2_sub=T_ax_2-T_SP_Sat

```

```

T_ax_3_sub=T_ax_3-T_SP_Sat
T_ax_4_sub=T_ax_4-T_SP_Sat
T_ax_5_sub=T_ax_5-T_SP_Sat
T_ax_6_sub=T_ax_6-T_SP_Sat
T_ax_7_sub=T_ax_7-T_SP_Sat
T_ax_8_sub=T_ax_8-T_SP_Sat

```

```

plt.figure(dpi=200)
save_file_name=filename+' Comparison of average subcooling at different axial
positions.png'
plt.ylabel('Degrees of Subcooling (C)')
plt.xlabel('Time (min)')
#plt.title('Comparison of average subcooling at different axial positions')
for i in [0,1,2,3,4,5,6,7,8]:
    plt.plot(Time/60,globals()['T_ax_'+str(i)+'_sub'],label=str(i)+' ft')

lgd=plt.legend(loc='upper left',bbox_to_anchor=(1.04,1))
plt.savefig(outputdir+'\\'+subdirectory+'\\'+save_file_name,bbox_extra_artists=(lgd,),bbo
x_inches='tight',dpi=200)

```

```

#%%% Output DataFrame
save_file_name=filename+' processed data.csv'
Output_df=pd.DataFrame()

```

```

for i in range(9):
    Output_df['T_ax_'+str(i)]=globals()['T_ax_'+str(i)]
    Output_df['T_ax_'+str(i)+'_sub']=globals()['T_ax_'+str(i)+'_sub']

```

```

Output_df.to_csv(outputdir+'\\'+subdirectory+'\\'+save_file_name)

```

```

#%%% Comparison of average temprature as a function of lateral position
subdirectory='Lateral Temperature Comparison'

```

```

T_ax_1_lat_Mid=data['TC 2']
T_ax_1_lat_Left=data['TC 3']
T_ax_1_lat_Right=data['TC 4']

```

```

T_ax_4_lat_Mid=data['TC 16']
T_ax_4_lat_Left=data['TC 17']
T_ax_4_lat_Right=data['TC 18']

```

```

T_ax_8_lat_Mid=data['TC 29']
T_ax_8_lat_Left=data['TC 30']
T_ax_8_lat_Right=data['TC 31']

```

```

try:
    os.makedirs(outputdir+'\\'+subdirectory)
except OSError:
    print ("%s directory already exists. Replacing current directory" % subdirectory)
else:
    print ("Successfully created the directory %s" % subdirectory)

plt.figure(dpi=200)
save_file_name=filename+' Lateral temperature comparison 1 foot from plate-side weld'

plt.ylabel('Temperature (C)')
plt.xlabel('Time (min)')
for i in ['Mid','Left','Right']:
    plt.plot(Time/60,globals()['T_ax_1_lat_'+i],label=i)
plot_strat()
lgd=plt.legend(loc='upper left',bbox_to_anchor=(1.04,1))
plt.savefig(outputdir+'\\'+subdirectory+'\\'+save_file_name,bbox_extra_artists=(lgd,),bbox_inches='tight',dpi=200)

plt.figure(dpi=200)
save_file_name=filename+' Lateral temperature comparison at the center of the tank'
plt.ylabel('Temperature (C)')
plt.xlabel('Time (min)')
for i in ['Mid','Left','Right']:
    plt.plot(Time/60,globals()['T_ax_4_lat_'+i],label=i)
plot_strat()
lgd=plt.legend(loc='upper left',bbox_to_anchor=(1.04,1),title='lateral position')
plt.savefig(outputdir+'\\'+subdirectory+'\\'+save_file_name,bbox_extra_artists=(lgd,),bbox_inches='tight',dpi=200)

plt.figure(dpi=200)
save_file_name=filename+' Lateral temperature comparison at the turbine-side weld'
plt.ylabel('Temperature (C)')
plt.xlabel('Time (min)')
for i in ['Mid','Left','Right']:
    plt.plot(Time/60,globals()['T_ax_8_lat_'+i],label=i)
plot_strat()
lgd=plt.legend(loc='upper left',bbox_to_anchor=(1.04,1),title='lateral position')
plt.savefig(outputdir+'\\'+subdirectory+'\\'+save_file_name,bbox_extra_artists=(lgd,),bbox_inches='tight',dpi=200)

#%% Output DataFrame

```

```

save_file_name=filename+' processed data.csv'
Output_df=pd.DataFrame()

for i in [1,4,8]:
    for j in ['Mid','Left','Right']:
        Output_df['T_ax_'+str(i)+'_lat_'+str(j)]=globals()['T_ax_'+str(i)+'_lat_'+str(j)]

Output_df.to_csv(outputdir+'\\'+subdirectory+'\\'+save_file_name)

#%% Miscellaneuous

T_exhaust=data['TC 40']
T_bubble=data['TC 41']
Output_df=pd.DataFrame()
subdirectory='Miscellaneous'
plt.figure(dpi=200)
save_file_name=filename+' Submerged Exhaust Exit'

try:
    os.makedirs(outputdir+'\\'+subdirectory)
except OSError:
    print ("%s directory already exists. Replacing current directory" % subdirectory)
else:
    print ("Successfully created the directory %s" % subdirectory)

plt.ylabel('Temperature (C)')
plt.xlabel('Time (min)')
plt.plot(Time/60,T_exhaust,label='Inside Exhaust Pipe')
Output_df.to_csv(outputdir+'\\'+subdirectory+'\\'+save_file_name+'.csv')

plt.ylabel('Temperature (C)')
plt.xlabel('Time (min)')
plt.plot(Time/60,T_bubble,label='Exhaust Outlet')
plot_strat()
#plt.title('Exhaust Line Outlet')
lgd=plt.legend(loc='upper left',bbox_to_anchor=(1.04,1))
plt.savefig(outputdir+'\\'+subdirectory+'\\'+save_file_name,bbox_extra_artists=(lgd,),bbox
x_inches='tight',dpi=200)
Output_df.to_csv(outputdir+'\\'+subdirectory+'\\'+save_file_name+'.csv')

# Pressures
plt.figure(dpi=200)
save_file_name=filename+' Suppression Tank Pressure'
plt.ylabel('Pressure (psig)')

```

```

plt.xlabel('Time (min)')
plt.plot(Time/60, data['Suppression Tank Pressure (psia)']-data['Barometric Pressure
(psia)'],label='Suppression Tank Pressure(psig)')
#plt.title('Suppression Pool Pressure')
lgd=plt.legend(loc='upper left',bbox_to_anchor=(1.04,1))
plt.savefig(outputdir+'\\'+subdirectory+'\\'+save_file_name,bbox_extra_artists=(lgd),bbo
x_inches='tight',dpi=200)
Output_df.to_csv(outputdir+'\\'+subdirectory+'\\'+save_file_name+'.csv')

```

```

plt.figure(dpi=200)
save_file_name=filename+' Steam Generator Pressure'
plt.ylabel('Pressure (psia)')
plt.xlabel('Time (min)')
plt.plot(Time/60, data['SG Pressure (psia)'],label='Steam Generator Pressure (psia)')
#plt.title('Steam Generator Pressure')
lgd=plt.legend(loc='upper left',bbox_to_anchor=(1.04,1))
plt.savefig(outputdir+'\\'+subdirectory+'\\'+save_file_name,bbox_extra_artists=(lgd),bbo
x_inches='tight',dpi=200)
Output_df.to_csv(outputdir+'\\'+subdirectory+'\\'+save_file_name+'.csv')

```

```

# Tank outlet temperature
plt.figure(dpi=200)
save_file_name=filename+' Tank Outlet Temperature'
plt.ylabel('Temperature (C)')
plt.xlabel('Time (min)')
plt.plot(Time/60, data['TC Tank Outlet'],label='Tank Outlet Temperature')
#plt.title('Tank Outlet Temperature')
lgd=plt.legend(loc='upper left',bbox_to_anchor=(1.04,1))
plt.savefig(outputdir+'\\'+subdirectory+'\\'+save_file_name,bbox_extra_artists=(lgd),bbo
x_inches='tight',dpi=200)
Output_df.to_csv(outputdir+'\\'+subdirectory+'\\'+save_file_name+'.csv')

```

```

# Differential Pressure
plt.figure(dpi=200)
save_file_name=filename+' Differential Pressure'
plt.ylabel('Pressure (in H2O)')
plt.xlabel('Time (min)')
plt.plot(Time/60, data['Post-Turbine to SP Differential Pressure'],'*',label='Differential
Pressure')
#plt.title('Differential Pressure')
lgd=plt.legend(loc='upper left',bbox_to_anchor=(1.04,1))
plt.savefig(outputdir+'\\'+subdirectory+'\\'+save_file_name,bbox_extra_artists=(lgd),bbo
x_inches='tight',dpi=200)
Output_df.to_csv(outputdir+'\\'+subdirectory+'\\'+save_file_name+'.csv')

```

```
#####Heat Removed
```

```
T_outlet = data['TC Tank Outlet'].values[strat_start:strat_end]  
TC_ave=((TC_3_ave+TC_7_ave+TC_11_ave+TC_15_ave+TC_19_ave+TC_23_ave+T  
C_27_ave+TC_31_ave)/8).values[strat_start:strat_end]  
T_SG_ave = (data['TC SG Top'].values+data['TC SG Upper'].values+data['TC SG  
Mid'].values+data['TC SG Lower'].values)/4
```

```
dt=Time.iloc[2]-Time.iloc[1]  
P_SP = data['Suppression Tank Pressure (psia)'].values[strat_start:strat_end]  
P_SG = data['SG Pressure (psia)'].values[strat_start:strat_end]
```

```
h_low=[SteamProp.SteamH(T_outlet[i], P_SP[i]) for i in range(strat_end-strat_start)]  
h_low_mix=[SteamProp.SteamH(TC_ave[i], P_SP[i]) for i in range(strat_end-  
strat_start)]
```

```
#using nominal values for steam generator temperature and pressure to remove effects of  
varied SG pressure between tests
```

```
T_SG_sat = SteamProp.SteamTsat(95)  
h_high = SteamProp.SteamH(T_SG_sat,95)  
m_flow = data['Feedwater mass flow rate (g/s)'].values[strat_start:strat_end]
```

```
heat_rem = sum([(h_high-h_low[i])*m_flow[i]/1000*dt for i in range(strat_end-  
strat_start)])
```

```
heat_rem_mix = sum([(h_high-h_low_mix[i])*m_flow[i]/1000*dt for i in  
range(strat_end-strat_start)])
```

```
heat_rem_improvement = heat_rem-heat_rem_mix
```

```
heat_rem_rate=heat_rem/(Time.iloc[strat_end]-Time.iloc[strat_start])
```

```
heat_rem_rate_mix=heat_rem_mix/(Time.iloc[strat_end]-Time.iloc[strat_start])
```

```
heat_rate_improvement=heat_rem_rate-heat_rem_rate_mix
```

```
#####
```

```
def heat_removal(T,P,m):
```

```
    h_low=[SteamProp.SteamH(T[i], P[i]) for i in range(strat_start,strat_end)]
```

```
    h_low_mix=[SteamProp.SteamH(TC_ave[i], P[i]) for i in range(strat_start,strat_end)]
```

```
    heat_rem = sum([(h_high-h_low[i])*m[i]/1000*dt for i in range(strat_end-  
strat_start)])
```

```
    heat_rem_mix = sum([(h_high-h_low_mix[i])*m[i]/1000*dt for i in range(strat_end-  
strat_start)])
```

```
    heat_rem_rate=heat_rem/(Time.iloc[strat_end]-Time.iloc[strat_start])
```

```
    heat_rem_rate_mix=heat_rem_mix/(Time.iloc[strat_end]-Time.iloc[strat_start])
```

```
    return heat_rem,heat_rem_mix,heat_rem_rate,heat_rem_rate_mix
```

```
#####
```



```

#sensitivity study for uncertainty in enthalpy
u_T=0.5
u_P=np.average(data['Pump 1 Outlet Pressure (psia)'].values*0.01)
#%
rho_feedwater = np.zeros(len(m_flow))
for i in range(len(rho_feedwater)):
    rho_feedwater[i] = SteamProp.SteamRho(data['TC US Feedwater
Valve'].values[i],data['Pump 1 Outlet Pressure (psia)'].values[i])
#%
S_rho_T = (SteamProp.SteamH(np.average(data['TC US Feedwater
Valve'].values)+u_T/2,np.average(data['Pump 1 Outlet Pressure (psia)'].values))-
SteamProp.SteamH(np.average(data['TC US Feedwater Valve'].values)-
u_T/2,np.average(data['Pump 1 Outlet Pressure (psia)'].values)))/u_T
S_rho_P = (SteamProp.SteamH(np.average(data['TC US Feedwater
Valve'].values),np.average(data['Pump 1 Outlet Pressure (psia)'].values+u_P/2))-
SteamProp.SteamH(np.average(data['TC US Feedwater
Valve'].values),np.average(data['Pump 1 Outlet Pressure (psia)'].values-u_P/2)))/u_P

u_rho = ((S_rho_T*u_T)**2+(S_rho_P*u_P)**2)**0.5

Flow_URV = 15*0.000063090196666667 #volumetric flowrate of feedwater in m^3/s
u_Flow = Flow_URV*0.002

u_m=((u_Flow*np.max(rho_feedwater) * 1000)**2 +
(u_rho*Flow_URV*1000)**2)**0.5 #uncertainty in mass flow rate g/s
#%
u_P=0.126
u_h_high = (SteamProp.SteamH(SteamProp.SteamTsat(95+u_P/2),95+u_P/2)-
SteamProp.SteamH(SteamProp.SteamTsat(95-u_P/2),95-u_P/2))

S_h_low_T_outlet =
(SteamProp.SteamH(np.average(T_outlet)+u_T/2,np.average(P_SP))-
SteamProp.SteamH(np.average(T_outlet)-u_T/2,np.average(P_SP)))/u_T
S_h_low_T_ave = (SteamProp.SteamH(np.average(TC_ave)+u_T/2,np.average(P_SP))-
SteamProp.SteamH(np.average(TC_ave)-u_T/2,np.average(P_SP)))/u_T
S_h_low_P_SP = (SteamProp.SteamH(np.average(T_outlet),np.average(P_SP)+u_P/2)-
SteamProp.SteamH(np.average(T_outlet),np.average(P_SP)-u_P/2))/u_P

u_h_low = ((S_h_low_T_outlet*u_T)**2+(S_h_low_P_SP*u_P**2))**0.5
u_h_low_mix = ((S_h_low_T_ave*u_T)**2+(S_h_low_P_SP*u_P**2))**0.5

```

```

u_heat_rem = np.sqrt((u_m/1000*sum((h_high-h_low[i])*dt for i in range
(len(h_low))))**2+(u_h_high*sum(m_flow[i]/1000*dt for i in range(len(m_flow))))**2
+ (u_h_low*sum(m_flow[i]/1000*dt for i in range(len(m_flow))))**2)
u_heat_rem_mix = np.sqrt((u_m/1000*sum((h_high-h_low_mix[i])*dt for i in range
(len(h_low_mix))))**2+(u_h_high*sum(m_flow[i]/1000*dt for i in
range(len(m_flow))))**2 + (u_h_low_mix*sum(m_flow[i]/1000*dt for i in
range(len(m_flow))))**2)
u_heat_rem_improvement = np.sqrt((u_m/1000*sum((h_low_mix[i]-h_low_mix[i])*dt
for i in range (len(h_low_mix))))**2+(u_h_low*sum(m_flow[i]/1000*dt for i in
range(len(m_flow))))**2 + (u_h_low_mix*sum(m_flow[i]/1000*dt for i in
range(len(m_flow))))**2)

```

```

u_heat_rate = u_heat_rem/(Time.iloc[strat_end]-Time.iloc[strat_start])
u_heat_rate_mix = u_heat_rem_mix/(Time.iloc[strat_end]-Time.iloc[strat_start])
u_heat_rate_improvement = u_heat_rem_improvement/(Time.iloc[strat_end]-
Time.iloc[strat_start])

```

```

T_room_SP = np.average(data['TC SP Side Room Temp'].values)
T_room_SG = np.average(data['TC SG Side Room Temp'].values)
T_room_ave=(T_room_SP+T_room_SG)/2

```

```

P_atm = np.average(data['Barometric Pressure (psia)'].values)

```

Readout

```

f = open(outputdir+'\\'+readout+'filename+'.txt,'w')
f.write('Average Room Temperature during test =' +str(T_room_ave)+' degrees C \n')
f.write('Average Barometric Pressure during test =' +str(P_atm)+' psia \n')
f.write('Average steam temperature leaving turbine =' +str(np.average(data['TC Post
Turbine']))+' Degrees C \n')
f.write('Steam mass flowrate = ' +str(np.average(data['Steam line Flow Rate
(g/s)'].values))+' g/s\n')
f.write('Thermal Stratification started at ' +str(Time.iloc[strat_start])+' seconds\n')
f.write('Bulk temperature at start of thermal stratification was
'+str(TC_31_ave.iloc[strat_start])+'degrees C\n')
f.write('Bulk subcooling at start of thermal stratification was
'+str(TC_31_sub_ave.iloc[strat_start])+'degrees C\n')
f.write('Total stratification duration was ' +str(Time.iloc[strat_end]-
Time.iloc[strat_start])+' seconds \n')
if 'mix_stop' in globals():
    f.write('lowest thermocouple steady state reached at ' +str(mix_stop/10)+' seconds\n')
else:
    f.write('lowest thermocouple never reached steady state\n')
f.write('Average Stratification was ' +str(np.average(T_strat))+' degrees C \n')
f.write('Maximum stratification was ' +str(max(T_strat))+' degrees C \n')

```

```

f.write('Maximum pressure was '+str(max(data['Suppression Tank Pressure (psia)']))+'
psia \n')
f.write('total heat removed = '+str(heat_rem)+' kJ\n')
f.write('heat removal rate = '+str(heat_rem_rate)+' kW\n')
f.write('Theoretical heat removed if fully mixed = '+str(heat_rem_mix)+' kJ\n')
f.write('Theoretical heat removal rate if fully mixed = '+str(heat_rem_rate_mix)+'
kJ\n\n')
f.write('Uncertainties:\n')
f.write('Heat Removal: \t\t\t+/-'+str(u_heat_rem)+' kJ\n')
f.write('Heat Removal (mixed): \t\t+/-'+str(u_heat_rem_mix)+' kJ\n')
f.write('Heat Removal Rate: \t\t\t+/-'+str(u_heat_rate)+' kW\n')
f.write('Heat Removal Rate (mixed): \t+/-'+str(u_heat_rate_mix)+' kW\n')
f.close()

```

```

filepath = outputdir+'\\'+output_'+filename+'.csv'

```

```

Output_df=pd.DataFrame()
Output_df['Nominal Water Mass Flow Rate (g/s)]=[np.average(data['Feedwater mass
flow rate (g/s)'].values)]
Output_df['U_massflow']=[u_m]
Output_df['Nominal Steam Mass Flow Rate (g/s)]=[np.average(data['Steam line Flow
Rate (g/s)'].values)]
Output_df['U_steam_massflow']=[0.01*np.average(data['Steam line Flow Rate
(g/s)'].values)]
Output_df['Average Pressure (psia)]=[np.average(data['Suppression Tank Pressure
(psia)'].values)]
Output_df['Maximum Pressure (psia)]=[np.max(data['Suppression Tank Pressure
(psia)'].values)]
Output_df['U_Pressure']=[u_P]
Output_df['Maximum Degrees of Stratification (C)]=[np.max(T_strat)]
Output_df['U_T_strat']=[u_T]
Output_df['Heat Removed (kJ)]=[heat_rem]
Output_df['U_heat removed']=[u_heat_rem]
Output_df['Theoretical Heat Removed for Mixed Pool (kJ)]=[heat_rem_mix]
Output_df['U_heat_removed_mixed']=[u_heat_rem_mix]
Output_df['Heat Removal Improvement (kJ)]=[heat_rem_improvement]
Output_df['U_heat removal improvement (kJ)]=[u_heat_rem_improvement]
Output_df['Heat Removal Rate (kW)]=[heat_rem_rate]
Output_df['U_Heat removal']=[u_heat_rate]
Output_df['Theoretical Heat Removal Rate for Mixed Pool (kW)]=[heat_rem_rate_mix]
Output_df['U_heat removal Theoretical']=[u_heat_rate_mix]
Output_df['Heat Removal Rate Improvement (kW)]=[heat_rate_improvement]
Output_df['U_heat removal rate improvement']=[u_heat_rate_improvement]

```

```
Output_df.to_csv(filepath,index=False,header=True)
```

```
###  
Processing_Time=time.time()-start_time  
#print('done')  
#print('Processing Time=',Processing_Time,'Seconds')
```

B.2.3 SteamProperties.py

```
### IAPWS Steam property calculator  
import numpy as np  
import math  
def n_set(x):  
    if x == 0:  
        n = [0.11670521452767e4,-0.72421316703206e6,-0.17073846940092e2,  
            0.12020824702470e5,-0.32325550322333e7,0.14915108613530e2,  
            -0.48232657361591e4,0.40511340542057e6,-0.23855557567849,  
            0.65017534844798e3]  
    if x == 1:  
        n = [0.14632971213167, -0.84548187169114, -3.7563603672040,  
            3.3855169168385,  
            -0.95791963387872, 0.15772038513228, -0.016616417199501,  
            0.81214629983568e-3,  
            0.28319080123804e-3, -0.60706301565874e-3, -0.018990068218419, -  
            0.032529748770505,  
            -0.021841717175414, -5.283835796993e-5, -0.00047184321073267, -  
            0.00030001780793026,  
            4.7661393906987E-5, -4.4141845330846e-6, -0.72694996297594E-15, -  
            3.1679644845054E-5,  
            -2.8270797985312E-6, -8.5205128120103e-10, -2.2425281908E-6, -  
            6.5171222895601e-7,  
            -1.4341729937924E-13, -4.0516996860117e-7, -1.2734301741641e-9, -  
            1.7424871230634e-10,  
            -6.8762131295531E-19, 1.4478307828521E-20, 2.6335781662795E-23, -  
            1.1947622640071E-23,  
            1.8228094581404E-24, -9.3537087292458E-26]  
    if x ==2:  
        n = [-0.96927686500217e1,0.10086655968018e2,-0.56087911283020e-2,  
            0.71452738081455e-1,-0.40710498223928,0.14240819171444e1,  
            -0.43839511319450e1,-0.28408632460772,0.21268463753307e-1]  
    if x == 3:
```

```

n = [-0.17731742473213e-2, -0.17834862292358E-1, -0.45996013696365e-1,
     -0.57581259083432e-1, -0.50325278727930e-1, -0.33032641670203e-4,
     -0.18948987516315e-3, -0.39392777243355e-2, -0.43797295650573e-1,
     -0.26674547914087e-4, 0.20481737692309e-7, 0.43870667284435e-6,
     -0.32277677238570e-4, -0.15033924542148e-2, -0.40668253562649e-1,
     -0.78847309559367e-9, 0.12790717852285e-7, 0.48225372718507e-6,
     0.22922076337661e-5, -0.16714766451061e-10, -0.21171472321355e-2,
     -0.23895741934104e2, -0.59059564324270e-17, -0.12621808899101e-5,
     -0.38946842435739e-1, 0.11256211360459e-10, -0.82311340897998e1,
     0.19809712802088e-7, 0.10406965210174e-18, -0.10234747095929e-12,
     -0.10018179379511e-8, -0.80882908646985e-10, 0.10693031879409,
     -0.33662250574171, 0.89185845355421e-24, 0.30629316876232e-12,
     -0.42002467698208e-5, -0.59056029685639e-25, 0.37826947613457e-5,
     -0.12768608934681e-14, 0.73087610595061e-28,
     0.55414715350778e-16, -0.94369707241210e-6]
return n

def I_set():
    I = [0,0,0,0,0,0,0,0,
         1,1,1,1,1,1,
         2,2,2,2,2,
         3,3,3,
         4,4,4,
         5,
         8,8,
         21,23,29,30,31,32]
    return I

def J_set(x):
    if x == 0:
        J = [-2,-1,0,1,2,3,4,5,-9,-7,-1,0,1,3,-3,0,1,3,17,-4,0,6,
             -5,-2,10,-8,-11,-6,-29,-31,-38,-39,-40,-41]
    if x == 1:
        J = [0,1,-5,-4,-3,-2,-1,2,3]
    if x == 2:
        J = [0,1,2,3,6,1,2,4,7,36,0,1,3,6,35,1,2,3,7,3,16,35,0,11,
             25,8,36,13,4,10,14,2,50,57,20,35,48,21,53,39,26,40,58]
    return J

def SteamPsat(T):
    """
    Parameters
    -----
    T : Float

```

Temperature in Degrees C.

Returns

Psat : Float

Saturation pressue in psia.

"""

T = T + 273.15 #convert to Kelvin

T_star = 1

n = n_set(0)

gamma=T/T_star

theta= gamma+ (n[8]/(gamma-n[9]))

A= theta*theta + n[0]*theta +n[1]

B= n[2]*theta*theta + n[3]*theta + n[4]

C= n[5]*theta*theta + n[6]*theta + n[7]

alpha = (2*C/(-B+math.pow((B*B - 4*A*C),0.5)))*(2*C/(-B+math.pow((B*B - 4*A*C),0.5)))*(2*C/(-B+math.pow((B*B - 4*A*C),0.5)))*(2*C/(-B+math.pow((B*B - 4*A*C),0.5)))*(2*C/(-B+math.pow((B*B - 4*A*C),0.5))

Psat = alpha/0.00689476

return Psat

def SteamTsat(P):

"""

Parameters

P : float

Pressure in psia.

Returns

Tsat : float

Saturation Temperature in Celsius.

"""

P=P*0.006894757293168361e6

P_star=1e6

n = n_set(0)

beta = math.pow((P/P_star),0.25)

A = beta*beta + n[2]*beta+n[5]

B = n[0]*beta*beta + n[3]*beta + n[6]

C = n[1]*beta*beta + n[4]*beta +n[7]

D = 2*C/(-B-math.pow((B*B-4*A*C),0.5))

Ts= 0.5* (n[9] + D -math.pow(((n[9]+D)*(n[9]+D)-4*(n[8]+n[9]*D)),0.5))

Tsat=Ts-273.15

return Tsat

```

#%%%
def SteamProp(T,P):
    """
    Parameters
    -----
    T : Float
        Steam Temperature in Celsius.
    P : Float
        Steam Pressure in psia.

    Returns
    -----
    rho : Float
        Steam density (kg/m^3).
    h : Float
        Steam Specific Enthalpy (kJ/kg).
    u : Float
        Steam Specific Internal Energy (kJ/kg).
    s : Float
        Steam Specific Entropy (kJ/kg*K).
    Cp : Float
        Specific Heat Capacity (kJ/kg*K).
    w : Float
        Speed of sound in medium (m/s).
    """
    Ts=SteamTsat(P)+273.15
    T = T +273.15
    P = P*0.006894757293168361e6
    R = 0.461526e3 #J/kg.K
    P_star = 16.53e6 #Pa
    T_star = 1386
    P_r = P/P_star
    T_r = T_star/T
    if T < Ts: #liquid phase region 1
        R = 0.461526e3 #J/kg.K
        P_star = 16.53e6 #Pa
        T_star = 1386
        P_r = P/P_star
        T_r = T_star/T
        I = I_set()
        J = J_set(0)
        n = n_set(1)
        g=[n[i]*math.pow((7.1-P_r),I[i]) * math.pow((T_r-1.222),J[i]) for i in range(34)]

```

```

g_pi = [-n[i]*I[i] * math.pow((7.1 - P_r),(I[i]-1)) * math.pow((T_r-1.222),J[i]) for i
in range(34)]
g_t = [n[i] * math.pow((7.1 - P_r),I[i]) * J[i]*math.pow((T_r - 1.222),(J[i]-1)) for i
in range(34)]
g_tt= [n[i] * math.pow((7.1-P_r),I[i]) * J[i]*(J[i]-1) * math.pow((T_r-1.222),(J[i]-
2)) for i in range(34)]
g_pit= [-n[i]*I[i]*math.pow((7.1-P_r),(I[i]-1)) * J[i] * math.pow((T_r-1.222),(J[i]-
1)) for i in range(34)]
g_pipi=[n[i]*I[i] * (I[i]-1) * math.pow((7.1-P_r),(I[i]-2)) * math.pow((T_r-
1.222),J[i]) for i in range(34)]
g_sum = sum(g)
g_pi_sum = sum(g_pi)
g_t_sum = sum(g_t)
g_tt_sum = sum(g_tt)
g_pipi_sum = sum(g_pipi)
g_pit_sum = sum(g_pit)
v= (R*T/P)*P_r *g_pi_sum #specific volume (m^3/kg)
rho= 1/v #density (kg/m^3)
h = (R*T*0.001)*(T_r*g_t_sum)
u = (R*T*0.001)*(T_r*g_t_sum-P_r*g_pi_sum)
s = (R*0.001)*((T_r*g_t_sum)-g_sum)
Cp= (R*0.001)*-1*T_r*T_r *g_tt_sum
w = math.pow(((R*T*g_pi_sum*g_pi_sum)/((g_pi_sum-
T_r*g_pit_sum)*(g_pi_sum-T_r*g_pit_sum)/(T_r*T_r * g_tt_sum)-g_pipi_sum)),0.5)
if T >= Ts: #steam Region 2
P_star=1e6
T_star=540
P_r = P/P_star
T_r = T_star/T
J0 = J_set(1)
n0 = n_set(2)
lr = [1, 1,1, 1, 1, 2, 2, 2, 2, 2, 3, 3, 3, 3, 3, 4, 4, 4, 5, 6, 6, 6,
7, 7, 7, 8, 8, 9, 10, 10, 10, 16, 16, 18, 20, 20, 20, 21, 22,
23, 24, 24, 24]
Jr = J_set(2)
nr = n_set(3)
g_o_pi= 1/P_r
g_o = np.log(P_r)+ sum((n0[i]*math.pow(T_r,J0[i])for i in range(9)))
g_o_t= sum(n0[i]*J0[i]*math.pow(T_r,(J0[i]-1))for i in range(9))
g_o_tt=sum(n0[i]*J0[i]*(J0[i]-1)*math.pow(T_r,(J0[i]-2)) for i in range(9))
g_r = [nr[i] * math.pow(P_r,lr[i]) * math.pow((T_r - 0.5),Jr[i]) for i in range(43)]
g_r_pi = [nr[i] * lr[i] * math.pow(P_r,(lr[i]-1)) * math.pow((T_r - 0.5),Jr[i]) for i in
range(43)]

```



```

    g_r_pipi = [nr[i] * lr[i] * (lr[i]-1) * math.pow(P_r,(lr[i]-2)) * math.pow((T_r -
0.5),Jr[i]) for i in range(43)]
    g_r_t = [nr[i] * math.pow(P_r,lr[i]) * Jr[i] * math.pow((T_r - 0.5),(Jr[i]-1)) for i in
range(43)]
    g_r_tt = [nr[i] * math.pow(P_r,lr[i]) * Jr[i] * (Jr[i]-1) * math.pow((T_r - 0.5),(Jr[i]-
2)) for i in range(43)]
    g_r_pit = [nr[i] * math.pow(P_r,(lr[i]-1)) * lr[i] * Jr[i] * math.pow((T_r - 0.5),(Jr[i]-
1)) for i in range(43)]

```

```

sum_g_r= sum(g_r)
sum_g_r_pi= sum(g_r_pi)
sum_g_r_pipi= sum(g_r_pipi)
sum_g_r_t= sum(g_r_t)
sum_g_r_tt= sum(g_r_tt)
sum_g_r_pit= sum(g_r_pit)

```

```

nom = 1 + 2*P_r*sum_g_r_pi + P_r*P_r * sum_g_r_pi*sum_g_r_pi
den1 = 1 - P_r*P_r * sum_g_r_pipi
nom_den2 = (1+ P_r*sum_g_r_pi - T_r*P_r*sum_g_r_pit)*(1+ P_r*sum_g_r_pi -
T_r*P_r*sum_g_r_pit)
den_den2 = T_r*T_r * (g_o_tt+sum_g_r_tt)
den = den1 + nom_den2/den_den2
v = (R*T/P) *P_r *(g_o_pi + sum_g_r_pi)
rho =1/v
h = (0.001*R*T)*T_r*(g_o_t+sum_g_r_t)
u = (0.001*R*T)*(T_r*(g_o_t+sum_g_r_t)-P_r*(g_o_pi+sum_g_r_pi))
s = (0.001*R)*(T_r*(g_o_t+sum_g_r_t)-g_o-sum_g_r)
Cp = (0.001*R) * -1 *math.pow(T_r,2) *(g_o_tt+ sum_g_r_tt)
w = (R*T *nom/den)
return rho,h, u, s, Cp, w

```

```
def SteamRho(T,P):
```

```
    """
```

```
    Parameters
```

```
    -----
```

```
    T : Float
```

```
        Temperature in Celsius.
```

```
    P : Float
```

```
        Pressure in psia.
```

```
    Returns
```

```
    -----
```

```
    Float
```

```
        Density (kg/m^3).
```

```

    """
    return SteamProp(T,P)[0]

def SteamH(T,P):
    """
    Parameters
    -----
    T : Float
        Temperature in Celsius.
    P : Float
        Pressure in psia.

    Returns
    -----
    Float
        Specific Enthalpy (kj/kg).
    """
    return SteamProp(T,P)[1]

def SteamU(T,P):
    """
    Parameters
    -----
    T : Float
        Temperature in Celsius.
    P : Float
        Pressure in psia.

    Returns
    -----
    Float
        Specific Internal energy (kj/kg).
    """
    return SteamProp(T,P)[2]

def SteamS(T,P):
    """
    Parameters
    -----
    T : Float
        Temperature in Celsius.
    P : Float
        Pressure in psia.

```

```

Returns
-----
Float
    Specific Entropy (kJ/kg*K).
"""
return SteamProp(T,P)[3]

def SteamCp(T,P):
    """
    Parameters
    -----
    T : Float
        Temperature in Celsius.
    P : Float
        Pressure in psia.

    Returns
    -----
    Float
        Specific Heat Capacity (kJ/kg*K).
    """
    return SteamProp(T,P)[4]

def SteamW(T,P):
    """
    Parameters
    -----
    T : Float
        Temperature in Celsius.
    P : Float
        Pressure in psia.

    Returns
    -----
    Float
        Speed of Sound (m/s).
    """
    return SteamProp(T,P)[5]

if __name__ == "__main__":
    Tsat=0 #saturation temperature (C)
    Psat=0 #saturation pressure (psia)
    rho=0 #density (kg/m^3)
    h=0 #Specific Enthalpy (kJ/kg)

```

```
U=0 #Internal Energy (kJ/kg K)
s=0 #Entropy (kJ/kg.K)
Cp=0 #Constant pressure heat capacity (kJ/kg.K)
w=0 #speed of sound (m/s)
```

B.2.4 search.py

```
# -*- coding: utf-8 -*-
"""
```

```
Created on Tue Dec 15 12:12:09 2020
```

```
@author: dkeeslin
"""
```

```
import os
import tkinter
import shutil
```

```
from tkinter import filedialog
Home = 'C:'
```

```
def search_for_file():
    root = tkinter.Tk()
    filename = filedialog.askopenfilename(parent=root,initialdir= Home,title='Choose
input file(s)')
    root.destroy()
    return filename
```

```
def search_for_directory():
    root = tkinter.Tk()
    directory = filedialog.askdirectory(parent=root,initialdir=Home, title='Please select an
output directory')
    root.destroy()
    return directory
```

```
def clean_directory(directory):
    print(directory)
    try:
        if len(os.listdir(directory)) != 0:
            shutil.rmtree(directory)
        else:
            os.remove(directory)
    except FileNotFoundError:
        print('target directory does not exist')
```

```

def search_for_files():
    root = tkinter.Tk()
    filenames = filedialog.askopenfilenames(parent=root,initialdir= Home,title='Choose
an input file')
    root.destroy()
    return filenames

```

B.2.5 SteadyStateDetection.py

```

# -*- coding: utf-8 -*-
"""

```

Created on Tue Apr 6 12:31:44 2021

@author: dkeeslin

Steady State Detection Algorithm from:

A Steady-State Detection (SSD) Algorithm to Detect Non-Stationary Drifts in Processes
(Jeff Kelly, John Hedengren, 2013)

```

"""

```

```

import numpy as np
def SSD(x,t_crit,n):
    t = np.linspace(1,n,n)
    m = sum(x[i+1]-x[i] for i in range(n-1))/(n-1)
    mu = 1/n *(sum(x)-m*sum(t))
    sigma = pow(1/(n-2)*sum((x-m*t-mu)**2),0.5)
    y_t=0
    for i in range(n):
        if abs(x[i] - mu) <= t_crit*sigma:
            y_t+=1
        else:
            y_t+=0
    return y_t/n >0.95,y_t/n

```